INVESTIGATION INTO THE EFFECTS OF TRACTION CONVERTERS ON LINESIDE TRANSFORMERS

Justine Muthen

Date: 20 July 2023

In fulfilment of the requirements for Masters of Science (Electrical Engineering), College of Agriculture, Engineering and Science, University of KwaZulu-Natal

Supervisor: Andrew Swanson

COLLEGE OF AGRICULTURE, ENGINEERING AND SCIENCE

DECLARATION 1 –SUPERVISOR AGREEMENT

I, Andrew Swanson, declare that;

1. I hereby verify that I have reviewed the final version of this thesis and approve this submission.

Signed

COLLEGE OF AGRICULTURE, ENGINEERING AND SCIENCE

DECLARATION 2 - PLAGIARISM

I, Justine Muthen, declare that;

1. The research reported in this thesis, except where otherwise indicated, is my original research.

2. This thesis has not been submitted for any degree or examination at any other university.

3. This thesis does not contain other persons' data, pictures, graphs or other information, unless specifically acknowledged as being sourced from other persons.

4. This thesis does not contain other persons' writing, unless specifically acknowledged as being sourced from other researchers. Where other written sources have been quoted, then:

a. Their words have been re-written, but the general information attributed to them has been referenced.

b. Where their exact words have been used, then their writing has been placed in italics and inside quotation marks and referenced.

5. This thesis does not contain text, graphics or tables copied and pasted from the Internet, unless specifically acknowledged, and the source being detailed in the thesis and in the References sections.

Signed

Abstract

In 25kV AC rail infrastructure applications, single-phase lineside transformers are used to supply power to lineside railway equipment. This consists of train condition monitoring and authorisation systems which are extremely sensitive to power supply inconsistencies. If there is a failure in the power supply to this lineside equipment, a resultant inaccuracy in the signals received from this equipment can affect the throughput of trains.

Due to the nature of the 25 kV traction power system, power quality issues can affect the lineside transformer. This study followed two key aspects, the first being the investigation of the lineside transformer. Here, the validity of the known parameters of the transformer are investigated and discussed. Since, there is little information available about these 16kVA, 25kV/230V lineside transformers and for the remaining parameters required for the simulation of the transformer model, a similar rated transformer was tested. Its behaviour was then modelled to suit the lineside application. Overvoltage's are studied in detail to determine the saturation limits for the transformer to be developed. This model, constructed using MATLAB, was then used to model the traction power system, which includes the traction substation, electrical infrastructure and train. The formation of all of these components have been detailed in the investigation.

The second aspect was studying the distortion in the voltage waveform experienced by the lineside transformer. This was analysed firstly, under two conditions, loaded, where the train is connected to the system and secondly, during regeneration, which is active via dynamic braking. The behaviour of the model was also observed, whilst increasing the switching frequency of the converter onboard the locomotive, increasing the fault level, as well as taking the over overvoltage situation into consideration. Here, the most prominent harmonic orders are determined and dsicussed. Specifically, noting that whilst analysing the model during over voltage characteristics, the magnetising current in the lineside transformer was found to have increased by approximately 70% due to the harmonics experienced at multiple frequencies.

Throughout this investigation it is clear that, the specification of the lineside transformer is ill-equipped to deal with the overvoltage characteristics required for this application and in some cases tends to saturate during operation. This became apparent at lower tap changer positions for core flux density levels of 1.7 T and 1.6 T. Hence, a dedicated lineside transformer specification is suggested, detailing

all the necessary design parameters, insulation level and harmonics, that should be adhered to, in order to prevent this.

Contents

List of Figures

List of Tables

Acronyms

AC – Alternating Current

DC – Direct Current

OHTE – Overhead Track Equipment

IGBT – Insulated Gate Bipolar Transistor

THD – Total Harmonic Distortion

UPS - Uninterruptable Power Supply

1 Introduction

In recent years there has been a drive to decrease carbon emissions and encourage the development of current railway infrastructure. South Africa's freight business has embraced this idea by increasing the quantity of commodities transported via the Rail Network infrastructure, as the majority of the freight logistics transport is by road. This contributes to approximately 85% of the transportation sector [1]. In South Africa, transportation contributes to almost 14% of the country's total carbon footprint, and of this approximately 90% is due to the road transport industry [1]. In order to decrease the amount of freight moved by road, the existing railway infrastructure will need to be upgraded which, warrants the extension of loop lines (electrical and civil components which make up a split on a single line, allowing for the staging of trains and alternate paths in the event of a breakdown), to aid in the venture. To this end the signalling equipment used for locomotive condition and authorisation needs to be reliable to ensure throughput and safety.

Transnet has three overhead power supply variations, 25kV AC, 50kV AC and 3kV DC. Dual voltage locomotives are used on 25kV and 3kV DC systems. This assists with decreasing the time taken to authorise a train moving through a section of rail with AC reticulation to DC reticulation, referred to as a change-over yard. However, with new technology, comes the concern of power quality within the locomotives. This refers to the conversion of power from AC to DC and back to AC. During braking and downhill movement of a train, power is regenerated into the system [2].

As mentioned, the railway entity aims to increase the tonnages of freight transported on rail, by upgrading infrastructure [2]. However, no indication is made to whether the existing infrastructure will be replaced, as is required with every increase in load from an electrical perspective. Increasing the length of a train, immediately indicates an increase in power consumption, which is not free from power quality issues. As a result, all electrical infrastructure connected to the 25 kV AC line is at risk.

Since the 25kVAC power supply system is more widely used around the world, in countries like India, France, Russia and Japan [3] [4], to name a few, the single phase 25kV/230V lineside transformer was

considered for this investigation. A typical lineside transformer steps down the overhead voltage to 230VAC in the case of single phase, and 400VAC, of three-phase, dependent on the line voltage. These lineside transformers are pole mounted and provide power to the lineside equipment through a 6 kVA UPS.

The lineside equipment, in question are referred to as signalling equipment. As the name suggest, this equipment is used to monitor the condition of the train passing through them and is also used for communication purposes. These need to function consistently and should they fail, this will result in the control room not knowing the location of the train as well the condition of the train. This is essential information especially when long-haul trains carrying more than 102 wagons are travelling between large sections of rail.

1.1 Research Question

The intention of this investigation is to find the effects of the overvoltages experienced at the secondary terminals of the lineside transformer. This essentially is the analysis of the source voltage used by the trackside signalling equipment.

Due to Transnet's plan to increase its freight capacity and hence improve on the existing infrastructure, little is known about the effects this would have on the existing electrical infrastructure, specifically the lineside transformer. As, this transformer is not exempt from failures owing to power quality issues experienced on the 25 kV AC line. It is therefore imperative to study the lineside transformer before these changes to infrastructure are implemented, in the hope of gaining a better understanding of the behaviour of the transformer and its specification.

This analysis was carried out by exploring the behaviour of the single-phase lineside transformer under typical load conditions as well as examining the surge in switching. The locomotives considered for this application are dual voltage, known to pose problems in power quality, especially whilst taking regenerative braking into consideration. The harmonics in the transformers output overvoltage is examined in this regard, whilst monitoring the saturation level of the transformer.

The investigation follows the two questions below.

1. Does the power quality issue that occurs with trains have an impact on the lineside transformer?
2. Is there something about the lineside transformer that needs to be specified differently?

1.2 Hypothesis

The hypothesis is that the lineside transformer is not rated to sufficiently handle the power supply conditions required for the transmission of trains.

1.3 Methodology

The process of this investigation follows a few aspects, which is briefly outlined by Figure 1. Firstly, the problem of voltage inconsistencies experienced by the lineside transformer is investigated. Thereafter the known design parameters of the transformer are scrutinised, and an appropriate transformer model is obtained to be tested. The effects of harmonics from the electrical railway infrastructure and trains on this lineside transformer are studied and the process is represented in Figure 2.

The simulation model was developed in MATLAB/Simulink. This accounts for the lineside transformer with non-linear characteristics, the train consisting of locomotives with the power electronics, the OHTE and its impedance.

To determine the validity of the developed locomotive model, the simulation was run with diodes or with the converter being uncontrolled, and thereafter IGBT's were added. The locomotive is then disconnected to mimic a steady state scenario, or when the transformer is idling. The model was then run under load and regenerative conditions at the different transformer tap settings.

Harmonics and voltage stability are two of main aspects under investigation and essentially whether the transformer possesses the sufficient specification to support the requirements of the lineside equipment.

The following scenarios were tested:

1. Voltage for normal operating conditions and regeneration from close to the sub and far away from the substation (low and high source impedance).

2. Harmonics for numerous switching frequencies for normal and regeneration conditions at various locations from the traction substation (low to high source impedance).

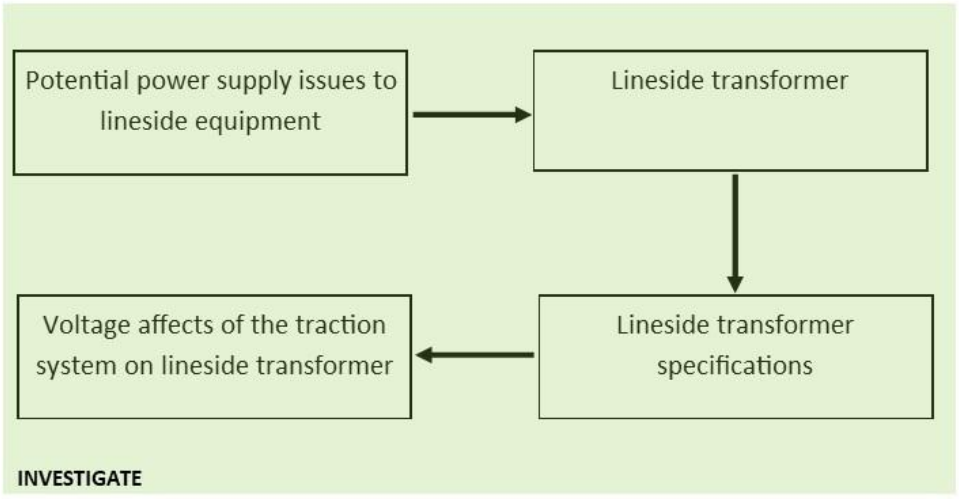

Figure 1: Methodology of overall investigation of lineside transformer.

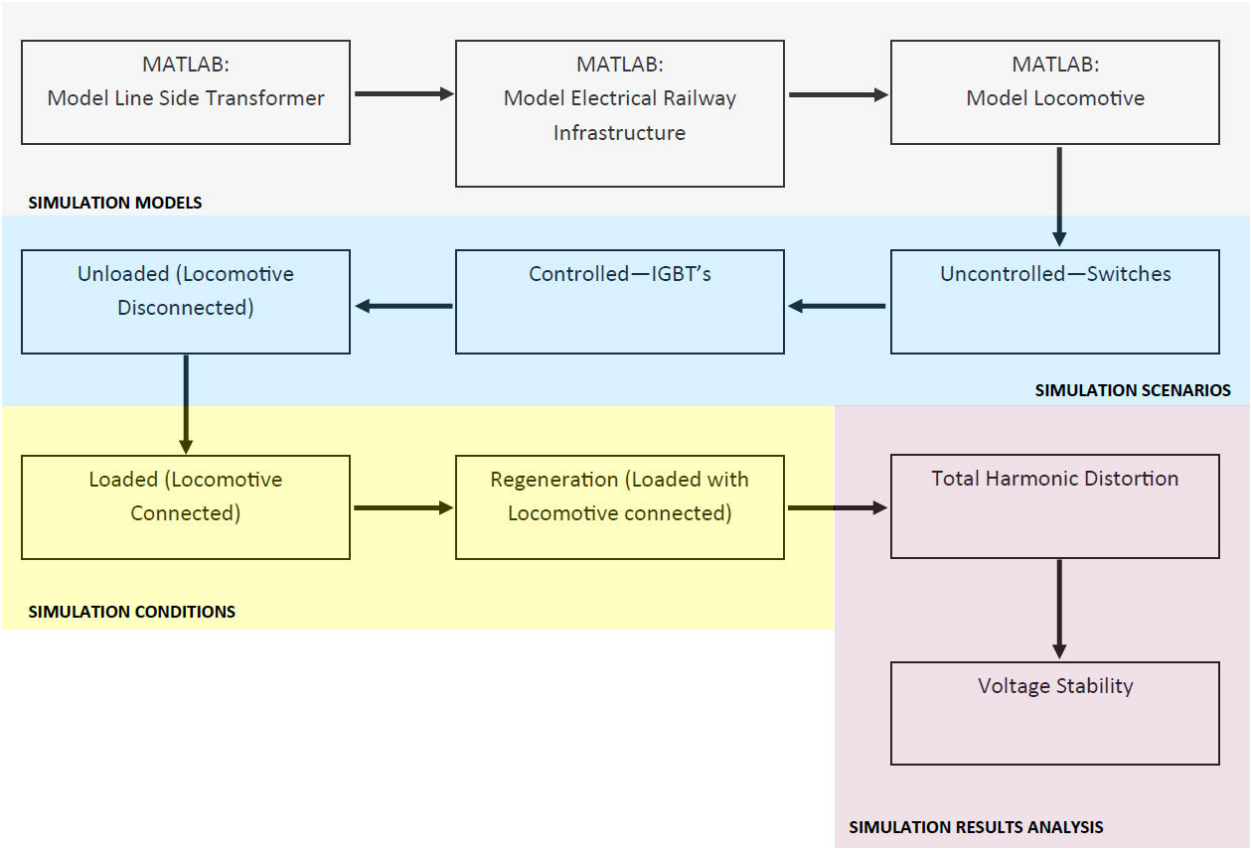

Figure 2: Methodology flow chart of harmonic study

1.4 Importance of Study and Contribution

The emphasis of this study is on the lineside transformer and its specification, as well as the effect that harmonics, over voltages and switching surges, caused by multiple locomotives in a train, have on them and thus the quality of power supplied to the lineside equipment.

There are limited technical resources available regarding this investigation, and more specifically regarding this type of lineside transformer, a contribution to the correct transformer parameters and requirements are hence made.

1.5 Dissertation Structure

The chapters encompassed in this dissertation is as follows.

Chapter 1 is the introduction and details the intentions of this study and the expected outcomes.

Chapter 2 details the contents of the background. This includes all the engineering principles and equipment used throughout this study.

Chapter 3 details the literature review. This includes all similar investigations and studies conducted in context of the experiment.

Chapter 4 investigates the possible design issues of the lineside transformer.

Chapter 5 investigates the potential impact of the electrical traction infrastructure on the lineside transformer. This includes the impact of harmonics according to the following cases: steady state, loaded train and thereafter, a train travelling by means of regenerative braking.

Chapter 6 mainly discusses and compares the results received, as well as highlights the issues experienced with the project. Special conditions implemented are also expressed.

Chapter 7 summarises and concludes all the objectives stated in chapter 4 and details the solutions to all setbacks found in chapter 5. This chapter also determines the validity of the solution.

2 Background and Literature Review

2.1 25kV Traction Power

South Africa has three railway infrastructure traction power systems, namely 3 kV DC, 25 kV AC and 50 kV AC, which span over 4935 km, 2309 km and 861 km, respectively [2]. This investigation focussed solely on the 25 kV AC power reticulation system and its corresponding infrastructure [5].

2.1.1 Electrical Rail Network Infrastructure

The electrical railway network infrastructure is divided into two parts. The first being the traction power system, which comprises of the equipment used to condition the power obtained from the power utility's distribution substation to a voltage befitting of the line of track designed for a specific area. The second part is referred to as the overhead track equipment (OHTE), this includes the overhead cables (catenary and contact), jumpers, droppers, section insulators and blade switches used for dividing the electrical infrastructure into sections.

Figure 3 Typical feeding arrangement of 25kV AC system, depicts electrical infrastructure configuration used to power the train. Two phases of the three-phase power (usually 132 kV) are taken from the power utility and is stepped down to 25 kVAC, in this case, at the traction substation. This voltage is then fed to the OHTE, ready to be used by the train. As noted, section insulators are used to create breaks in the circuit, this is mainly done to separate the different phases. A traction sectioning switch is used to assist with feeding between traction substations to ensure the availability of the line. In the event of a traction substation being unavailable, the breaker will be closed [5] [6].

As shown, the return circuit's path moves from the pantograph of the locomotive, through the wheels of the train onto the rail through bonding back to the traction substation. It is important to note that an earth wire, which runs adjacent to the catenary wire is sometimes used, and forms part of the return circuit [5].

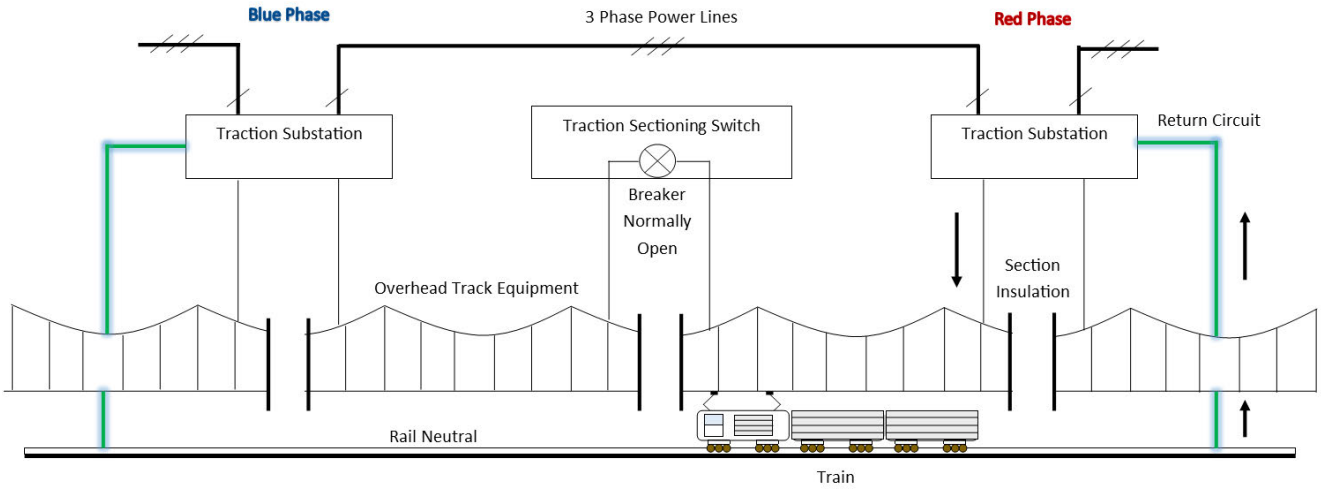

Figure 3 Typical feeding arrangement of 25kV AC system [5]

Figure 4, depicts the line diagram of the conversion of power, from power utility to the line side transformer which supplies the signalling equipment.

This equipment is made up of train authorisation equipment, used to communicate with train drivers and lineside equipment used to set the track. As well as condition assessment equipment, this makes use of trackside equipment which monitors the state and completeness of the train. All of these are voltage sensitive equipment and power supplied to them needs to be regulated and mostly free from harmonics, as this would affect the functioning of the trackside equipment and jeopardise its communication of critical information. The lineside pole mounted transformer is single phase, rated at 25kV/230V, 16kVA, and receives power from the 25kV OHTE. This suggests that any voltage insistencies on the over lines will be passed onto the transformer.

Baxter [7] states that the United Kingdom has a similar railway infrastructure network approach and uses the 25kV AC reticulation system. The difference is that previously booster transformers were used every 3km to 8km, to help with the voltage drop along the OHTE. These have been replaced by the autotransformer system which boosts the line voltage and reduces the number of traction substations required. The autotransformers also assist in reducing the power interruptions on the line to ensure a reliable

power supply. Most countries still use the 3kV DC reticulation system on their railways, resources specific to this issue is hence limited.

Table 1: Lineside Transformer Characteristics

Parameter	**Value**
Un	25kV
Um	27.5kV
BIL	52kV

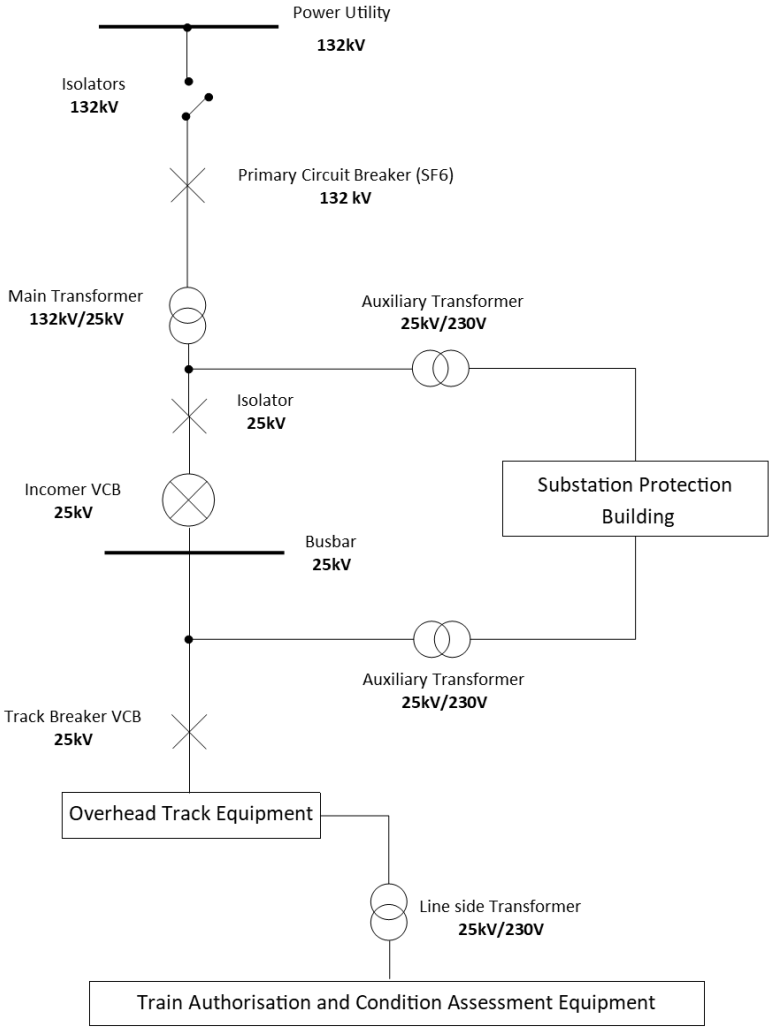

Figure 4: Rail Network AC Traction Substation Power Flow [5]

The auxiliary transformer provides power to the auxiliary power supply, used for the lighting inside the traction power substation building, which houses the protection intelligent electronic devices [8].

Another important component of the electrical infrastructure is the changeover yard. Since South Africa has both AC and DC traction systems, a section of rail between these systems needs to hold the capability of switching to either system when the need arises [2].

2.2 Locomotive Traction Converters

Locomotives are used to haul coaches or wagons containing different commodities. They form the basis of transportation for the train and can be completely electrically driven, diesel driven, or hybrid diesel electric. For the purpose of this investigation, AC powered locomotives are outlined, since this is the type of traction power being surveyed.

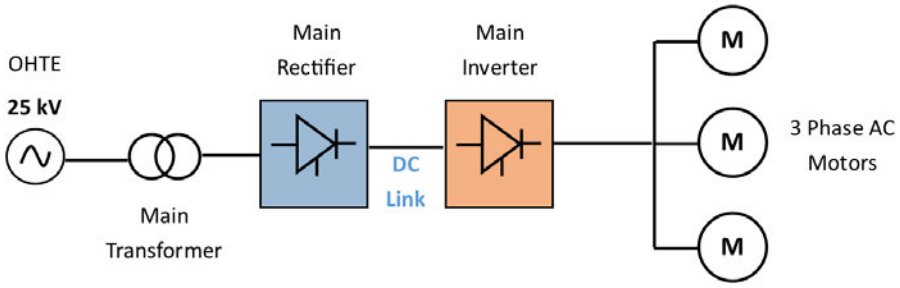

Figure 5: General illustration of AC Locomotive Power conversion

The locomotive is energised through the pantograph, obtaining power from the contact wire. There is usually more than one pantograph on a locomotive, a skid/skate, which forms the point of interaction between the pantograph and OHTE. AC motors are used in almost all newly designed locomotives, due to their low maintenance characteristic. The internal circuitry follows the AC to DC, back to AC power conversion.

The flow of power to a locomotive is as follows, current flows from the OHTE through the pantograph to the locomotive transformer. Here, the voltage is stepped down, and rectified to the DC link, required to power all internal DC components. Next, the power flows through the main inverter, and is converted back to AC to power the three phase AC motors. The bonded rails form part of the return circuit back to the traction substation.

Four-quadrant converters are typically used in modern locomotives, since they can deliver power in either direction, which makes them ideal for applications, where regeneration is concerned. Harmonics in the AC input can be easily controlled by adjusting the switching frequency accordingly.

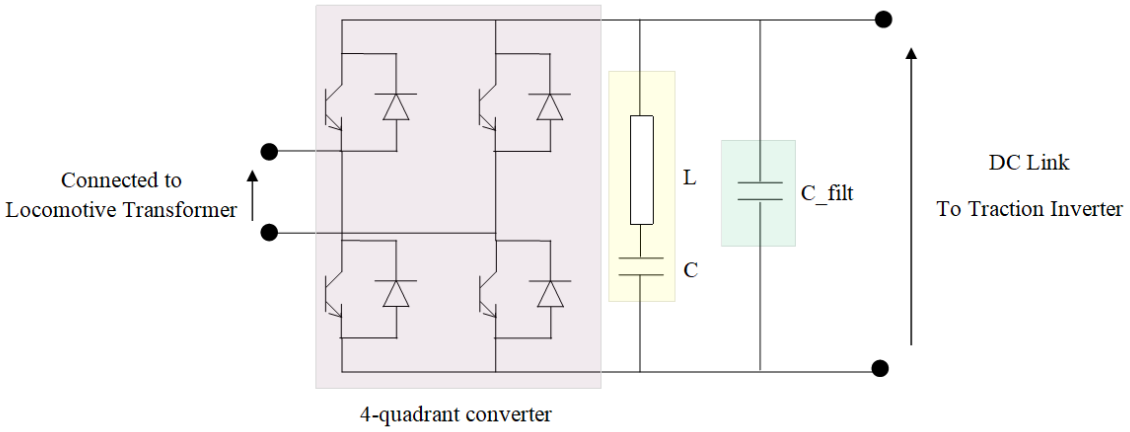

Figure 6: 4-quadrant converter circuit [9]

The converter circuitry has inductance *L* and capacitance *C*, representing the second harmonic filter. The main filter capacitor is shown as *C_filt*.

The switching devices considered for this investigation are the diodes, GTO thyristors and IGBT's. The railway industry internationally has moved towards implanting IGBT's instead of GTO's due to its efficiency, especially at higher frequencies. This significantly reduces the current required during operation and reduces noise due to traction [10], [11].

2.3 Power Quality Issues

The issue of power quality supply to the train can be largely attributed to the constant change in operation mode. This includes powering up and down of the locomotives, coasting (travelling at a steady speed with a constant load) on a flat gradient, and the regeneration of power through braking or travelling on a descending gradient.

Three notable power supply disturbances in the context of the traction power system are harmonic waveform distortion, oscillatory transients and overvoltages.

2.3.1 Harmonic Waveform Distortion

Harmonic waveform distortion is defined as the disturbance in the fundamental sinusoidal waveform at multiples of the fundamental frequency. Modern locomotive converters will emit these harmonics depending on the switching frequency and the configuration of the power electronics.

The OHTE is seen as a distributed RLC circuit. Due to this characteristic the network can experience resonances which accentuate harmonics in the reticulation. The presence of harmonic voltages in the system is also dependent on the strength of the system. A low fault level on long lines means that the harmonics are larger than on a system with a high fault level [12] [13] [14].

The amount of distortion can be quantified by the following equation, referred to as the total harmonic distortion (THD) [14]:

$$\%THD = \frac{\sqrt{\sum_{n=2}^{\infty}(V_{n_{RMS}})^2}}{V_{fund_{RMS}}} X\ 100 \quad (1)$$

Where, n is the harmonic order, V_{n_RMS} is the RMS voltage of the corresponding order and V_{fund_RMS} is the fundamental RMS voltage of the signal sample.

2.3.2 Oscillatory Transients

Oscillatory Transients, this refers to the change in a signal's voltage (or current) and usually occurs when a load is turned off and on. Modern locomotives do this over a neutral/ dead section, where magnets are responsible for switching the locomotive off, preventing a flashover. These transients may affect lineside equipment [14].

2.3.3 Overvoltage's

Overvoltages, are steady state increases in the voltage. Modern locomotives allow for regeneration in the region of 3%, which attributes to the locomotive loading. These overvoltages may affect lineside transformers where the tap changer settings are incorrect, and a non-linearity may occur as the voltage would be closer to the non-linear region of operation [12] [13] [14].

2.3.3.1. Regeneration

Typical motor operation is classified by the conversion of electrical energy to mechanical energy, this is when the motor turns at a speed slower than that of the speed set by the applied frequency, at the motor shaft. However, when the rotor turns faster than the synchronous speed of the motor, the mechanical energy from the motor shaft is transformed into electrical energy and this condition is referred to as regeneration.

A trains regeneration occurs when a locomotive is either coasting or braking. The term coasting refers to the train driver operating the train on a downward gradient, without accelerating. The train's locomotives, coaches, and wagons are being transported with the existing inertia possessed by the train [14] [15].

2.3.4 Interferences

The process of transmission and distribution of power in the railway environment cannot proceed without experiencing interferences which result in unwanted power losses. The following is a list of the most common interferences found in railway systems [16].

- Conductive interference –The voltage increases due to short-circuit or operational currents flow to the earth near the track and at substations earth-mat, this is determined by the substation earthing resistance and by the current flowing through the resistor. These voltages could cause problems, such as potential differences in the vicinity of the substation. Designing adequate return circuits will minimise stray currents by properly insulating the rails and return cables to the traction substation.

- Inductive interference – Electrical and magnetic fields around substations and on OHTE cause these interferences, which induce voltages and currents in signalling and technical equipment. The alternating magnetic field generated by the operating current of AC railway systems as well as by the higher harmonics, can induce voltages. The harmonics here are mainly caused by frequency converters on locomotives and in substations, and by transformers. It should be noted that resonance can be generated by harmonics on the OHTE.

  In transformers, saturation effects lead to magnetic flux which diverges from a precise sine wave. In power electronic circuits, switching characteristics produce higher voltage harmonics at various frequencies.

- Capacitive interference – Causes voltages in isolated unearthed conductors close to OHTE and could lead to voltages being dangerous to living beings who are in contact.

- High frequency emissions – occur from arcing between the contact wire and pantographs, as well as over neutral sections [16].

2.4 Transformers

2.4.1 Transformer Background

The transformer usually comprises of two or more electric circuits, which is coupled by a common magnetic circuit and is hence used in power generation and transfer. The fundamental operation of the transformer is that if the primary winding is connected to an AC power source, then dependent on the frequency and amplitude of this applied voltage, a magnetic flux will be induced, which will in turn introduce a voltage in the secondary winding of the transformer [17].

An ideal transformer and load are depicted in the Figure 7 below, where the symbols and corresponding parameters are indicated in the table below.

Table 2: Ideal Transformer Parameters

Symbol	Parameter
v_1	Primary Voltage (V)
i_1	Primary Current (A)
N_1	Number of Primary winding turns
v_2	Secondary Voltage (V)
i_2	Secondary Current (A)
N_2	Number of Secondary winding turns
Φ	Core flux (Wb)

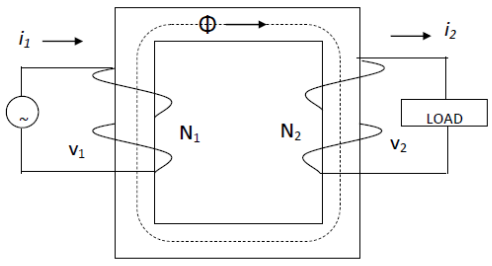

Figure 7: Ideal Transformer [17]

For practical scenarios, the alternating flux links with the secondary windings and an emf is induced on the secondary side. And can be calculated according to the equation below.

$$e_2 = 4.44 * f * N_2 * \Phi m \quad (2)$$

Where, *f* refers to the frequency of the secondary voltage.

2.4.2 Transformer Losses

Generally, transformers possess an efficiency which exceeds 95%, however the remaining transformer losses can be described as the no-load/ excitation loss, also referred to as the core loss and load loss/ impedance loss. These components collectively represent the total loss of the transformer.

$$P_{Total} = P_{Core} + P_{Load\ Loss} \ (3)$$

Where, P_{Total} is the total loss in watts, P_{Core} is the no-load loss and $P_{Load\ Loss}$ is the loss due to the load.

The load loss can further be divided into three components, the copper losses, or winding loss or eddy-current loss and stray loss due to the core clamps, magnetic shields and other components within the transformer.

$$P_{Load\ Loss} = P + P_{EddyCurrents} + P_{Stray} \quad (4)$$

Where, $P_{Load\ Loss}$ is the load loss, P is the copper loss, $P_{EddyCurrents}$ are the eddy-current losses and P_{Stray} represents the stray losses [18].

2.4.3 The effect of Harmonics on Transformers

Harmonic currents contribute to various loss components in transformers, which are subsequently transferred to the load side. The following are some of the main constituents.

- The RMS load current is increases, which is turn results in an increase in the copper losses.

- Excessive winding losses are experienced causing an increase in the eddy-current loss. This eventually leads to a rise in the winding temperature and may result in overheating.
- The stray losses will increase at a rate proportional to the square of the load current.
- Harmonic currents usually have a DC component, and these will affect the transformer by increasing the core loss marginally. It will also increase the magnetising current. It will also cause affect the top oil rise in liquid-filled transformers [19].

3 Literature Review

3.1 Harmonics

Vo, Palecek and Kolar [20] explored the effect that AC Traction have on harmonic distortion in a 110kV voltage supply network. The analysis discussion showed that odd harmonics from the 1st to the 19th were simulated and the results indicated that the 3rd, 5th and 7th current harmonics were the most prevalent. Thyristors were used as the switching component in the study. And all simulated results were found to be in line with IEEE 519-1992 (the edition available at the time of print) [20].

Hu *et al.*, [21] stated that harmonics are influenced by the power system, traction system and the locomotive control system. The length of the OHTE, impedance of the traction transformer and various other parameters contribute to the resonance. Installing filters on the locomotive or in the traction substation yard can be employed as harmonic suppression methods [21].

Siranec *et al.*, [22] discussed the power quality of electrical traction based in the Slovak Republic. It was found that the magnitude of 15th voltage harmonic order exceeded the expected results according to EN 50 160, due to the parallel resonance in the power line. At higher voltages, it was noted that there was a spread of current and voltage harmonics along the OHTE. From the results of the simulation, it can be stated, that when the traction vehicle is further from traction substation, the lower harmonic orders are higher [22].

3.2 Transformers

Transformers are important components of power supply systems. Non-sinusoidal loads connected to a transformer tend to increase the iron losses in the magnetic core. These are commonly referred to as harmonic loads and may seriously affect the transformer by increasing the eddy current losses, since eddy currents are larger at the end of the transformer windings. The increase in loss of current due to harmonics, influences the operating temperature of the transformer. Transformers required to supply loads which are non-linear in nature should be derated based on harmonic components in the load current and the eddy current loss [23].

3.3 Technical Standards

The following technical standards were researched and deemed relevant to the investigation under discussion.

3.3.1 NRS 048

NRS 048-2 [24] details the quality of supply specification of the power supply received from the power utility. According to this standard the maximum voltage of the 132kV feed is 145kV, which suggests a maximum of approximately 27.5kV at the secondary terminals of the Traction transformer. Hence, the expected maximum peak voltage at the primary side of the lineside transformer is approximately, 38.9kV.

3.3.2 IEEE 519

This standard outlines the harmonic limits in power systems at the point of common coupling, which for the purpose of this investigation, is at the traction substation. The voltage distortion limits for 132kV should reflect a maximum of 2%. However, it should be noted that for harmonic orders lower than 50 individual harmonic distortions should not exceed 1.5% [25].

3.3.3 SANS 780 and IEC 60076 – 3

The specification for single and three phase transformers immersed in oil are detailed in SANS 780 [26]. This standard indicates the insulation levels for a transformer with a nominal voltage of 33kV, which is the closest to the 25kV single phase transformer under test in this investigation. The withstand voltage according to the power-frequency test is at 70kV [27]. It should be noted, however that this applies to a three-phase transformer and although the standard is referenced in most railway specifications, the maximum nominal voltage covered by SANS 780 is 36 kV.

4 The Lineside Transformer

This chapter explores the specification of the lineside transformer for the purpose of this investigation. As stated previously, little literature on the design parameters of this transformer and its application exists. A model is hence developed by comparing the behaviour of a 32 kVA, 19 kV/2x240 V dual phase transformer to the known ratings of the lineside transformer. Possible changes that need to be made when specifying a lineside transformer is also evaluated, by looking at the range specified for the tap changers, and the magnetic flux design point of the transformer. As well as whether the insulation levels should be increased and the potential resonance of the transformer by measuring the frequency response.

This is done by detailing the experimental process and the model simulation explored to ascertain the specifications and behaviour of the single phase 16 kVA 25 kV/230V. This is primarily done, since there is a lack of information and engineering standards. Specifically, the design limits of the transformer affecting the magnetisation curve, while the saturation characteristics are scrutinised during this investigation under low and high voltage scenarios.

According to NRS 048-2, switching on the power utility network can cause a voltage change of less than 10% on medium voltage network. This is also applicable to the local plant network, which in this case refers to the traction substation. It can therefore be noted that the overvoltage and undervoltage experienced by the lineside transformer system is 27.5 kV and 22.5 kV, respectively.

It can be stated that these voltage variations can be minimized by adjusting the tap changer on the 132kV/ 25kV traction transformer, however the 10% voltage change is still present in the system due to the movement of trains and the switching operations onboard multiple locomotives.

On traction power systems the issue is that the voltage varies significantly more than this, as well as varying dynamically. Thus, the applicable of SANS standard specification may not be appropriate. Which, the lineside transformer will also be affected by. The seriousness of this issue can increase by the application of locomotives that have the capability to regenerate into the system.

There is a possibility of an increase in nominal voltage on the 25kV network which could range between 80% to 120% or from 20kV to 30kV. However, the specification for the tap changer on the lineside transformer at minimum and maximum is ± 5% of the nominal voltage. Hence, the tap changer needs to accommodate a much larger range of voltage. The intensity of the issue under discussion currently, may again increase if the tap changer were to be set to its extremities, as it is ill equipped by design to handle instances of risky overvoltage's. This is particularly concerning on the lowest setting where there is a possibility of a significant overload. Generally, in transformer specifications, tap changers are according to the user's requirement. The transformer's load, the signaling equipment, is fed through a UPS and as a result can handle a range of voltages.

4.1 Specifications of the Transformer

According to SANS 1019 (2017), low voltage is classified as anything below 1 kV and medium voltage is between 1 kV and 45 kV. The table below list the standard medium voltage information from 11 – 44 kV, the single-phase voltage for a 44 kV system, is 25 kV. As the traction power systems are single phase systems, this means that lineside equipment and insulation should be rated according to the 44 kV level.

According to various engineering standards for supply and transformers the following tables indicate the standard voltages of operation and insulation levels.

Table 3: Standards

Number	**Standard**	**Name**
A	SANS 1019	Standard voltages, currents and insulation levels for electricity supply
B	IEC 60076-3	Power Transformers- part 3: Insulation Levels, dielectric tests and external clearances in air
C	NRS 048-2	Electricity Supply – Quality of Supply

D	SANS 780	Distribution Transformers
E	NRS 054	Guidelines for the design of large power transformers up to 132 kV, in the rating range of 1.25 MVA to 16 MVA.
F	CEE0111.99	Spoornet – Specification for 25 kV AC Traction Substations
G	TI/SPC/PSI/AT/0200(03/2020)	Technical specification for 25kV/240V, 5kVA, 10kVA, 25kVA, 50kVA & 100 kVA, 50Hz, Single phase, oil filled auxiliary transformers for Indian railway AC traction system

Table 4: Standard operating voltages and Insulation levels

Un (kVrms)	**Um (kVrms)**	**Uphase (kVrms)**	**Rated Power-Frequency Withstand (kVrms)**	**LIWL (kV)**	**Present in Standards Numbered**
11	12	6.35	28	95	A, B, D, E
22	24	12.70	50	150	A, B, D, E, F
33	36	19.05	70	200	A, B, D, E
44	52	25.40	95	250	A, B, E, G

The exercise above was conducted to outline that there exists a lack of information available, specific to the 25 kV/230 V single phase transformers under investigation. Most railway engineering documentation refer to SANS 780, which stipulates the transformer specifications for up to a nominal voltage of 33 kV.

4.2 Development of a Transformer Model

The issue of the applied voltage fluctuations on the line, results in the lineside transformer experiencing overvoltage's on the high voltage side. A transformer model was developed to investigate the behaviour of medium voltage transformers and apply the outcome to the lineside transformer.

The issue of the applied voltage was explored, and an experiment was performed to compare the results to the simulated model developed using MATLAB, through transformer design first principles. The description and equipment used is detailed below.

4.2.1 Experiment

A 32 kVA, 19 kV/2x240 V dual phase transformer was used to develop the model of the single-phase transformer under investigation. The focus of the model was the supply voltage and the magnetising current.

The equipment used in the experiment includes:

- 32 kVA, 19 kV/2x240 V Dual Phase Transformer
- 2 x FLUKE 189 True RMS Multimeter
- 2 x FLUKE i30s AC/DC Current Clamp
- Pico Differential Probe TA 057
- 2.6 kVA, 230 V Variac
- FLUKE MDA-550 Motor Drive Analyzer
- 28 kV High Voltage probe
- 10 kVA 240V/480V Transformer

The experiment was conducted by supplying voltage onto the secondary (low voltage) winding of the 19 kV/2x240 V transformer using a 2.6 kVA Variac and a 10 kVA 240 V/480 V step up transformer. The step-up transformer was using to supply voltage across the whole secondary winding (up to 480 V). Figure 8 shows the transformer, step-up transformer and Variac.

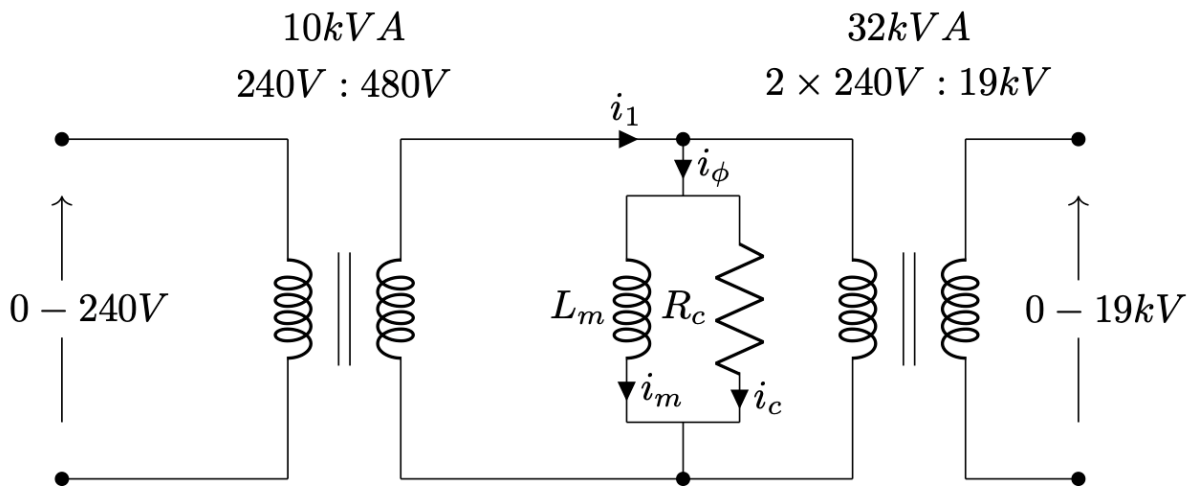

Figure 8: Experimental Circuit Diagram

The waveforms are of particular interest and the voltage across the low voltage winding was recorded using a differential probe (Picotech Differential Probe TA 057), while the current was recorded using a current probe. A Fluke motor drive analyser was used to record the waveforms as well as the power loss. The RMS voltages at the secondary and the primary windings were also recorded and can be seen in Table 5: Experiment ResultsTable 5. Pictures of the experimental setup are presented below.

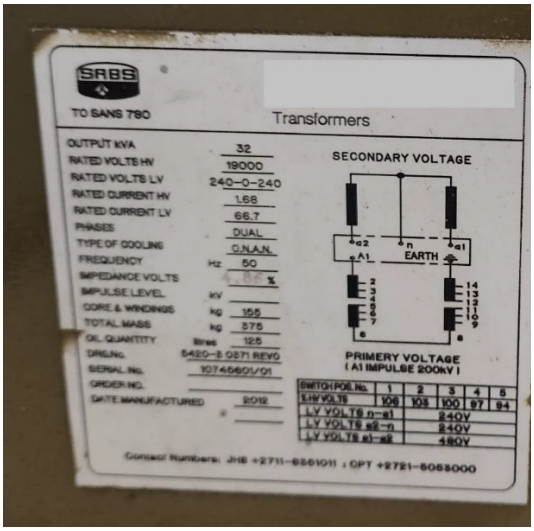

Figure 9: Transformer Name Plate

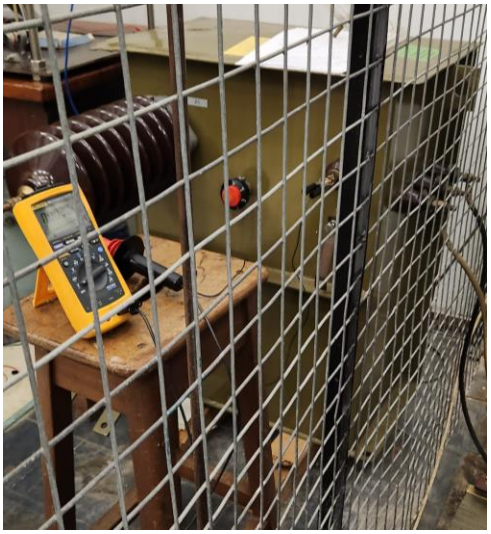

Figure 10: Transformer HV measurement during Experiment

Figure 11: Experimental Set up with Step up Transformer

Figure 12: Variac used in Experiment.

Figure 13: Motor Drive Analyser

The results obtained from the experiment are presented below, as well as the measured waveforms at approximately 65% and 100% of the rated low voltage output of the transformer.

Table 5: Experiment Results

LV (V)	I2rms (A)	Power (W)	HV (kV)
128	0,0682	8,7	5,167
240	0,1269	29,5	9,66
299	0,2123	48	12,11
327	**0,3126**	**60**	**13,25**
403	0,8423	110	16,31
420	1,0327	120	16,98
444	1,4289	150	17,91
471	2,1691	200	19,06
480	**2,5043**	**220**	**19,41**

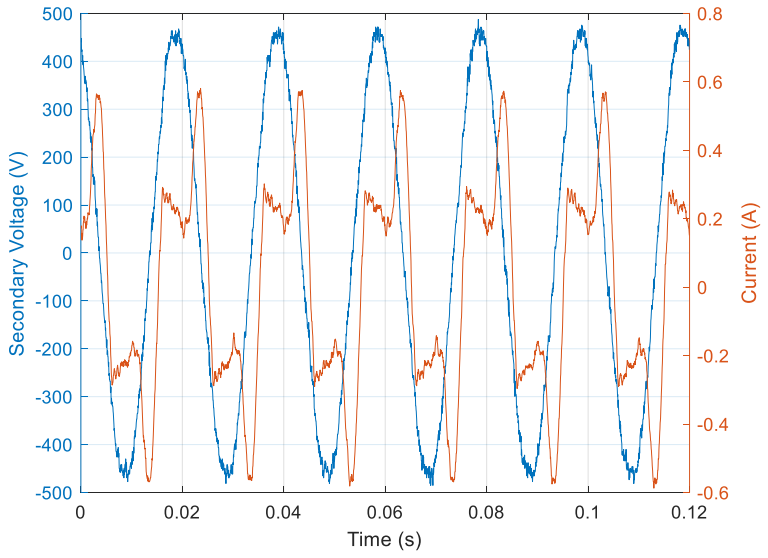

Figure 14: Measured Voltage and Current on the Secondary side at 327V

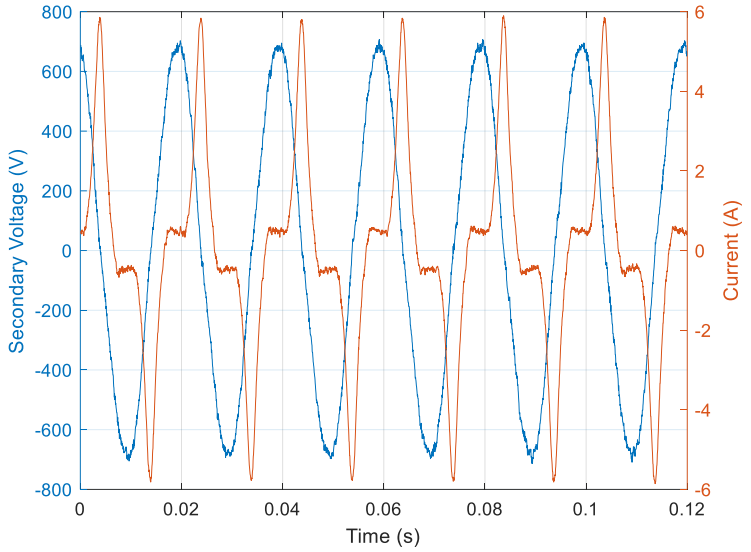

Figure 15: Measured Voltage and Current on the Secondary side at 480V

Figure 14 and Figure 15 show a sinusoidal voltage in blue and the current in red. The current consists of two components, the core loss current and the magnetising current. The core loss current is linear, while the magnetising current is non-linear and is dependent on the design of the transformer. By examining the behaviour of experimental transformer, it is noted that minor disturbances in the waveforms exist. Considering that under load conditions the secondary side of the transformer will be connected to a UPS, any amplification to these disturbances can be considered negligible.

4.2.2 Model

A model of a distribution transformer was formed in order to investigate important design aspects of the line side transformer such as the magnetic flux design point and the impact of overvoltages. This was developed from basic design equations and available information. The behaviour of a transformer is largely determined by the core, which refers to the material type and the size of the core. Considering the fundamental machine equation [17], the size of transformer core is inversely proportional to the magnetic flux.

$$E = 4.44\ x\ f\ x\ B\ x\ A\ x\ N \quad (5)$$

Transformer manufacturers have developed their designs to optimise the amount of material used in the transformer and can use a magnetising point that is relatively high to reduce the overall cost of the transformer.

The method used to develop a model of the transformer to match the experimental results is shown in the figure below. Note: It was not expected to be a perfectly designed transformer, however the model has been developed to investigate key parameters that may would to be better specified.

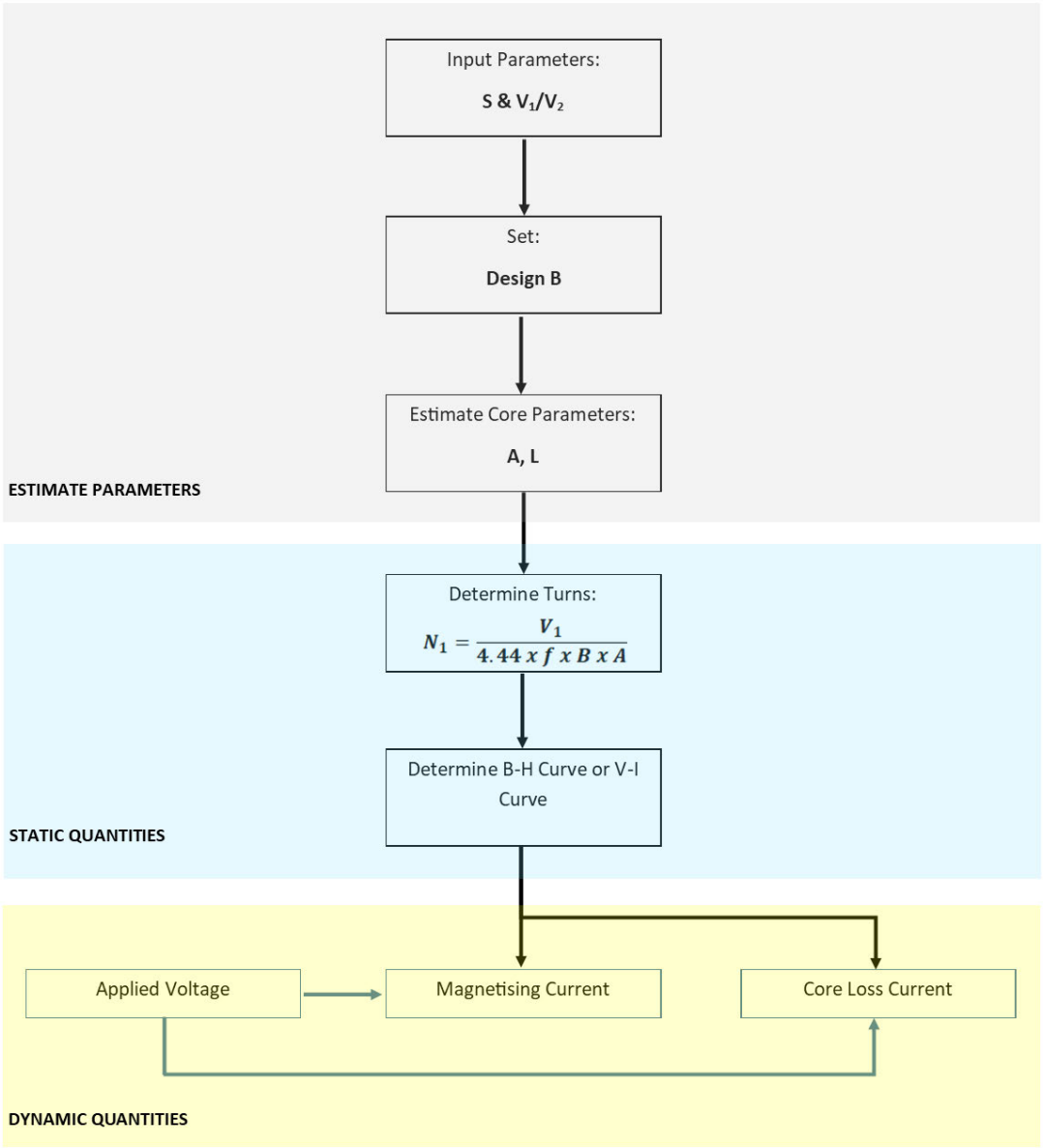

Figure 16: Flow Diagram of Model development

The following table lists the parameters used in the figure above.

Table 6: List of Parameters and Symbols used in Flow Diagram

Symbol (SI Unit)	**Parameter**
A (m^2)	Area
L (m)	Length
M (kg)	Mass
v (m3)	Volume
N	Number of Turns
B (T)	Magnetic Flux Density
H (W/ m^2)	Magnetic Flux Intensity
f (Hz)	Frequency
V_1 (V)	Primary Voltage

An iterative method was used to best align to the measured data, using a 32kVA 19kV/2x240V.

The B-H curve which is used to describe the magnetic properties of M-5 Steel is shown in Figure 17. The B-H curve was derived from the AK Steel M-5 grain oriented steel [28]. Clearly, the material can be seen to reach saturation at a flux density of approximately 2 T. The typical core loss values of the steel are 0.89 W/kg at 1.5 T and 1.3 W/kg at 1.7 T. The transformer model used a design flux density, B, of 1.7 T to ensure that the transformer was close to the knee point of the B-H curve.

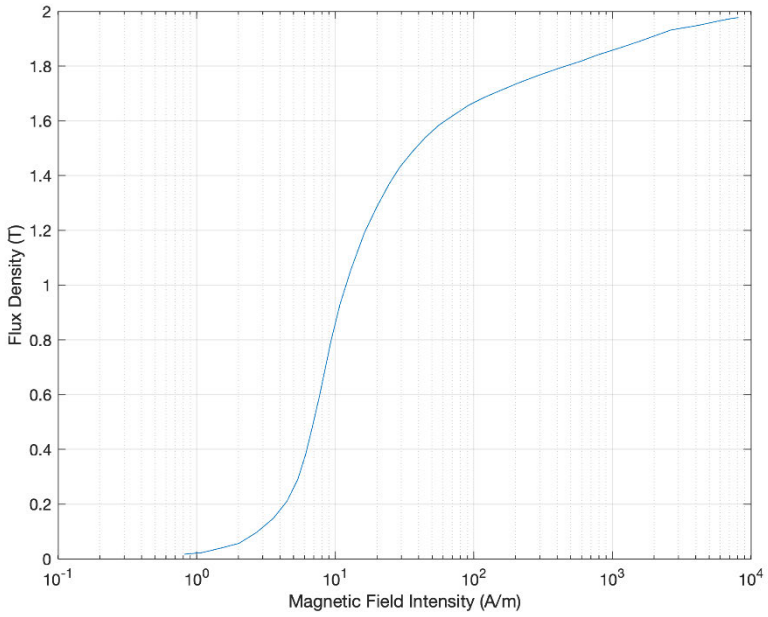

Figure 17: B-H Curve of M-5 Electrical Steel of 0.012 thickness

The area of the core was estimated using the following equation [29]:

$$A = \frac{\pi d^2}{4}\ x\ 0.95 \quad (6)$$

Where 0.95 is the fill factor for the core, which is the ratio between the magnetic and non-magnetic material in the core.

The dimensions of the core were adjusted to including length of the core. The area and length were iterated through a few times to better fit the measured information.

The number of turns were estimated from the fundamental machine equation (5) and were set. These were also adjusted to better fit the measured information.

The number of turns and dimension of the core for the static design parameters were used with the varying voltage to look at the waveshape of the current for the applied voltage. The dimensions of the core were also used to determine the core loss current.

It is important to note that the developed transformer model was implemented using MATLAB, and the corresponding code can be found in Appendix A.3. Transformer Model. MATLAB was also used to analyse the acquired transformer model. To match the experiment, the same applied voltages were used and a comparison of the results are shown in Table 7 and Figure 21: V-I curve for Measured and Simulated Current.

Table 7: Comparison of Measured and Model Results

LV (V)	Measured I2 (A)	Simulated I2 (A)	HV1 (kV)
128	0,0682	0,1311	5,167
240	0,1269	0,1901	9,66
299	0,2123	0,2405	12,11
327	**0,3126**	**0,2757**	**13,25**
403	0,8423	0,4924	16,31
420	1,0327	0,6079	16,98
444	1,4289	0,9269	17,91
471	2,1691	2,2959	19,06
480	**2,5043**	**3,3396**	**19,41**

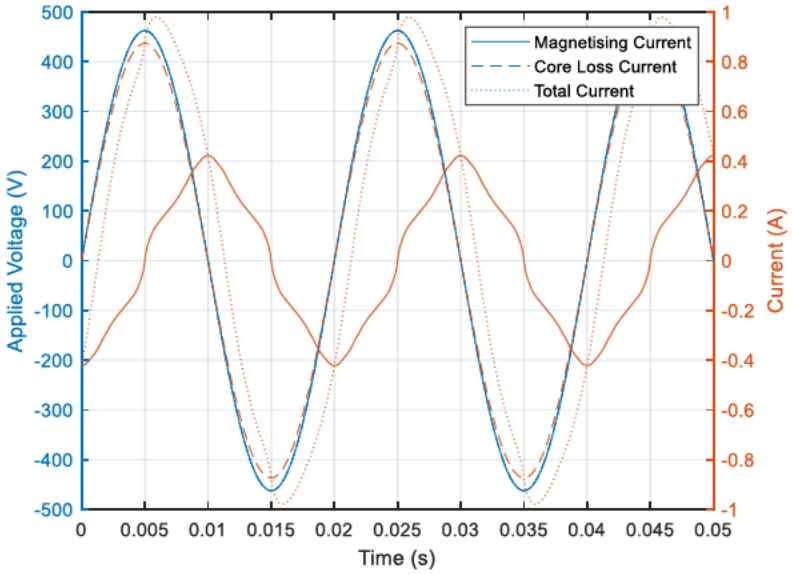

Figure 18: Model Voltage and Current on the Secondary at 327V

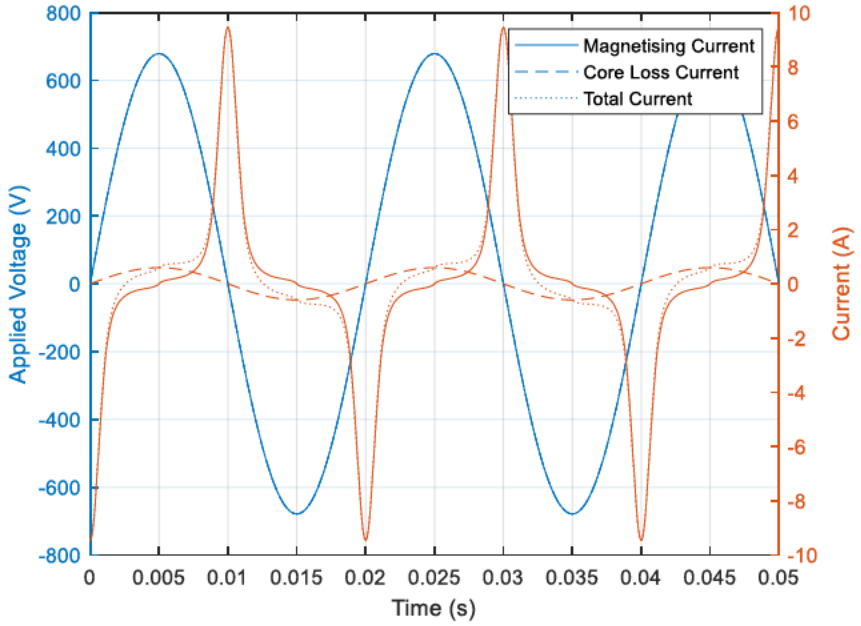

Figure 19: Model Voltage and Current on the Secondary at 480V

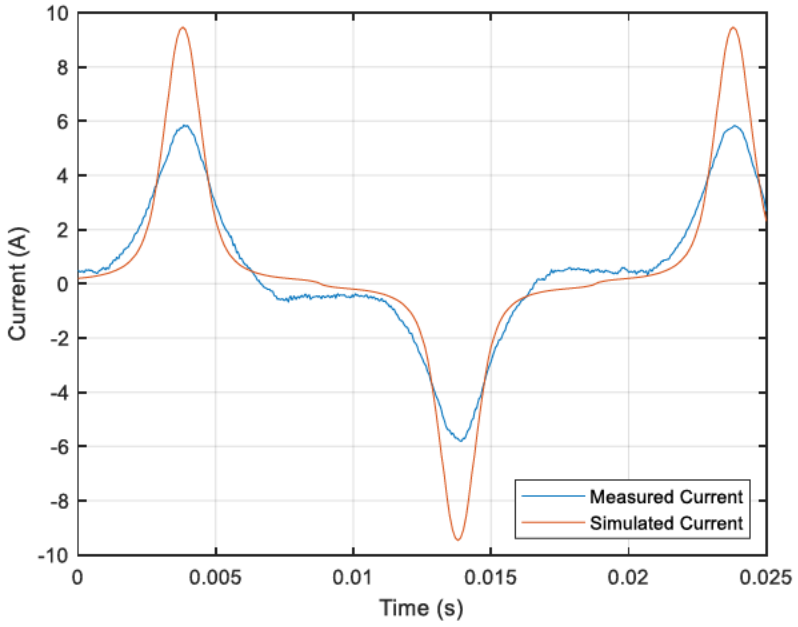

Figure 20: Measured Current vs Simulated Current at 480V

The following V-I curve was obtained using the voltage and the current on the secondary side of the transformer. The non-linear shape of the curve is similar to that of a B-H curve for typical steel material used in transformer cores.

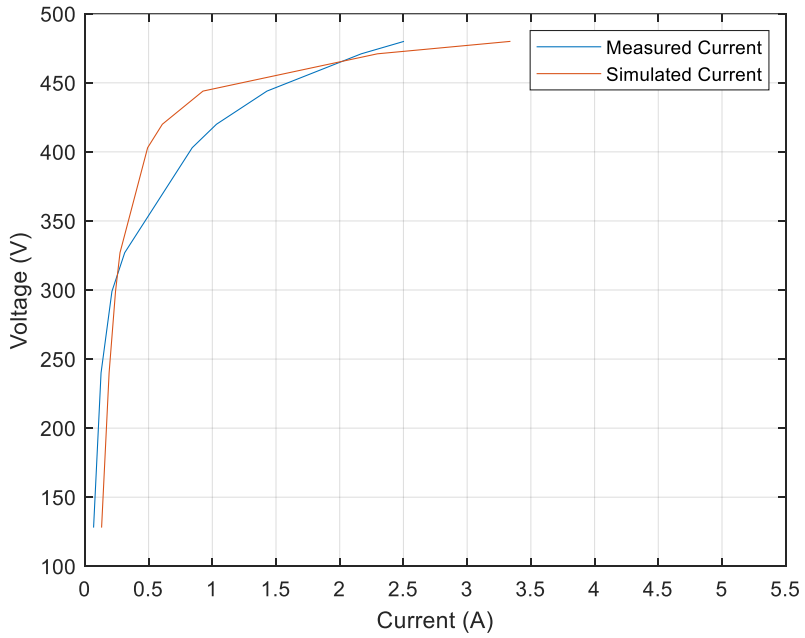

Figure 21: V-I curve for Measured and Simulated Current

4.2.2.1 Conclusion

The model was developed to determine the design parameters of the lineside transformer. Specifically designed for the 25 kV railway power system and did not consider the load conditions, as the signal equipment, representing the load, is first connected to a UPS. This allows the load side to remain stable and has a miniscule effect on the transformer. The results are not a perfect match and has an approximate error of 7%, as noted on Figure 21. As the model approaches the rated voltage the error reduces to 5%. This was the region of interest and was considered a suitable model to use.

4.3 Analysis of Lineside Transformer with Transformer Model

Now that the transformer model has been developed, the outputs of flux density, applied voltage and magnetising current can be analysed. To demonstrate possible inclusions in the future specification of the transformer, the 16 kVA, 25kV/230V lineside transformer under investigation was analysed according to the following cases,

- Case 1: Specified 25kV lineside transformer with tap changers set to 0%, -5%, and +5% at B = 1.7T.
- Case 2: Specified 25kV lineside transformer with tap changers set to - 10% and +10% at B = 1.7T.
- Case 3: Specified 25kV lineside transformer with tap changers set to 0%, -5% and +5% at B = 1.6T.
- Case 4: Specified 25kV lineside transformer with tap changers set to 0%, -5%, and +5% at B = 1.5T.

The tap changer was firstly varied whilst the flux density of the transformer remained at 1.7T. this was done to analyse the magnetising current at the most extreme case possible which, would be under overvoltage conditions at the lowest tap position. The flux density is then reduced to determine whether the specified transformer can operate comfortably at a lower design level which suggests a lower volume of core material will be required. This will largely affect the cost if the transformer, as well as the overall weight.

The process explained above is followed to obtain the following plots. The number of turns needed to be altered in the transformer model, since the rating of the transformer has now changed.

Table 8: Over and under voltage multiplication factors used for various tap changer settings.

Tap (%)	Tap Voltage (kV)	Over Voltage Factor	Under Voltage Factor
0	25.00	1,2	0,80
-5	23.75	1,26	0,84
+5	26.25	1,14	0,76
-10	22.50	1,33	0,89
+10	27.50	1,09	0,73

4.3.1 Case 1: Specified 25kV lineside transformer with tap changers set to 0%, -5%, and +5% at B = 1.7T.

During the first case, the lineside transformer was designed to the core flux density level of 1.7 T. This was done to induce the most extreme boundaries of the transformer and determine the behaviour of the saturation characteristics and the magnetising current. Firstly, the number of turns needed to be calculated, which was simulated by comparing the ratings of the 32kVA, 19kV/2x230V. The number of primary turns was found to be 5578. This was used to simulate the model at different tap changer settings. The absolute over voltage for the lineside transformer was 30kV and the under voltage, 20kV. The ratios used for these limits are stated in Table 8.

Figure 22 shows the Flux density versus magnetising current curve (BI Curve) for the simulation case where the operating voltage is set to 25kV, it is seen that the transformer saturates before it reaches the over voltage condition of 30kV. The next set of plots, Figure 23 depicts the applied voltage and magnetising current waveforms, where it is affirmed that the transformer set at 25kV saturates, as noted by the broken-line magnetising current plot.

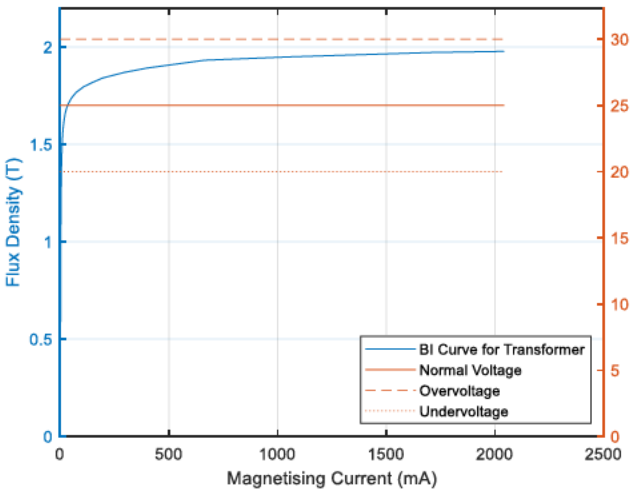

Figure 22: BI Curve for tap set at 0% and B = 1.7T

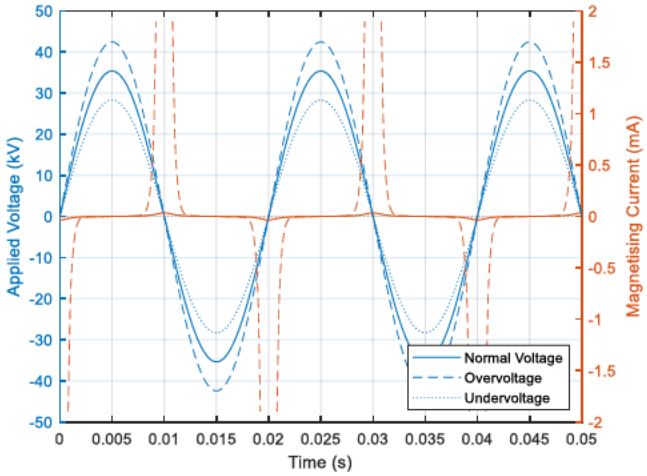

Figure 23: Applied voltage and magnetising current for tap set at 0% and B = 1.7T

The BI curve in Figure 24 also shows that the transformer saturates, reaching the over voltage condition quicker than the previous results, and this is largely due to lower operating voltage. This is also apparent from Figure 25, which also shows an increase in magnetising current.

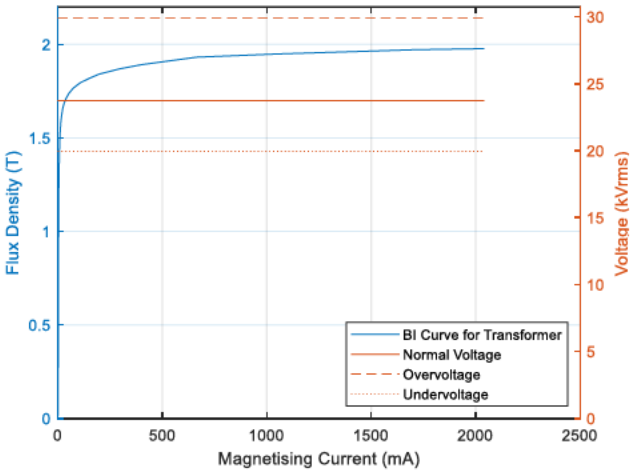

Figure 24: BI Curve for tap set at -5% and B = 1.7T

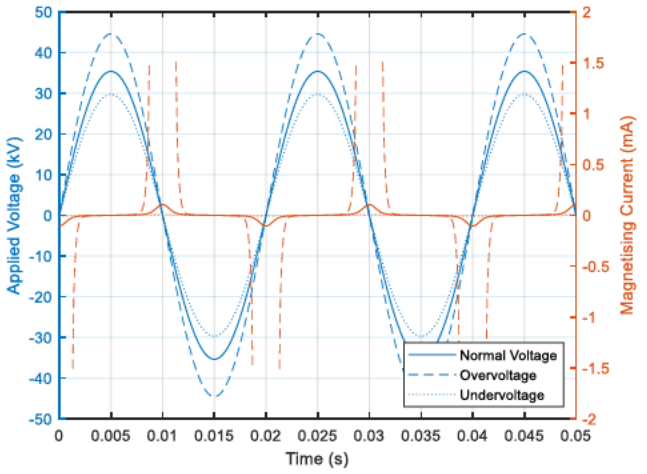

Figure 25: Applied voltage and magnetising current for tap set at -5% and B = 1.7T

The following graphs are obtained by simulating the transformer model at a tap changer setting of +5%. According to Figure 26 the transformer can function at the overvoltage condition and not saturate before

reaching it. Figure 27, show that for this case, the magnetising current is the lowest and this is mainly due to the higher operational voltage.

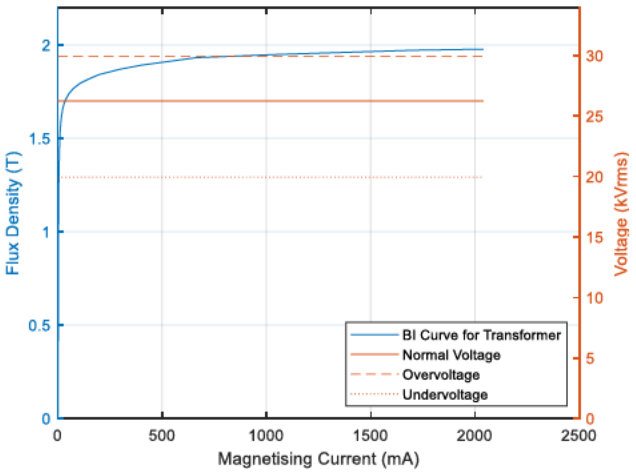

Figure 26: BI Curve for tap set at +5% and B = 1.7T

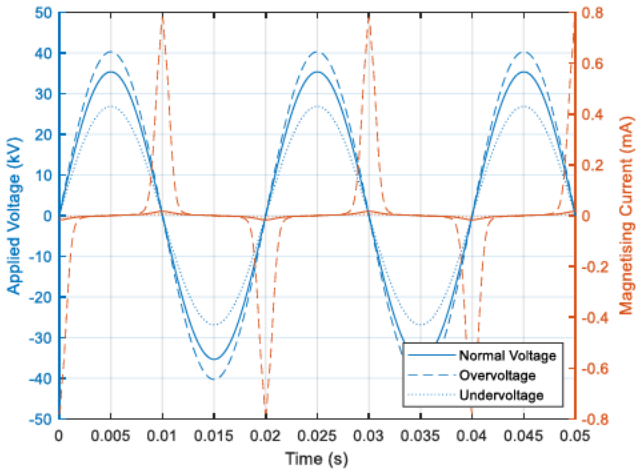

Figure 27: Applied voltage and magnetising current for tap set at +5% and B = 1.7T

4.3.2 Case 2: Specified 25kV lineside transformer with tap changers set to - 10% and +10% at B = 1.7T

Here, the flux density remained at 1.7 T and the transformer was simulated at -10% and +10% tap changer settings. It is again noted that at -10%, illustrated by the BI curve in Figure 28 and the magnetising current waveforms in Figure 29, that the transformer becomes saturated under over voltage conditions. The magnetisation current has also increased significantly, and this is largely due to the increase in core losses.

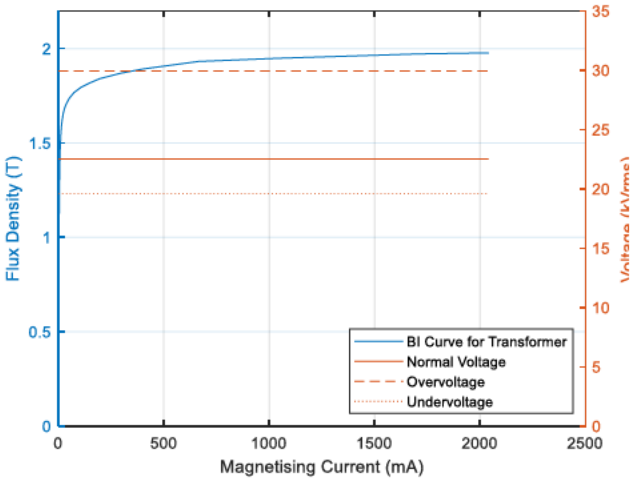

Figure 28: BI Curve for tap set at -10% and B = 1.7T

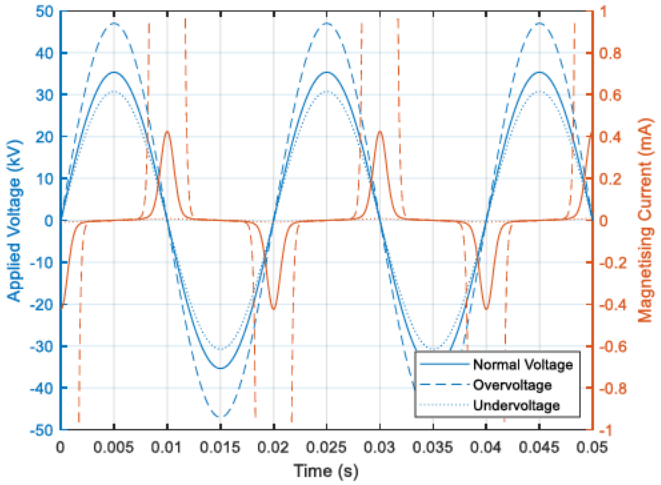

Figure 29: Applied voltage and magnetising current for tap set at -10% and B = 1.7T

Figure 30, below shows the BI curve of the transformer model simulated at the operating voltage of 27.5kV. It shown that the model is able to perform comfortably at 30kV. And that the magnetising current is the lowest at this designed flux density level.

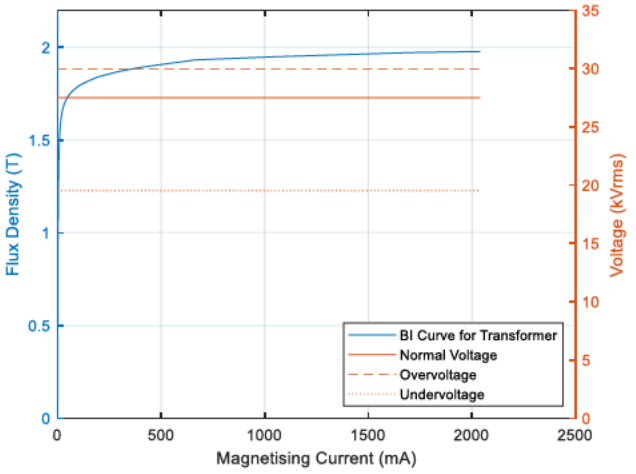

Figure 30: BI Curve for tap set at +10% and B = 1.7T

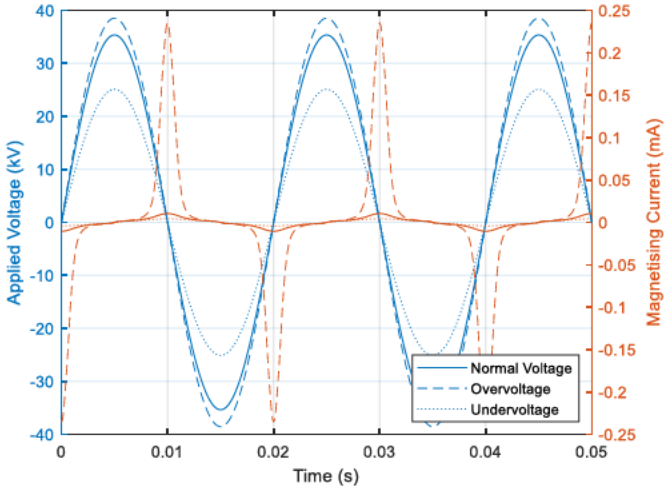

Figure 31: Applied voltage and magnetising current for tap set at +10% and B = 1.7T

4.3.3 Case 3: Specified 25kV lineside transformer with tap changers set to 0%, -5% and +5% at B = 1.6T

For the next case, the flux density is set to 1.6 T, and as a result, the number of turns will need to be recalculated. Following the same method as the first case, the number of primary side turns for this transformer was found to be 5928. The increase in number of turns, can be substantiated by Faraday's Law of Induction, which states that a changing magnetic flux induces and emf in a coil [17]. Since the specified flux density has been reduced (thus, the change in flux through one turn per unit of time) and the emf kept the same, the number of primary turns has increased.

As noted by Figure 32 and Figure 33, is it shown that the transformer does not saturate at an operating voltage of 25kV and the magnetising current is significantly low, which is desirable.

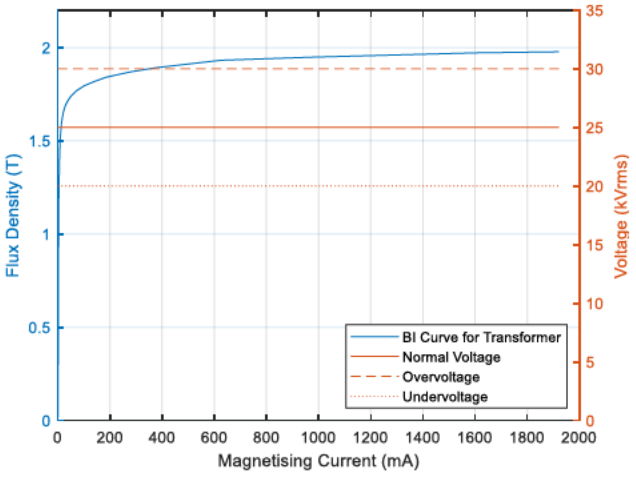

Figure 32: BI Curve for tap set at 0% and B = 1.6T

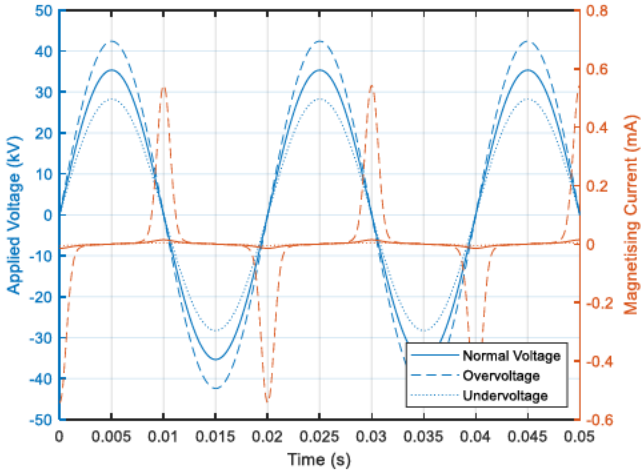

Figure 33: Applied voltage and magnetising current for tap set at 0% and B = 1.6T

The BI curve in Figure 34, below clearly shows the behaviour of the transformer at a flux density of 1.6T and an operating voltage of 23,75kV, with both over and under voltage limits. Figure 35 shows the magnetising current is lower than that of the simulation at 1.7 T, however, the transformer still tends to saturate.

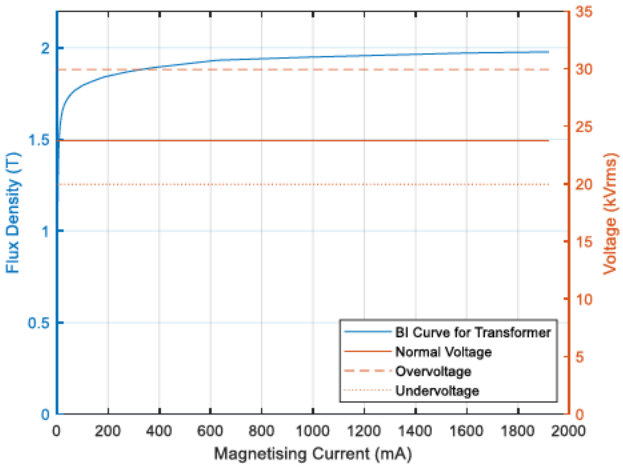

Figure 34: BI Curve for tap set at -5% and B = 1.6T

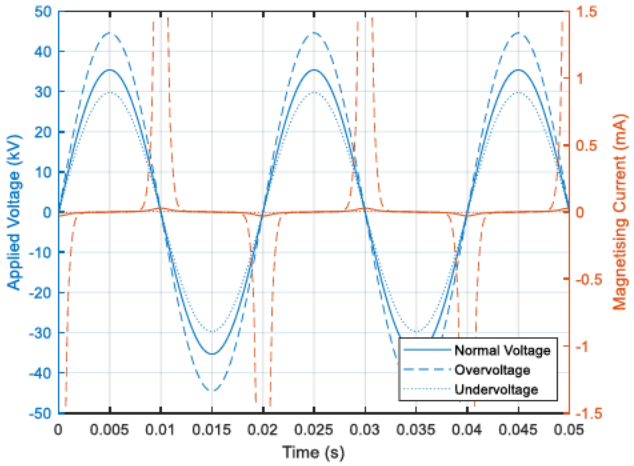

Figure 35: Applied voltage and magnetising current for tap set at -5% and B = 1.6T

Figures 36 and 37, indicate that at a tap changer setting of +5% the transformer model has a much lower magnetising current, which is required for this investigation. The transformer is also able to function within the design limits.

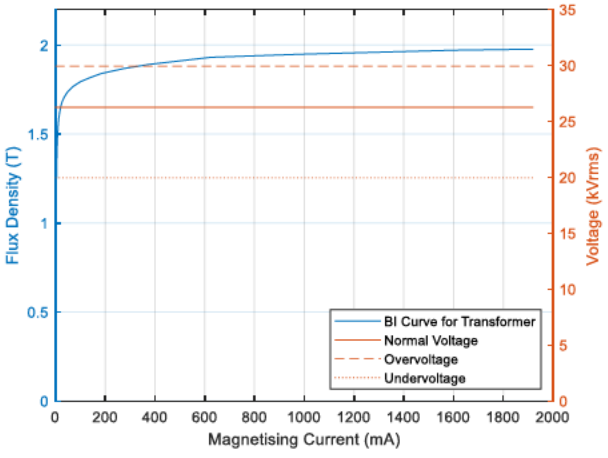

Figure 36: BI Curve for tap set at +5% and B = 1.6T

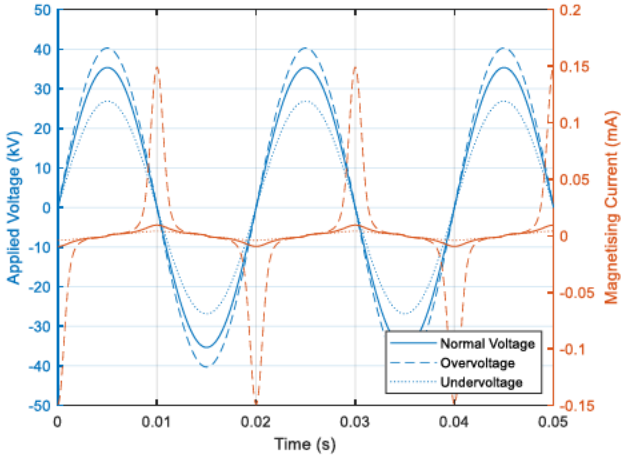

Figure 37: Applied voltage and magnetising current for tap set at +5% and B = 1.6T

4.3.4 Case 4: Specified 25kV lineside transformer with tap changers set to 0%, -5%, and +5% at B = 1.5T

The flux density was decreased to 1.5 T and the number of primary turns were determined to be 6338. According to the waveforms obtained from simulating the transformer model to the corresponding parameters in Table 9, it is noted that transformers does not saturate at any of the tap changer settings under discussion. This suggests that it would be prudent to consider specifying that the lineside transformer be manufactured at a magnetic flux density of 1.5 T, or lower, without compromising the integrity of the transformer and the cost.

The figures below show the BI curve, applied voltage and magnetising current plots at operating, under and over voltage conditions. It is evident that the simulated transformer set at an operating voltage of 25kV, does not saturate when the flux density is lowered to 1.5T.

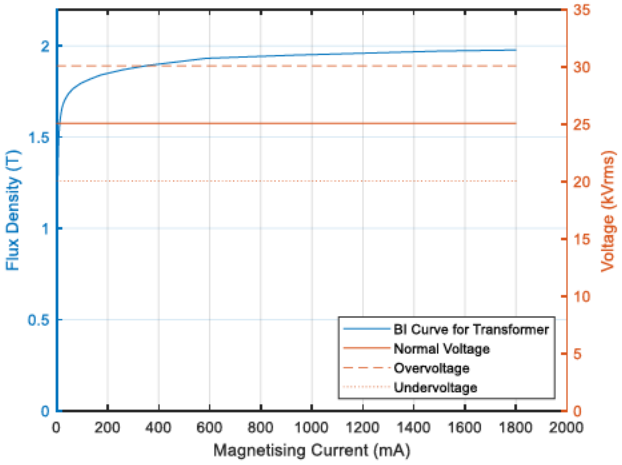

Figure 38: BI Curve for tap set at 0% and B = 1.5T

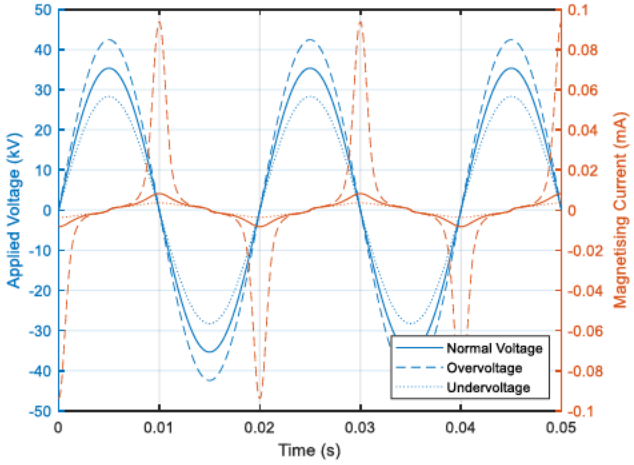

Figure 39: Applied voltage and magnetising current for tap set at 0% and B = 1.5T

Figure 40 shows the BI curve of the simulated transformer at an operating voltage tap changer setting of -5%, the transformer can operate sufficiently between the over and under voltage limits set for the transformer. Further to this, Figure 41 indicates that the transformer does not saturate and has much higher magnetising current, than the previous set of figures. This is consistent with the decrease in operation voltage.

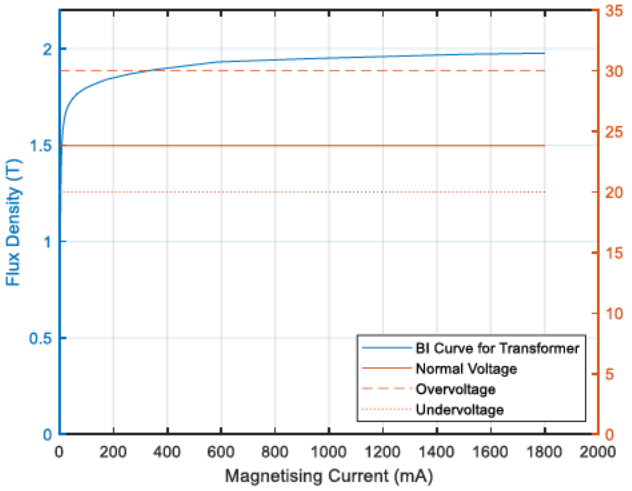

Figure 40: BI Curve for tap set at -5% and B = 1.5T

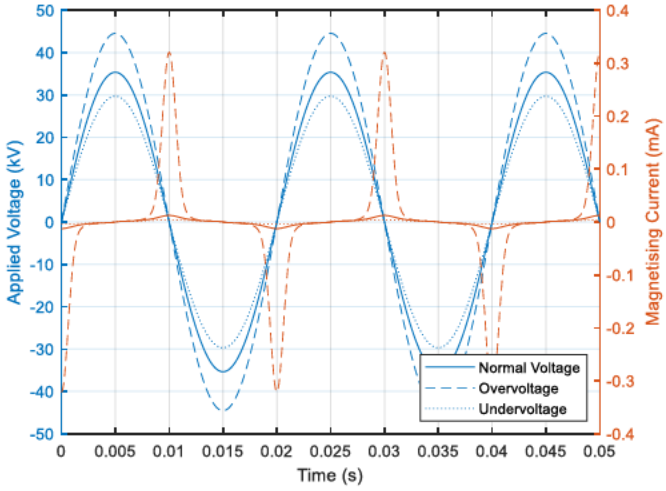

Figure 41: Applied voltage and magnetising current for tap set at -5% and B = 1.5T

The final plots for this case, below, show that the at a tap changer setting of +5%, the transformer does not saturate and is able to function within the required maximum and minimum limits. The magnetising current is noted to be much lower than the previous cases, at this voltage.

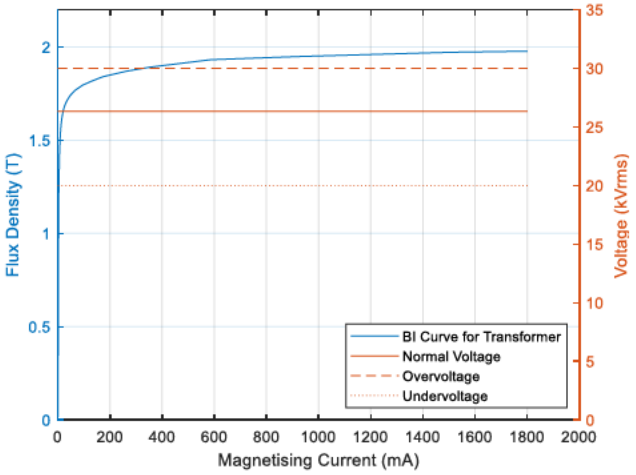

Figure 42: BI Curve for tap set at +5% and B = 1.5T

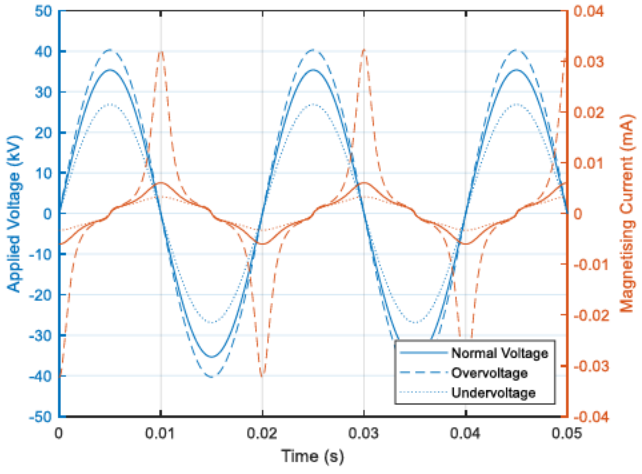

Figure 43: Applied voltage and magnetising current for tap set at +5% and B = 1.5T

4.3.5 Summary of Results

The results of the various simulated cases are tabled below, with reference to the waveforms obtained during the exercise.

Table 9: Comparison of Results

B (T)	Tap (%)	Operating Voltage (kV)	Over Voltage (kV)	Under Voltage (kV)	Magnetising Current (mA)	Number of Turns	Saturated
1,7	0	25,00	30,00	20,00	1,42	5578,00	Yes
	-5	23,75	29,92	19,95	3,82	5299,10	Yes
	+5	26,25	29,92	19,95	0,79	5856,90	No
	-10	22,50	29,92	19,57	14,83	5020,20	Yes
	+10	27,50	29,97	19,52	0,55	6135,80	No
1,6	0	25,00	30,00	20,00	0,75	5928,00	No
	-5	23,75	29,93	19,95	1,31	5631,60	Yes
	+5	26,25	29,93	19,95	0,54	6224,40	No
1,5	0	25,06	30,08	20,05	0,52	6338,00	No
	-5	23,81	30,00	20,00	0,71	6021,10	No
	+5	26,32	30,00	20,00	0,41	6654,90	No

4.3.5.1 Conclusion

As previously mentioned, the key elements under analysis in this section is the designed flux density level of the transformer and the rated nominal voltage. For this reason, the flux density is varied and simulated against different tap changer settings to mimic the transformer operating under different applied voltages.

Throughout all the cases, the transformers tend to perform better at higher tap changer extremities. This is largely due to the lower magnetisation or excitation current required to produce the required flux in the transformer. Which suggests that the core loss is also significantly lower, with an increase in the number of turns on the primary coil. Tabulated below are the conclusive advantages and disadvantages of this simulation.

Table 10: Summary of Advantages and Disadvantages of Transformer Model Simulation

Statement	**Advantages**	**Disadvantages**
Fewer number of primary turns	Decrease in transformer manufacture cost	Increase in magnetising current and core losses leading to insulation failure.
Higher number of primary turns	Lower magnetising current and core losses. Higher efficiency. Transformer can function at overvoltage limit.	Increase in transformer manufacture cost
Higher design flux density level	Over voltage is at the applicable value.	Higher magnetising current. Increase in saturation characteristics rate.
Lower design flux density level	The transformer can perform within the required limits.	The transformer will need to be rated higher than the required operational voltage.

Based on the table above, it is recommended that the transformer be specified to a flux density lower than 1.7 T, to ensure that the core size and effectively material is decreased, to ensure that the cost of the transformer is reduced. The magnetising current will also be decreased, hence ensuring that the insulation

is also maintained, which increases the life span of the transformer. The rated operation voltage will also need to be increased for this application, beyond 25 kV. This is to ensure that the transformer will be able to sufficiently provide power to the lineside equipment, this would preferably need to be 27.5kV, according to the behaviour noted in Figure 31.

4.4 Resonance

While a transformer is predominantly inductive at lower frequencies, it does have a capacitive component that are notable at higher frequencies. While there are not normally issues for harmonics on distribution systems, the traction system has significant harmonics driven by the IGBT driven locomotives that may cause problems with the transformer, particularly if there is a resonance in the transformer.

To this end a frequency response analysis was done using a PicoScope and the experimental setup is shown in the figure below. This was applied to the dual phase transformer, 32kVA 19kV/2x240V. where the frequency was varied according to the following cases.

- Tap changer setting at 1 with LV earthed.
- Tap changer setting at 5 with LV earthed.
- Tap changer setting at 1 with LV floating.
- Tap changer setting at 5 with LV floating.

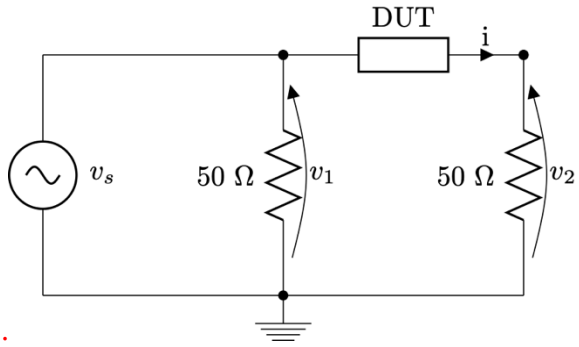

Figure 44: Circuit for frequency response analysis

4.4.1 Results

The following figures were obtained from the response analysis. It should be noted that the maximum frequency of the total harmonic distortion analysis was 2500Hz.

Figure 45 shows the bode plot of the dual phase transformer when the tap changer setting is at position one. This indicates that it is set to the lowest operation voltage extremity and the magnitude and phase follow a similar pattern, in that they both begin to dip at approximately 6 kHz. Several peaks are noted between 10 kHz and 1 MHz Which suggests that resonance is present at this operating voltage in the transformer when the transformer is under short circuit test, due to the core and windings.

The same can be said for Figure 46, however, on closer analysis some peaks seem to have additional disturbances when set to a higher tap setting, this could possibly be due to the additional number of turns.

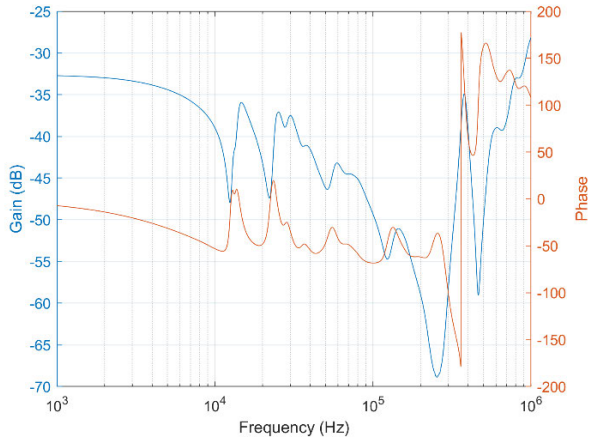

Figure 45: Frequency response of Tap1 with LV Earthed

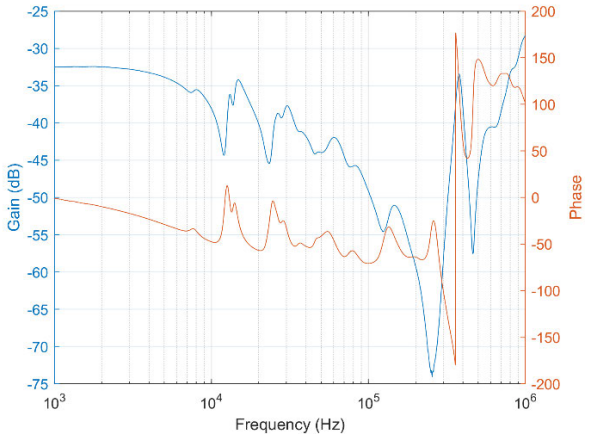

Figure 46: Frequency response of Tap5 with LV Earthed

The following figures represent the next two cases during the open circuit test. In Figure 47, the transformer is set tap changer setting 1, and the first peak appears after 11 kHz, which refers to the core region. The resonance within the transformer is heightened at Figure 48, which is in line with the tap changer setting of 5, referring to a higher operating voltage.

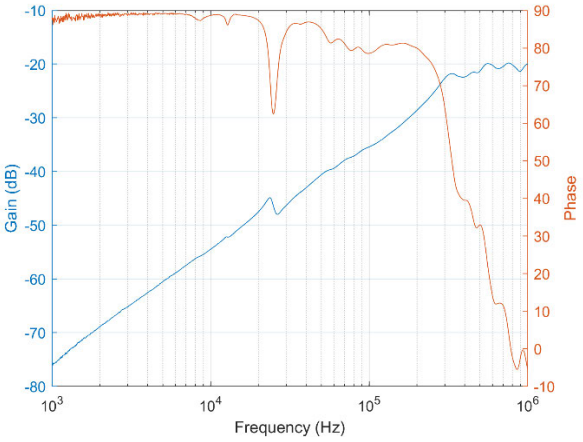

Figure 47: Frequency response of Tap1 with LV Floating

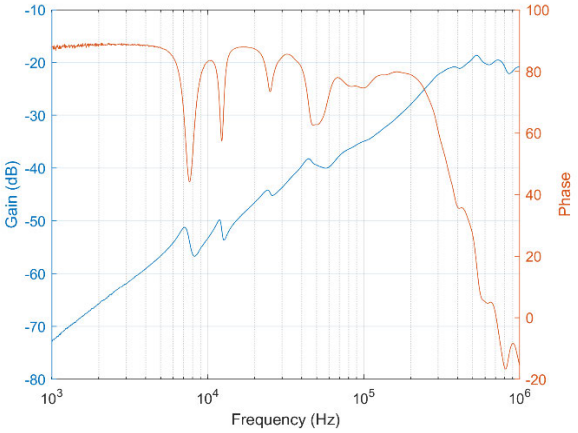

Figure 48: Frequency response of Tap5 with LV Floating

4.4.2 Conclusion

From this experiment regarding the transformer resonance, it can be concluded that there should be a resonance expected in the transformer after the 6 kHz point. This becomes more prevalent at higher voltages experienced by the primary side of the transformer. It is important to note that although during the FFT for the THD analysis, the maximum frequency is set to 2500 Hz, it is beneficial to study the harmonics beyond this frequency, to ascertain if they cause additional harm to the lineside transformer over time.

5 Traction System Model Development

The previous chapter detailed the investigation into the lineside transformer design parameters and specification for the application of railway engineering. A suitable transformer model was developed, based on tests and comparisons conducted on a similarly rated dual voltage transformer. This model is used in the configuration of the electrical railway infrastructure and hence, a few other key parameters were determined before, the process of analysis took place.

This chapter, therefore, details all the variables used in developing the complete traction system SIMULINK model. This was formulated in two parts. The first being the electrical railway infrastructure which includes the traction substation, overhead traction equipment and the line side transformer currently under test. The second was the locomotive which represents the load connected to the infrastructure. The simulation is carried out using MATLAB/SIMULINK.

The following subsections are used to further develop components which make up the main model.

5.1 Electrical Railway Infrastructure

The main components of this infrastructure are listed and described in the subsections as follows:

- Lineside Transformer
- Source impedance (Incoming Power Supply)
- Traction Substation
- Overhead Track Equipment and Rail

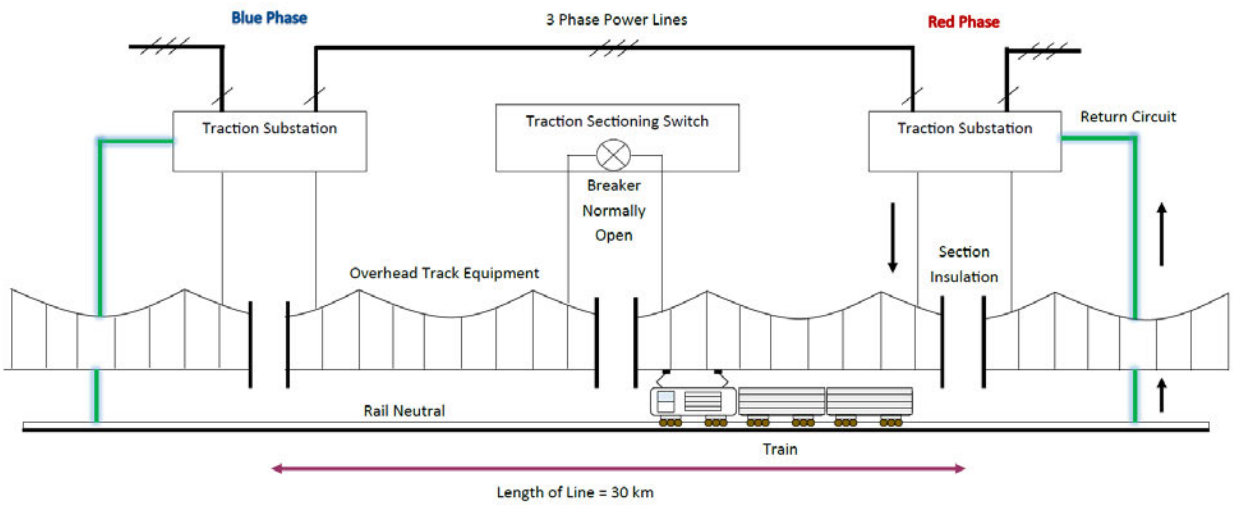

Figure 49: Electrical Infrastructure

5.1.1 Lineside transformer

The 16 kVA, 25 kV / 230 V transformer provides power to lineside equipment used for train authorisation and condition assessment, which essentially informs a centrally located control room of the location of the train and the condition of the bearings and other components onboard the train. Power is also supplied to the track sectioning switch base station, which is used to isolate consecutive traction substations from each other. This transformer is modelled using a saturable transformer block. Here the primary voltage is varied according to the tap changer settings and the base parameters are listed below.

Table 11: Lineside Transformer Parameters

Lineside Transformer Parameters	
Power Rating (kVA)	16
High Voltage (kV)	25
Low Voltage (V)	230
Impedance (%)	4.4
Frequency (Hz)	50

Table 12: Tap Changer Settings

Line Side Transformer Tap changer values					
Tap No.	**1**	**2**	**3**	**4**	**5**
%	-5,0%	-2,5%	0,0%	2,5%	5,0%
HV (V)	23750	24375	25000	25625	26250

The saturation characteristics of a typical 25kV/ 230V single phase transformer were determined using transformer design principles as stated in the previous chapter, considering that the transformer is single phase with the above-mentioned constraints and has an iron core.

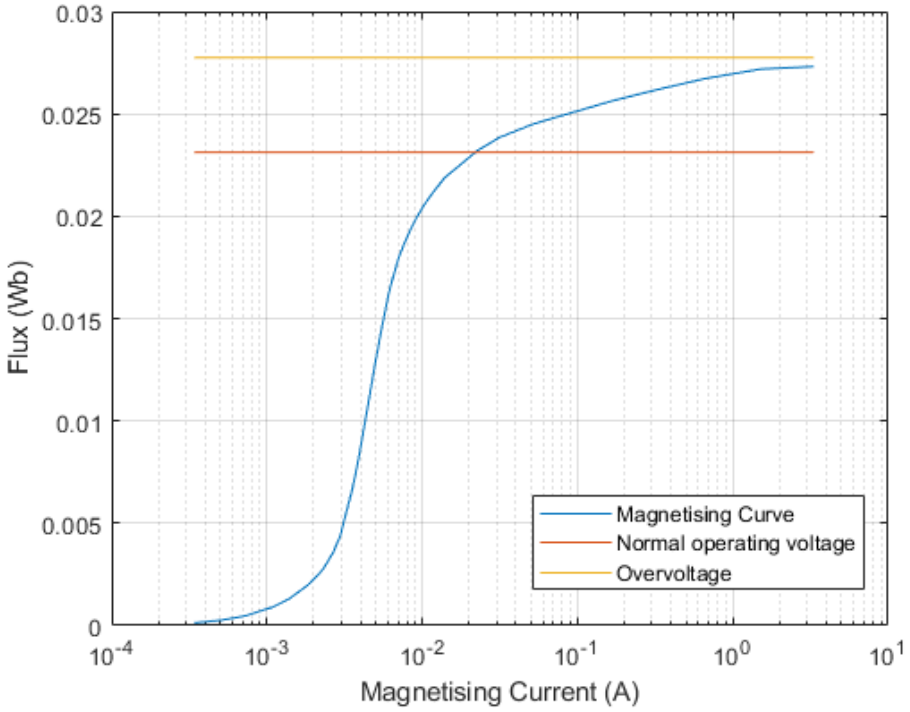

Figure 50: Magnetisation Curve of 25kV/230V Lineside Transformer

Next, the inter-winding and stray capacitances for the representation of an accurate transformer model are determined using a similarly configured dual phase transformer, 32kVA 19kV/2x240V, available in the High Voltage Laboratory. The following diagram displays the configuration of the measured capacitances.

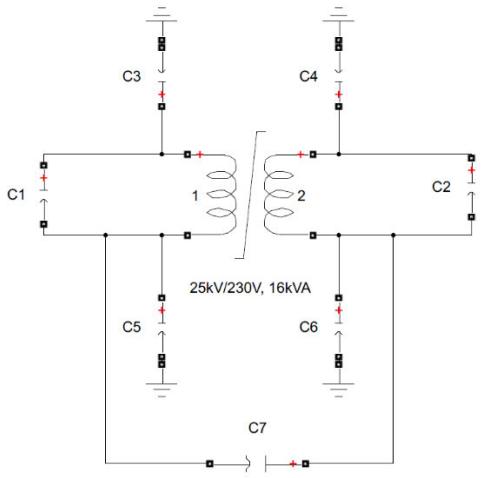

Figure 51: MATLAB Model of Lineside Transformer

Measured Capacitances	
C1 (F)	678.5e-12
C2 (F)	1e-9
C3 (F)	544.5e-12
C4 (F)	1206.7e-12
C5 (F)	545.7e-12
C6 (F)	1206.7e-12
C7 (F)	564.5e-12

To determine the validity of the measured capacitances a model of the transformer is simulated with both an increase and decrease in the measured capacitances with an order of 10%. An impedance measurement tool is used to conduct a frequency sweep of the transformer model whilst disconnected from the system. And according to the following figures, the peak in phase differs marginally from the transformer model with initial measured capacitances. This indicates that these are acceptable and there are no disturbances experienced by the model.

The figures below show the resultant waveforms of the frequency sweep of the lineside transformer with the measured capacitances implemented onto the transformer model. The magnitude indicates no instabilities and the peak of the phase is at approximately at 80 Hz.

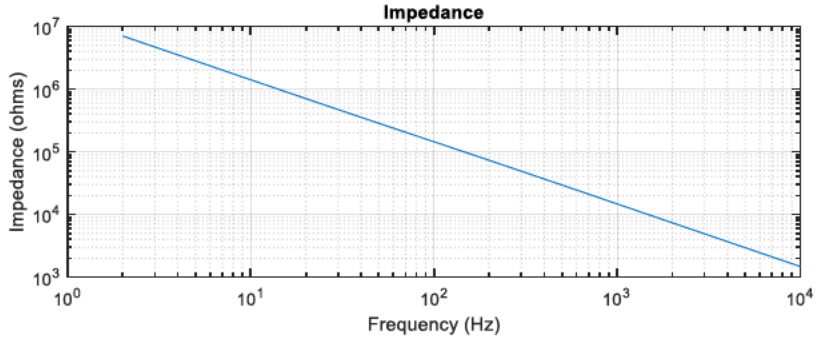

Figure 52: Magnitude Component Waveform of Impedance Frequency Sweep of measured (100%) Transformer Capacitances

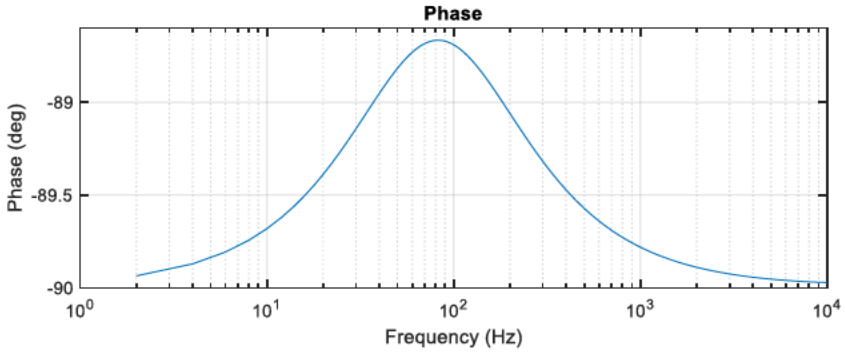

Figure 53: Phase Component Waveform of Impedance Frequency Sweep of measured (100%) Transformer Capacitances

Figure 54 and Figure 55 show the magnitude and phase plots of the frequency sweep. It is shown that the magnitude at 90% of each of the measured capacitances, is a smooth downward slope. And the phase plot has it's peak slightly shifted to the right.

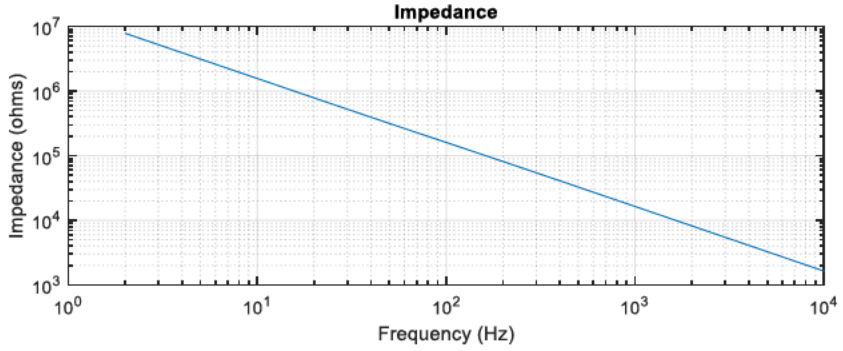

Figure 54: Magnitude Component Waveform of Impedance Frequency Sweep of measured (90%) Transformer Capacitances

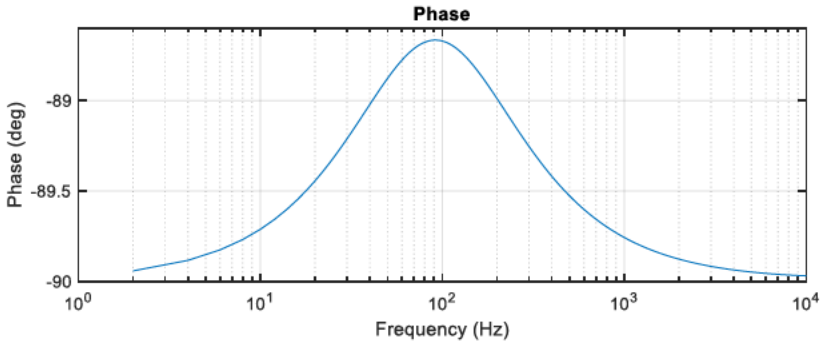

Figure 55: Phase Component Waveform of Impedance Frequency Sweep of measured (90%) Transformer Capacitances

The figures below for the transforemr capacitances calculated at 10% more than the measured values, follow a similar shape as those previously discussed. The phase plot is noted to shift slightly to the left, as expected.

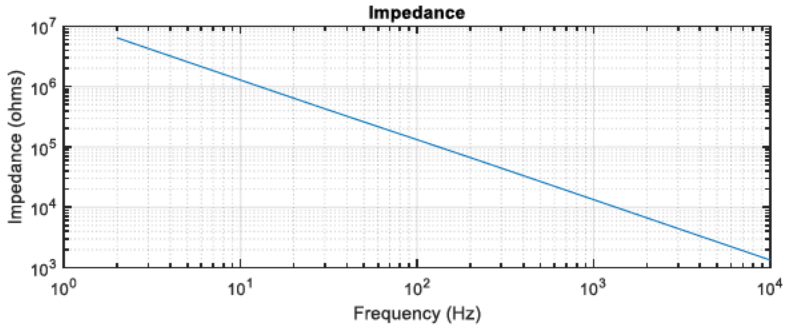

Figure 56: Magnitude Component Waveform of Impedance Frequency Sweep of measured (110%) Transformer Capacitances

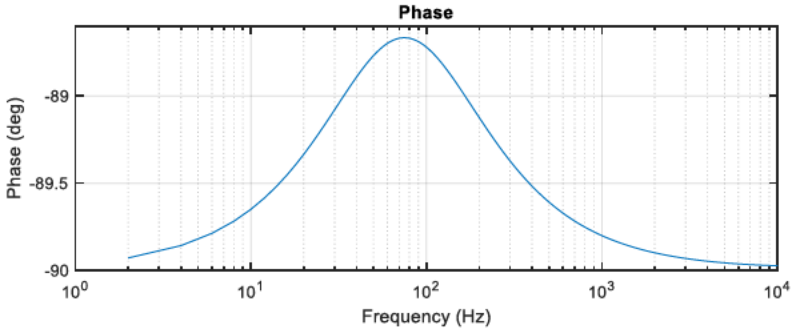

Figure 57:Phase Component Waveform of Impedance Frequency Sweep of measured (110%) Transformer Capacitances

5.1.2 Source Impedance

To mimic the power utility, the source consists of a 132 kV feeder with a 50 MVA fault level. Typically, each traction substation receives two of the three phases provided and maintained by the power utility. These phases are sequentially alternated at each traction substation to maintain phase balance at the power utility.

5.1.3 Traction Substation

The sole purpose of the traction substation is to step down or condition the power received from the power utility (rated at 132kV) to the overhead track equipment (rated at 25kV), which then provides power to the locomotive. The traction substation also houses the protection equipment which alerts a centrally located control room if there are issues at the substation as well as on the line. Especially if there are detections in overcurrent and undervoltage.

Table 13: Transformer Specification

Traction Transformer Parameters	
Impedance (%)	11
Primary Voltage (kV)	132
Secondary Voltage (kV)	25
Power Rating (MVA)	20

5.1.4 Overhead Track Equipment and Rail

The overhead track equipment comprises of contact and catenary wire, jumpers, clamps, and section insulators. For building the electrical infrastructure model, these will be shown as two PI sections. The overhead line parameters are determined using the Power Line Parameters application in the powergui block available in MATLAB/Simulink. The Rail as well as the double line consisting of both catenary and contact wires at a maximum height of 4.5m, for 25kV reticulation system were considered for the

calculation of the parameters of the line. These are represented by the PI Section Line in the following model.

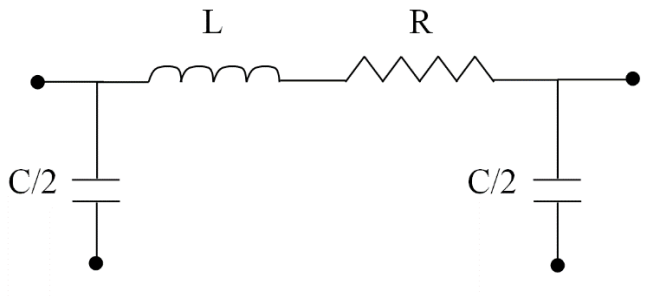

Figure 58: Equivalent Circuit of PI section

Table 14: OHTE Parameters

Overhead Line Parameters		
Line Resistance (Ω/km)	R	0.074
Inductance (H/km)	L	1.18e-3
Capacitance (F/km)	C	10e-8

It is important to note that the rail is representative of the main return conductor and is therefore included in the calculation of the parameters within the model. The rail together with bonding cables (negligible in this case) form the return current path to the traction substation.

To simulate the locomotive's movement through the section of 30km between two substations, two PI section blocks were added. The length of the respective piece of OHTE either before or after the locomotive is represented by these blocks and are changed accordingly. The entire length of 30 km is used to simulate the worst-case scenario of the failure of one traction substation. This requires the closure of the TSS, allowing the adjacent traction substation to supply all the electrical infrastructure previously supplied by the failed substation, to prevent delays in train movement. A PI section was also used to represent the length of cable which links the OHTE to the lineside transformer.

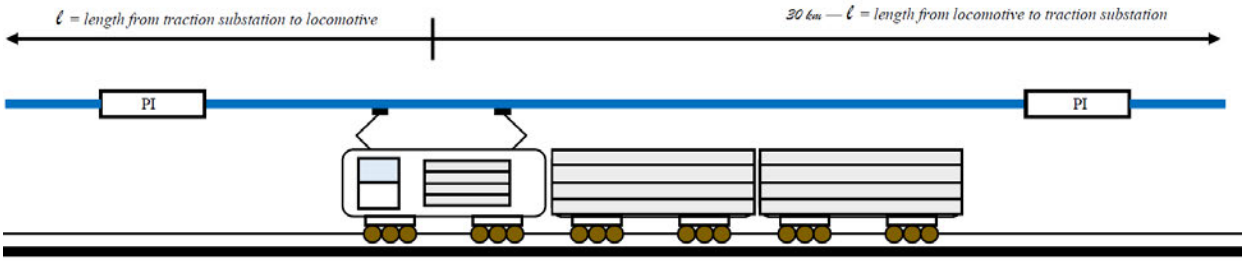

Figure 59: Train Movement on Rail

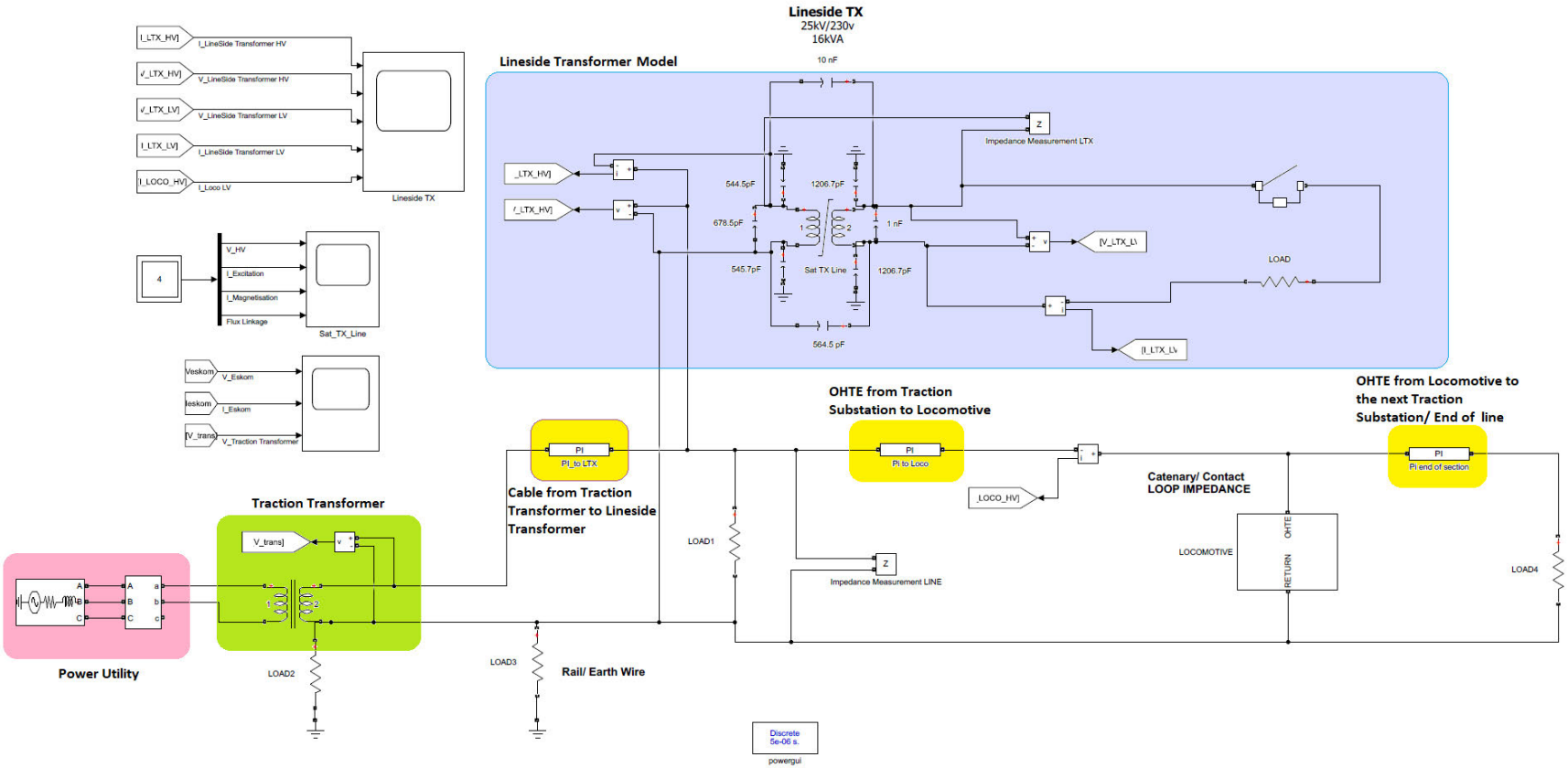

Figure 60: MATLAB Model of Electrical Infrastructure

5.2 Locomotive

The locomotive serves as the load under test on the electrical infrastructure and its components are as follows.

- Locomotive main transformer
- Traction converter

5.2.1 Locomotive main transformer

The main transformer, for the purpose of this AC locomotive, powers four AC motors and subsidiary electronic equipment onboard the locomotive. The parameters used to model this are detailed in the table below.

Table 15: Locomotive Parameters

Locomotive Main Transformer	
Impedance (%)	38
Primary Voltage (kV)	25
Secondary Voltage (kV)	1.98 x 4
Power Rating (MVA)	5.6

5.2.2 Traction Converter

This model utilises four 4-quadrant converters (4QC) to change the AC power to DC and the switches used in this investigation were IGBT's due to their high frequency switching capabilities, as opposed to the obsolete GTO's (Gate Turn-Off Thyristors). Their higher switching frequency is known to assist with smoothening acceleration and reducing traction noise. IGBT's also have high current carrying capability and dissipates low current when conducting.

The 4QC parameters used for simulation are as follows.

Table 16: 4QC Parameters

4-Quadrant Converter	
Switch Type	IGBT
Controller Type	PI
Pre-charged Capacitor (mF)	40
Second Order Filter	0.01Ω+0.5mH+5mF
Load (Ω)	5

The traction converter unit is developed to mimic the harmonics and possible resonances which could be expected. The controller type used to formulate the signal for driving the IGBT's is the Proportional Integral (PI). The Load resistor represents the load carried by the locomotive; this includes wagons. The RLC filter is designed to reduce the effects of disturbances in lower order frequencies. The pre-charged capacitor is necessary to filter any resonance emanating from the converter model.

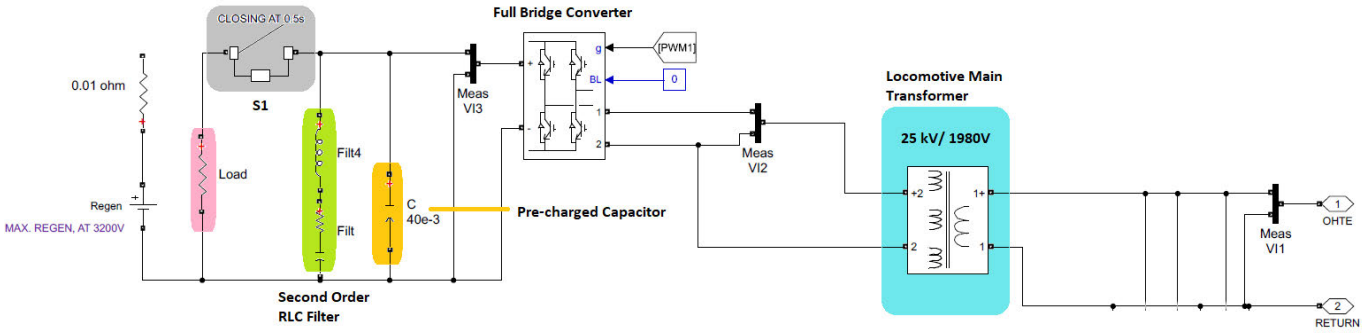

Figure 61: MATLAB Model of Traction Converter

Before the controller can be modelled, the uncontrolled converter is simulated with the above parameters. This simply refers to the converter configuration using diodes in place of IGBT's and with the omission of a controller used to regulate the PWM signal. The following figure is the DC-link voltage output as per the previously mentioned conditions, which indicates that the waveform does not reach the desired output of 3kVDC.

The simulation run time is 2.5s and the circuit breaker S1 is set to close at 0.5s. according to the DC Voltage plot that the waveform peaks at 2750 V, through the pre-charged capacitor at 0.5s, and drops significantly when the load and RLC filter are energised. The voltage then oscillates at just above 2000V.

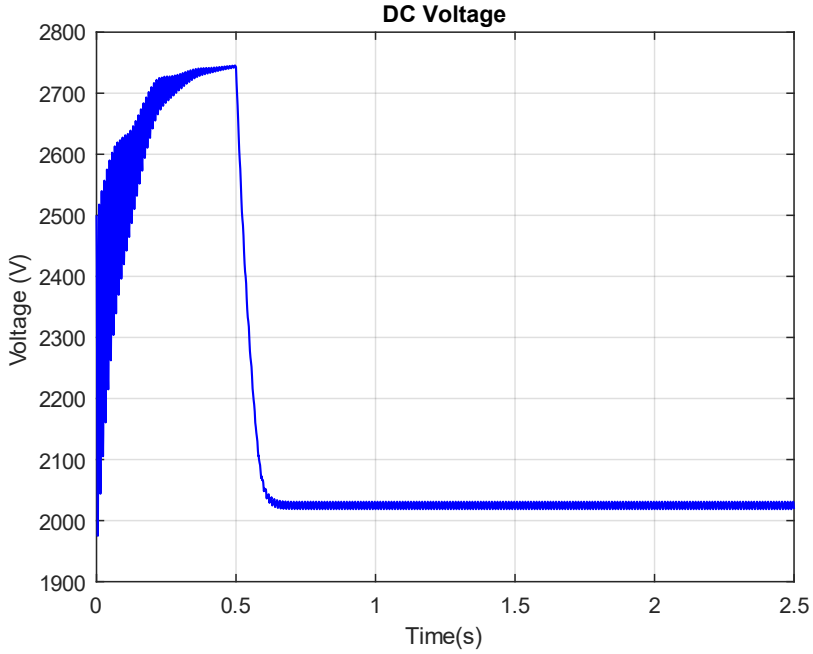

Figure 62: DC-Link Voltage of Uncontrolled System

A PI controller was designed in order to regulate the feedback signal, which in this case is the DC output voltage of the converter, received from the system. The controller is implemented and tuned to manage the error signal, using the transformer parameters and to ensure that the output was stable for most simulation scenarios. The output of the controller function in conjunction with the automatic gain control determines the PWM pulses. The PWM generator block is later used to vary the switching frequency of the full-bridge converter in multiples of the operating frequency, which is set to 50 Hz [30].

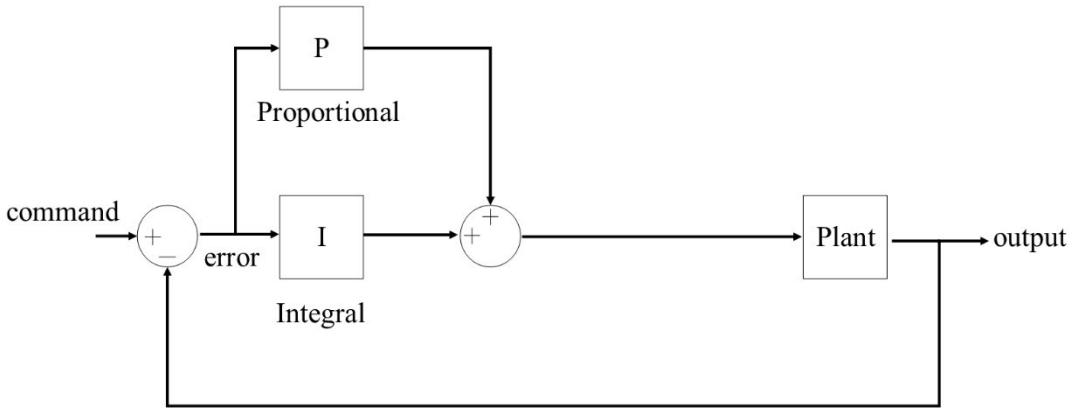

Figure 63: Block Diagram of PI Controller

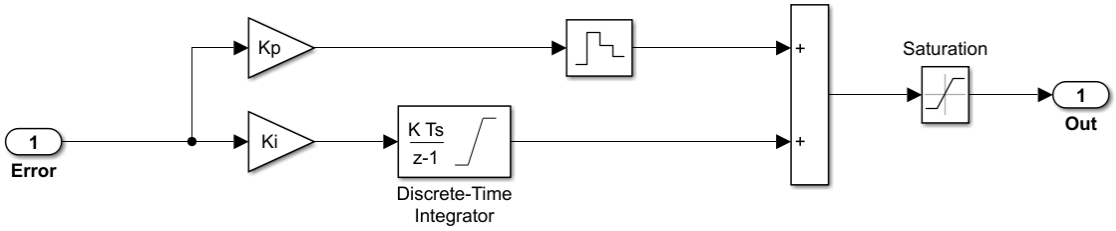

Figure 64: MATLAB model of PI Controller

The firing pulses required for the switching operation of the IGBT's is controlled by the PWM generator. V1 represents the plant input signal, which in this case is the overhead line voltage. A second order band pass filter is then used to retain the relevant 50Hz signal components. The sinusoidal measurement is implemented to assist in the estimation of the angle of the filtered input signal. This phase angle is then used in the automatic gain control and the PWM generator. Udc refers to the DC output of the full bridge rectifier and is used as the input to the PI controller to determine the error signal in the model.

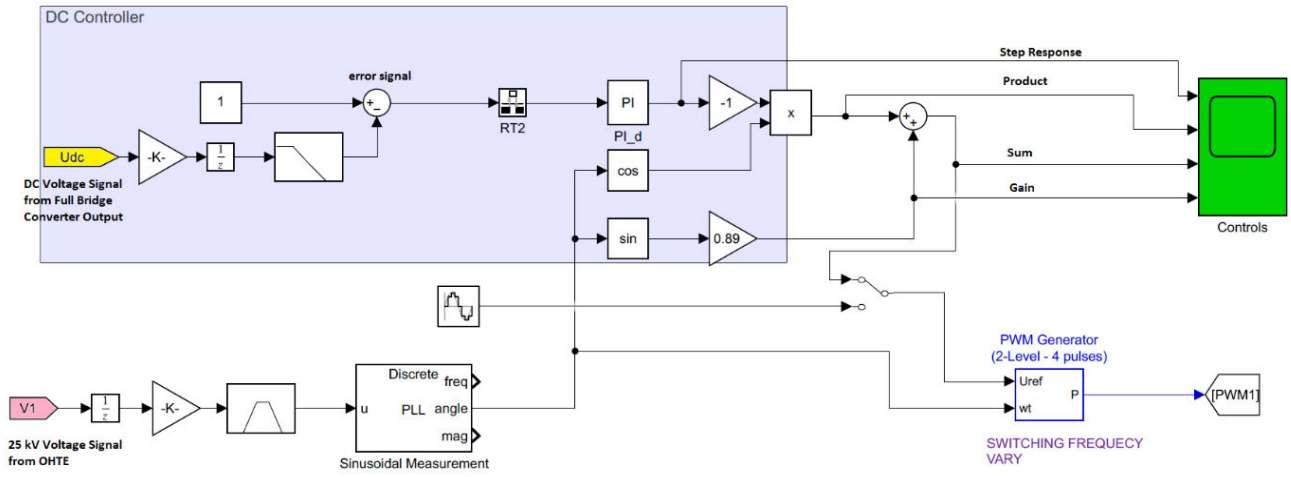

Figure 65: MATLAB Model of Controller

Figure 66: Controller Waveforms, depicts the output of the Controls scope and it is noted that the step response meets steady-state conditions at approximately 0.8s, once connecting the load at 0.5s. the waveforms labelled Product and Gain collectively make up the sinusoidal reference signal input of the PWM generator.

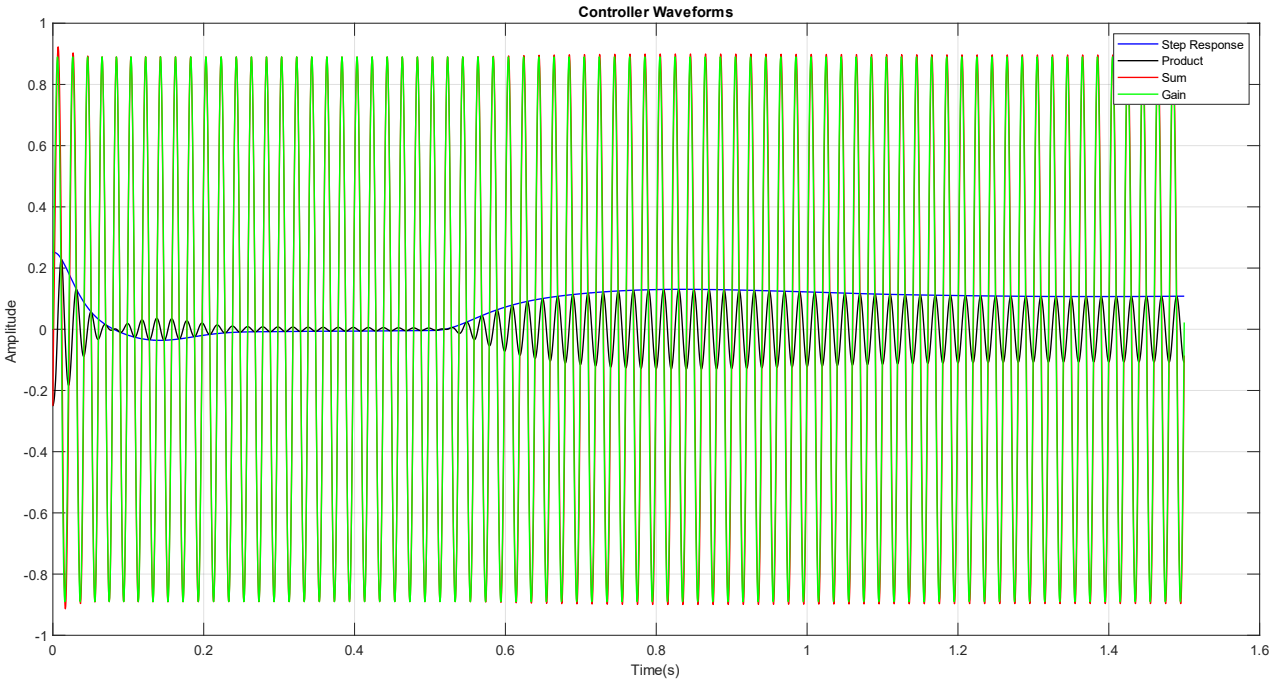

Figure 66: Controller Waveforms

5.3 Sample Waveforms for Base Model

This sub-section depicts the input voltage received by the lineside transformer under test. This is done to ascertain the validity of the developed model. The following headings form the basis of the conditions considered during the investigation.

5.3.1 No-Load (Locomotive disconnected)

As stated previously, the locomotive is referred to as the load on the railway network's electrical infrastructure, which is disconnected under no-load conditions. This indicates the removal of the converters and hence the expected power supply to the lineside transformer, ideally should represent a smooth sinusoidal waveform. The plot below shows that as expected the input signal appears to be sinusoidal in nature oscillating between -35kV and 35kV, which is the peak voltage of the waveform.

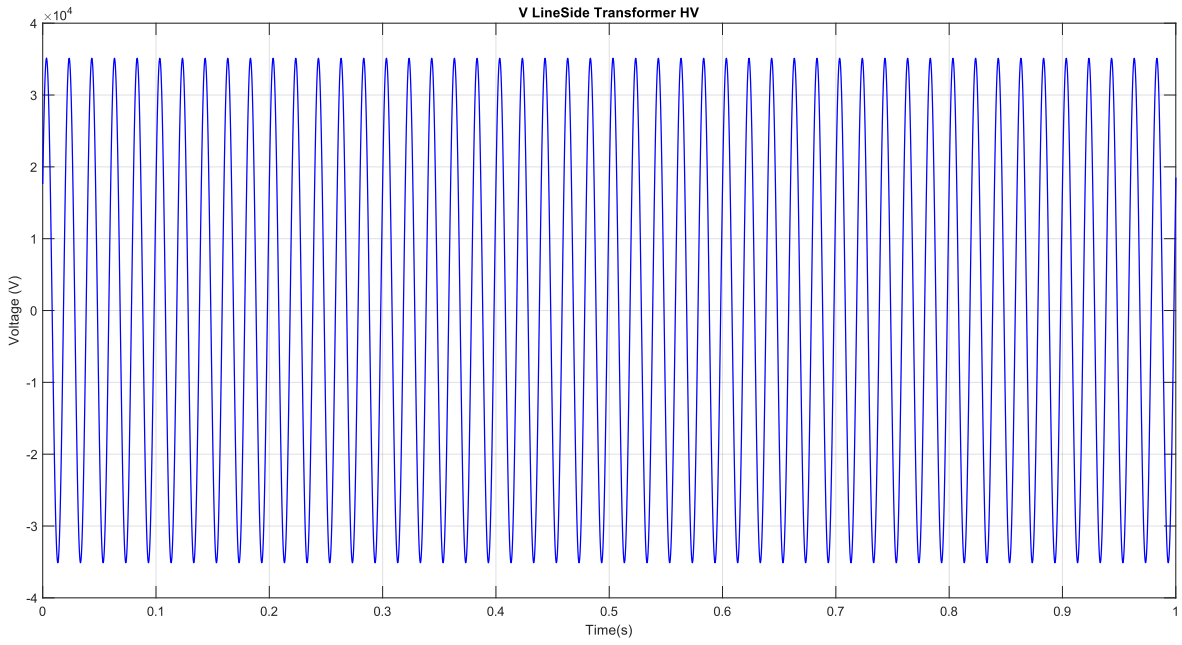

Figure 67: Primary Side Voltage Waveform of Line Side Transformer under No-Load Conditions

5.3.2 Load (Locomotive connected)

The system under load conditions indicates that the locomotive is connected to the model and hence, the converters become active. The effect of the switching now becomes apparent and is noted by the

spikes shown in the figure below. As expected, this is indicative of resonances within the system which can lead to an increase in the harmonics [21]. The locomotives load is switched on at 0.5s and the initial decrease in voltage thereafter settles with the activation of the system controller. The initial spike noted in the voltage is due to immediate introduction of the lineside transformer as a load onto the power system, which induces inrush currents.

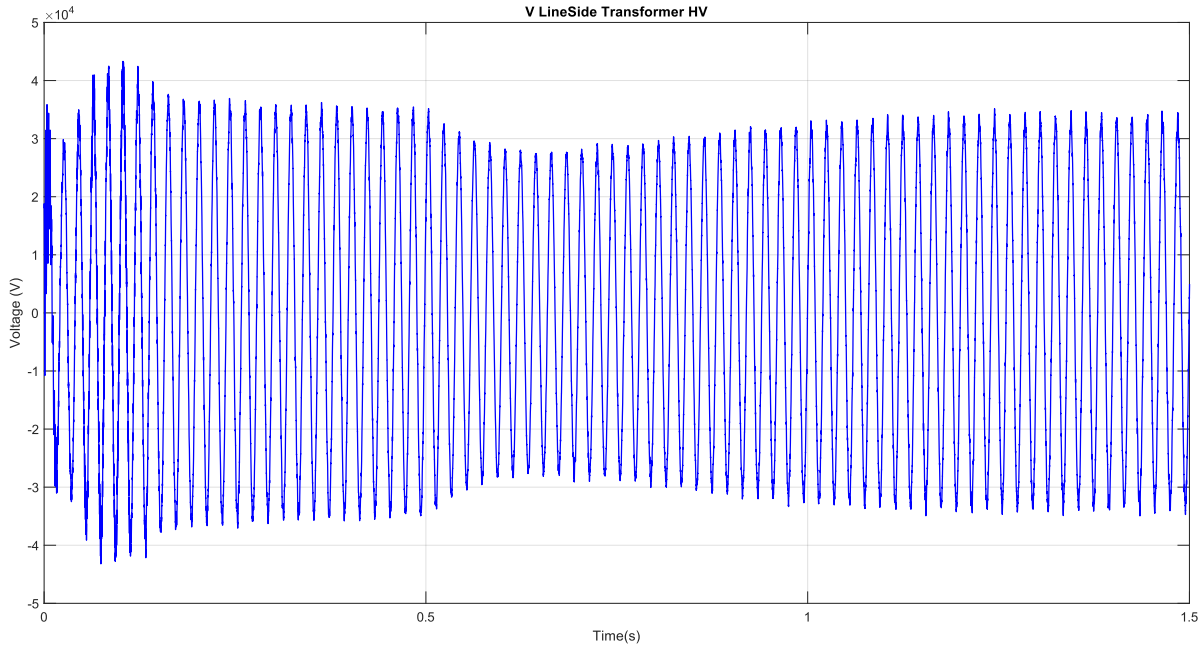

Figure 68: Primary Side Voltage Waveform of Line Side Transformer under Load Conditions

In Figure 69: DC Voltage Waveform of Converter under Load Conditions, the output voltage of the converter is shown. The controller stabilises the output from the closure of the breaker at 0.5s to 1.5s. The waveform tends to consistently oscillate at 3kVDC which is the required output of the of the converter.

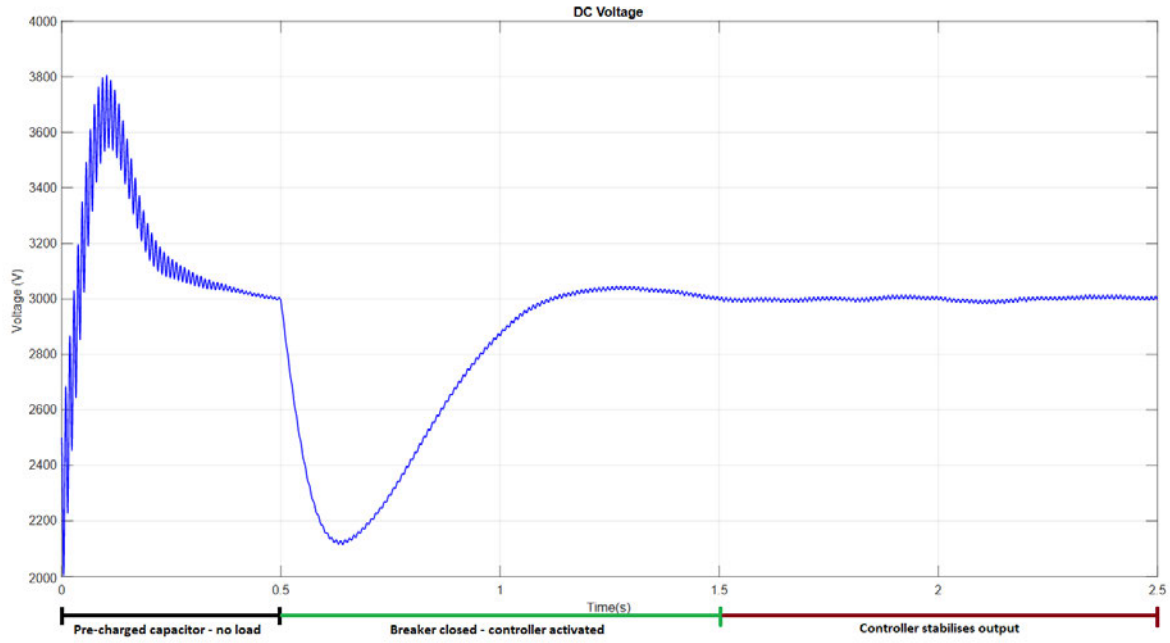

Figure 69: DC Voltage Waveform of Converter under Load Conditions

5.3.3 Regeneration

The model is also tested under regeneration conditions to monitor the harmonics and supply inconsistencies experienced by the lineside transformer, should the locomotive travel on a downward gradient or coast, resulting in the regeneration of power from the locomotive onto the OHTE.

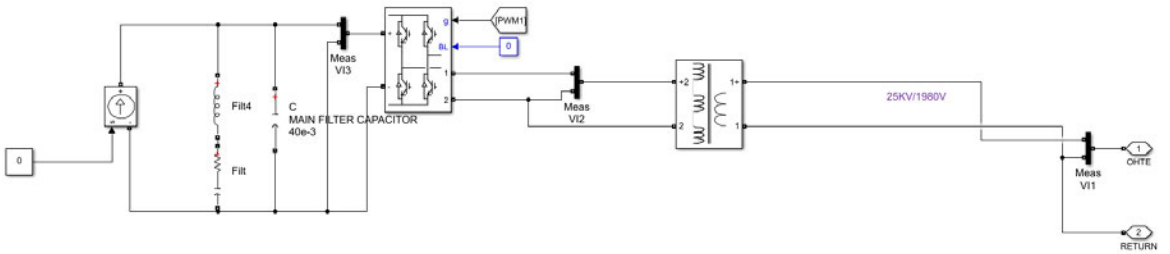

Figure 70: Regeneration Model

A current source represents the regeneration component of the locomotive. The current signal is set to +178A, assuming that the train is undergoing 100 % of dynamic braking. As noted in Figure 72: DC Voltage Waveform of Converter under Regenerative Conditions, the DC link voltage waveform immediately increases to 3100 VDC when the locomotive begins to regenerate back into the system at 0.5s, as anticipated, since there is power dissipation in the circuit. The waveform tends to settle towards

3000 VDC due to controller stabilisation. The spikes or voltage inconsistencies are also more intense, as compared to the normal operation load conditions. These spikes represent harmonics from the DC link voltage which are transferred to the OHTE and the lineside transformer. [31].

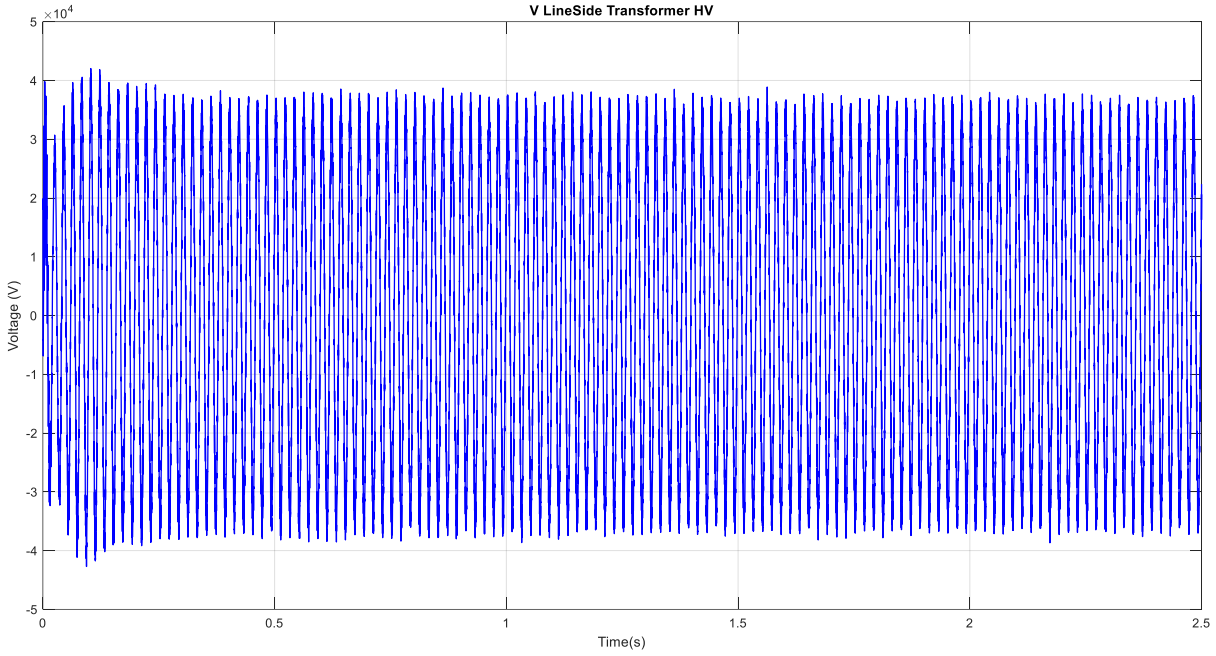

Figure 71: Primary Side Voltage Waveform of Line Side Transformer under Regenerative Conditions

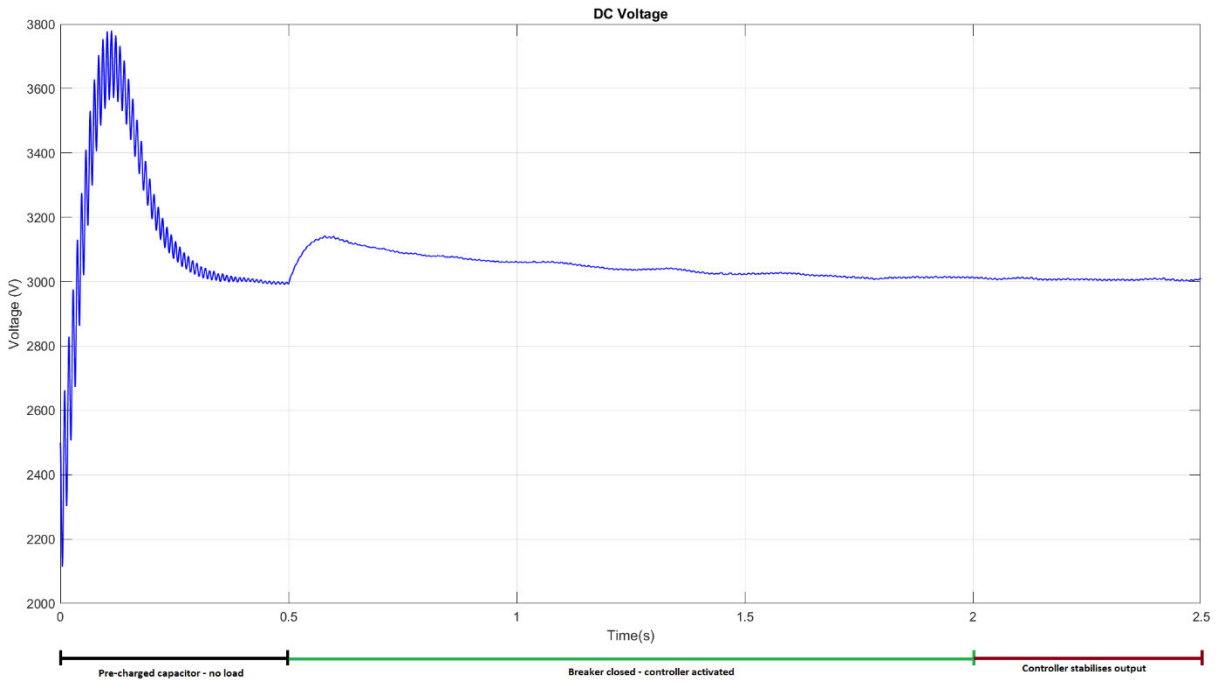

Figure 72: DC Voltage Waveform of Converter under Regenerative Conditions

6 Simulation Results and Discussion

The primary focus of this chapter is to determine the effect that the traction converters onboard a locomotive have on the lineside transformer, which shares its power source with the locomotive. This is carried out by analysing the lineside transformer's input power supply using MATLAB Simulink's FFT Analysis tool in the powergui block. The model is simulated at varying distances from the traction substation to show movement of the locomotive between two substations approximately 30 km away from each other (worst case). The THD is measured and analysed at different transformer tap changer settings to ascertain which harmonics are the most dominant. The following scenarios are explored.

- Case 1: Unloaded system – this refers to the train being disconnected.
- Case 2: Loaded system - this refers to the train being connected.
- Case 3: Loaded system under Regenerative conditions – refers to the train being connected to the system and pushing power back into the system.

Cases 2 and 3 are simulated by taking measurements as the train moves to different distances, namely 0.5km, 10km, 15km, 20km, 25km and 29.9km. All whilst varying the tap changer settings from 1 to 5.

It is vital to note that the voltage used for the THD calculation is found on the high voltage side of the lineside transformer, since this is the supply under investigation. This is indicated in the figure below.

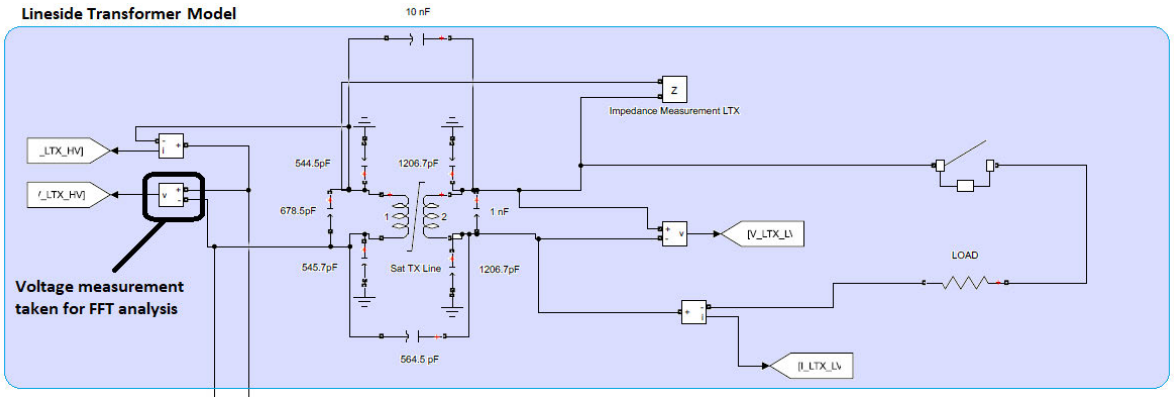

Figure 73: Lineside Transformer Model

6.1 Unloaded (Train Disconnected)

In order to test the developed model under various conditions, the unloaded system with the locomotive disconnected is used as the steady-state model. Here, the source (power utility) fault level is set to 50 MVA and the tap changer setting for the lineside transformer is set at 0 %. The FFTDATA structure was setup as follows.

Table 17: FFT Analysis Settings

Parameter	**Value**
Input	V1
Runtime	2 s
Start Time	1.5 s
Number of Cycles	2
Maximum Frequency	2500 Hz

The runtime, start time and cycles are set to ensure that the sample considered for analysis would settle sufficiently to assist with the precision of the exercise.

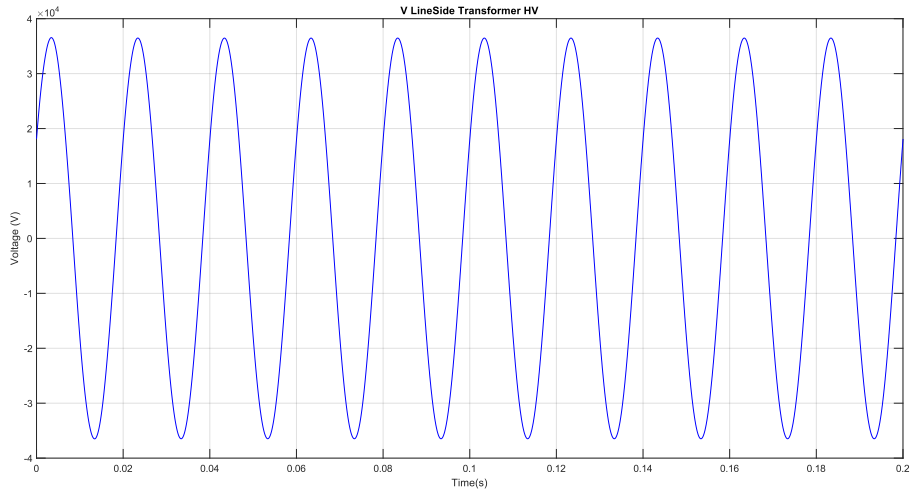

Figure 74: Unloaded Lineside Primary Voltage

The voltage output presents a smooth sinusoidal waveform oscillating between 35kV, as projected, without the presence of any disturbances. The THD at all intervals is expected to be zero due to the

absence of the locomotive. As the traction converter is suspected to be one of the causes of the harmonic distortion experienced on the line. Overvoltage's on the OHTE due to regeneration or an increase in the train load could also be a contributing factor. As well as the transformer resonance at higher frequencies.

6.2 Loaded (Train Connected)

The analysis of the loaded system follows a similar approach as the previous, with the addition of the locomotive being configured at a switching frequency of 1750 Hz. The current source signal was set to -712A, representative of the maximum current on the DC link side of the locomotive. The THD was calculated at various distances away from the traction substation, with the maximum being 29.9km which is usually just before the next traction substation, following a sectioned or split feeding arrangement. The last measurement is taken at this point since the locomotive will never cross the 30km point or conduct at the traction substation due to the presence of the section insulators. The results obtained are tabulated below.

Table 18: THD Values under loaded conditions

Distance (km)	THD at Tap 1 (%)	THD at Tap 2 (%)	THD at Tap 3 (%)	THD at Tap 4 (%)	THD at Tap 5 (%)
0,5	17.42	18.49	19.05	18.89	21.19
10	2.16	2.26	2.36	2.53	2.62
15	8.05	8.37	8.9	9.55	9.8
20	6.49	6.98	7.52	8.05	8.36
25	9.15	10.56	10.05	11.41	12
29,9	8.56	9.17	9.65	10.56	11.41

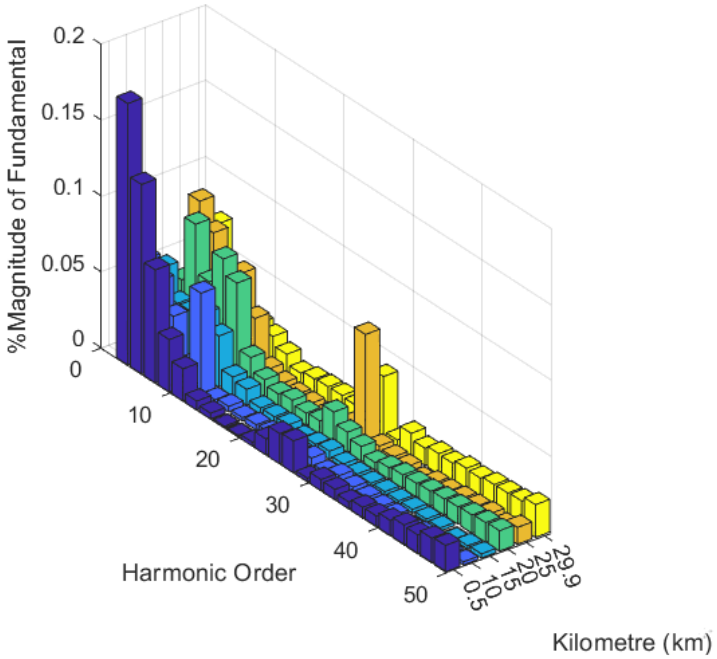

Figure 75: 3D View of THD at Varying distances for Tap1

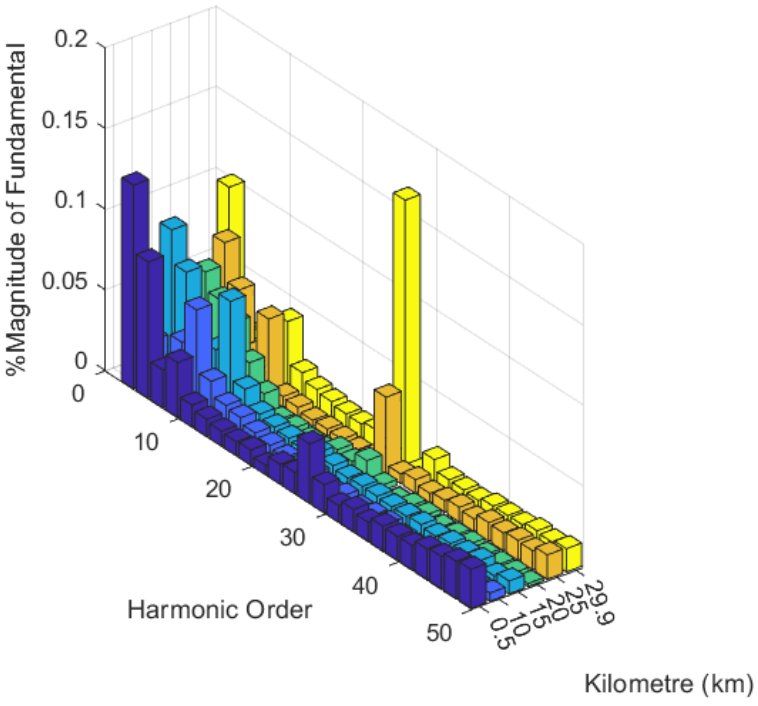

Figure 76: 3D View of THD at Varying distances for Tap2

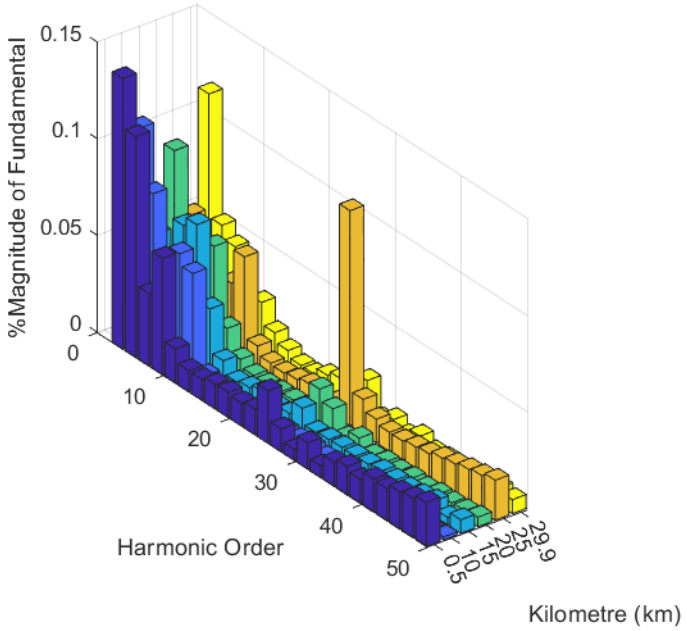

Figure 77: 3D View of THD at Varying distances for Tap3

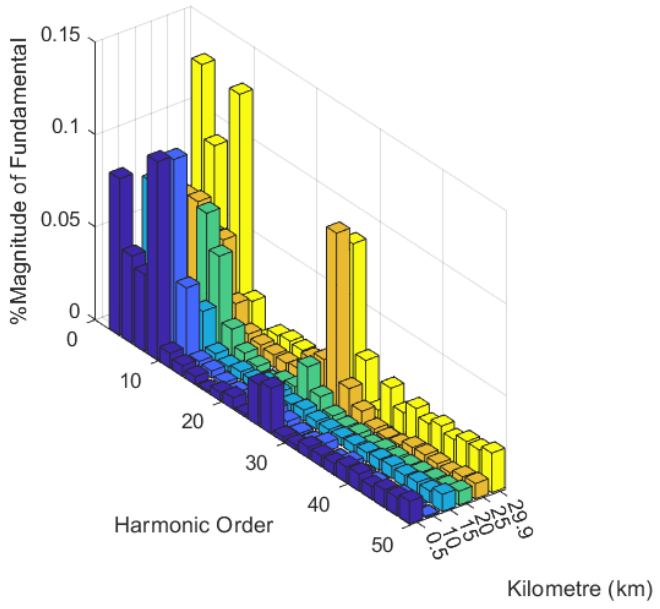

Figure 78: 3D View of THD at Varying distances for Tap4

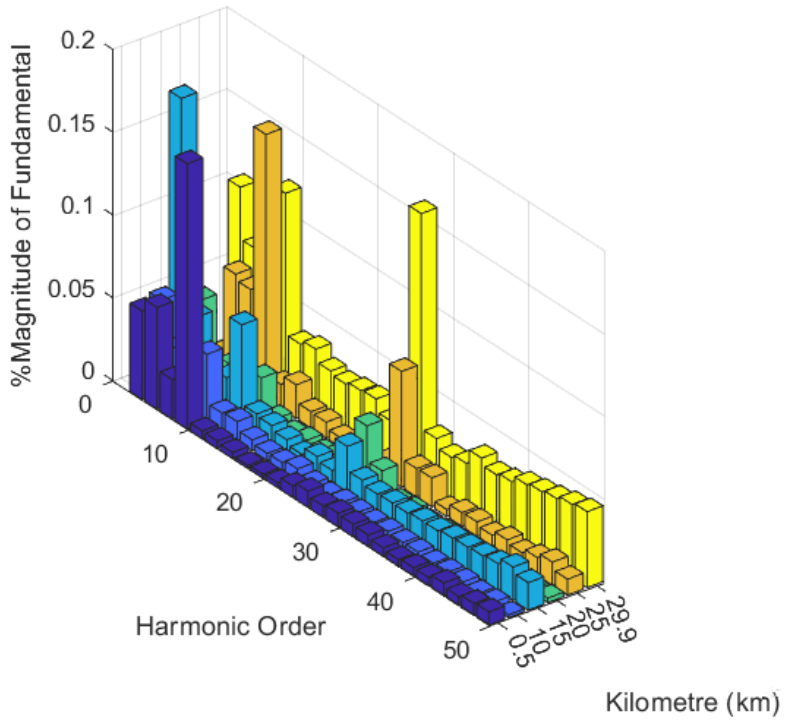

Figure 79: 3D View of THD at Varying distances for Tap5

According to the table of results, the primary input side of the lineside transformer experiences the greatest distortion due to harmonics at 0.5 km. This was largely due to the locomotive position being the closest to the traction substation, with the resultant line impedance being the lowest at this point. The traction transformer at the substation contributes to the disturbances noted in the waveform. It is also noted that the THD decreases significantly at 10km, which is just before the train reaches the location of the lineside transformer. Here, the line length assists in dissipating some of the distortion. The gradient of the line as well as auxiliary equipment, like switches and section insulators need to be compensated. The THD calculated between 10km and towards the end of the line is within the region of 10%. However, it tends to increase again at the end of the line, and this is due to the train approaching the next traction substation. As shown in Table 18, the THD is lower at the lower order tap changer settings, with the lowest being at -2.5%. This mainly affirms that the disturbances experienced in the signal increases, with an increase in magnitude.

Taking the THD expression (equation 1) into account, the THD should be lower at lower voltages, represented in this case as the lower tap changer intervals. The main reason for this is, due to the voltage being sufficient to satisfy energising the core of the transformer and emitting the desired output at the secondary terminals. It is important to note that, in order to obtain the rated output, the magnetising

current will drastically increase to compensate this undervoltage. This in turn will cause the transformer to saturate, based on its design parameters.

The converters are responsible for the development of the odd ordered harmonics; hence these are explored. The FFT plots indicate that with the increase in the distance, a large amount of the harmonics is subdued, and this was as a result of an increase in the current carrying capacity. The 3rd, 5th, 7th, 9th and 27th order harmonics, at 150Hz, 250Hz, 350Hz, 450Hz and 1350Hz, respectively, are the most dominant during loaded conditions.

The worst calculated THD was when the locomotive was at 0.5km with the lineside transformer having a tap changer setting of 5 and can be compared with the results at the same location with the tap changer setting of 1. The sample current waveforms are shown below. It was noted that the presence of multiple harmonics attributing to the THD were evident early in the samples. The disturbance experienced is extremely irregular and prevents the peaks from attaining the projected voltage of 35kV at the primary side of the transformer.

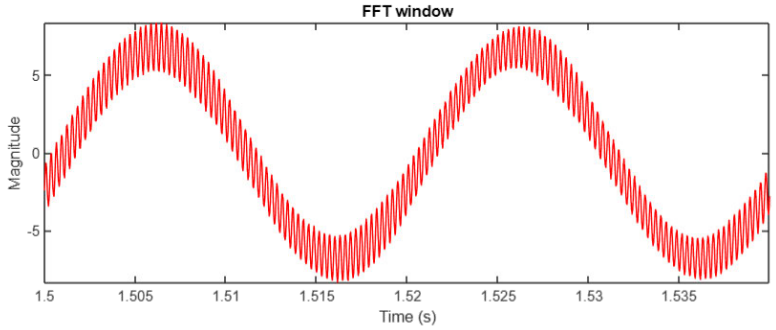

Figure 80: Lineside sample for 0.5km at Tap 1

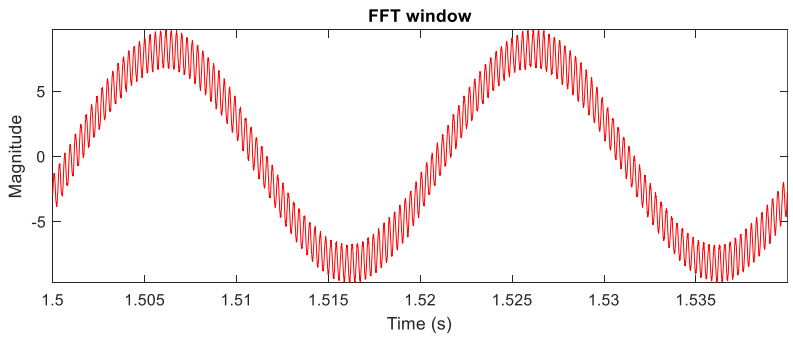

Figure 81: Lineside sample for 0.5km at Tap 5

To better understand this, the output of the converter is analysed at 0.5km at Tap 5. Both voltage and current waveforms show that the controller is unable to completely stabilise, once initiated and experiences fluctuations in the output. This affirms the statement that the instabilities in power supply at the lineside transformer does partially emanate from the locomotive traction converter.

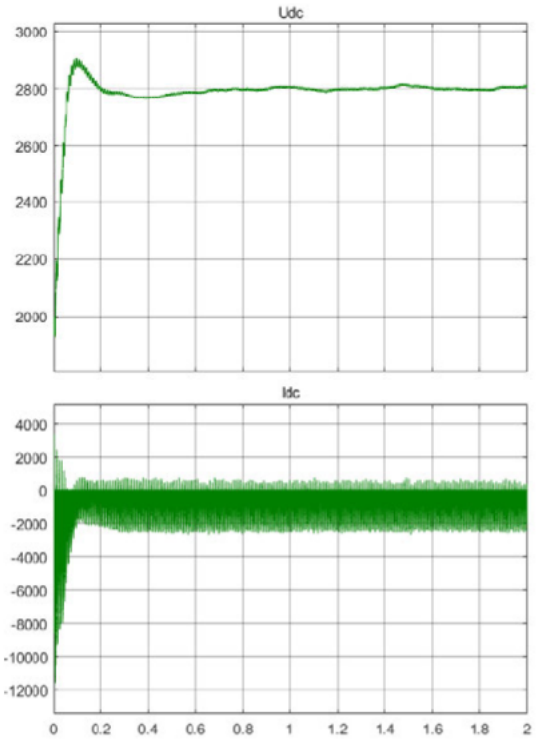

Figure 82: DC Link Voltage and Current output of Converter

The magnetising current of the lineside transformer is also investigated at the highest THD, of 21.19% at the tap changer setting of 5, which is an operational voltage of 26.25kV, whilst at 0.5 km from the traction substation. This is shown in Figure 83 when the load is disconnected from the transformer, and it is noted that the waveform has an additional disturbance in the plot. The magnetising current is known to be low at this voltage, however these additional harmonics in the transformer will aid in inaccuracies and transfer them to the lineside equipment.

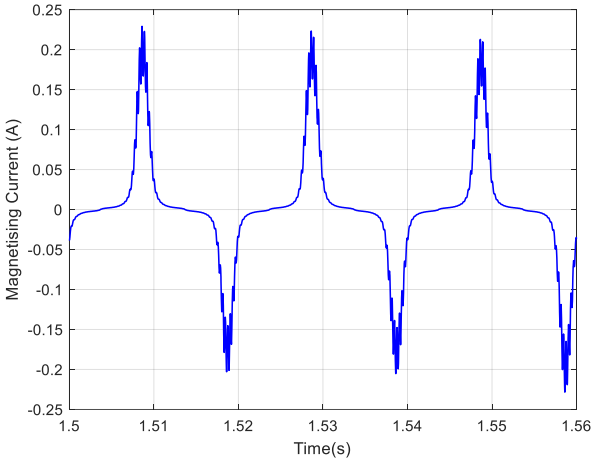

Figure 83: Magnetising current waveform at Tap 5 at 0.5km

6.3 Regeneration

The conditions of the regeneration of power back into the system is dependent on the gradient or inclination of the railway track. These are usually achieved when the locomotive is travelling downhill, without accelerating. The AC motors on the bogie act as generators and the traction converter operates in the opposite direction to invert the signal.

The model is set to 25% the current signal used under loading conditions, and this was done, since 100% dynamic braking was assumed, hence one third of the current should be considered fed back into the system. [32] +178A is used to push current back into the system and account for any losses. This is done to ascertain whether the model can be used to accurately depict the harmonic distortion under regeneration, by not saturating at this value. As shown in the table below, the THD follows a similar pattern as the system under loaded conditions. The harmonic distortion is within the allowable 27%.

Table 19: THD Values under Regenerative conditions

Distance (km)	**THD at Tap 1 (%)**	**THD at Tap 2 (%)**	**THD at Tap 3 (%)**	**THD at Tap 4 (%)**	**THD at Tap 5 (%)**
0,5	16.68	17.77	18.91	19.17	19.76
10	2.14	2.28	2.40	2.55	2.64
15	8.06	8.45	8.87	9.44	9.84
20	6.82	6.85	7.5	7.7	8.25
25	9.02	10.39	10.58	11.91	12.18
29,9	8.66	9.17	9.79	10.71	10.97

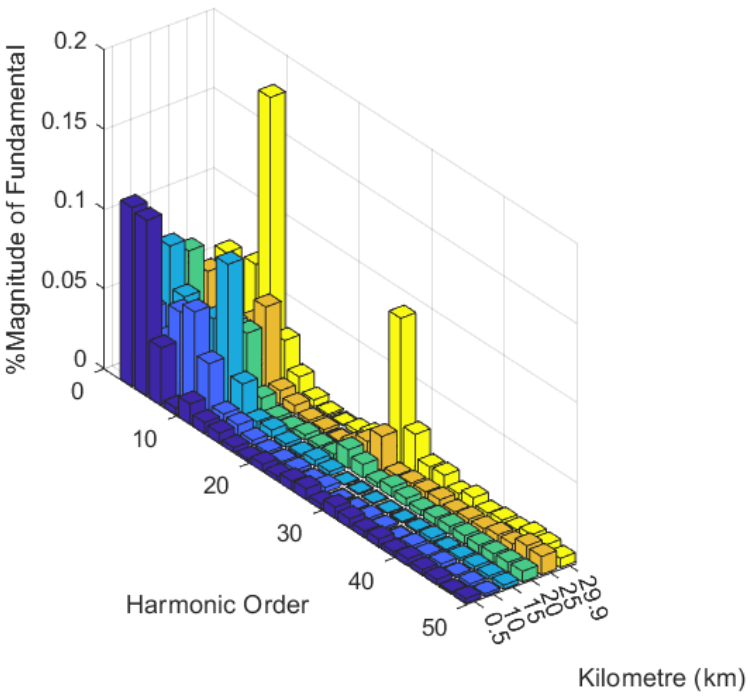

Figure 84: 3D View of Regenerative THD at Varying distances for Tap1

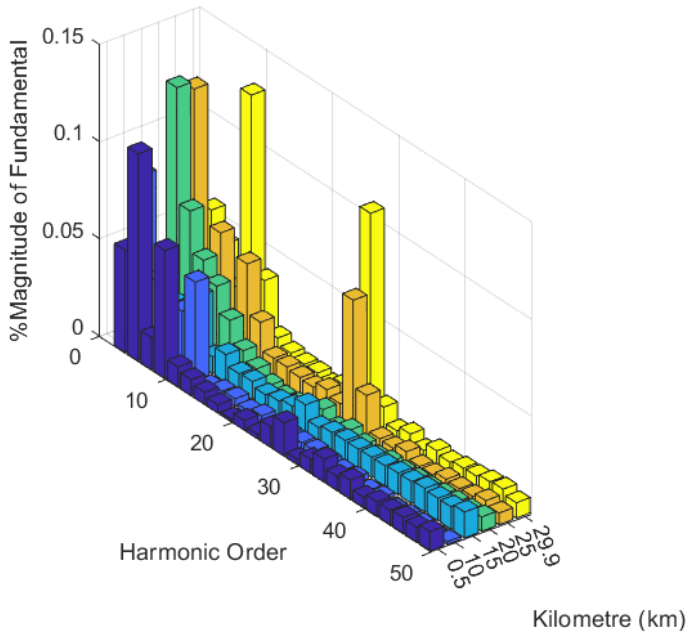

Figure 85: 3D View of Regenerative THD at Varying distances for Tap2

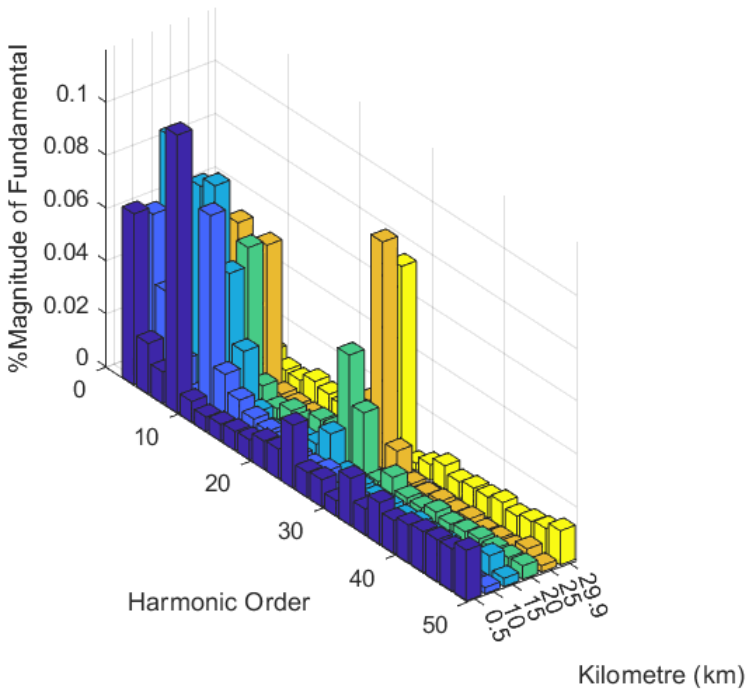

Figure 86: 3D View of Regenerative THD at Varying distances for Tap3

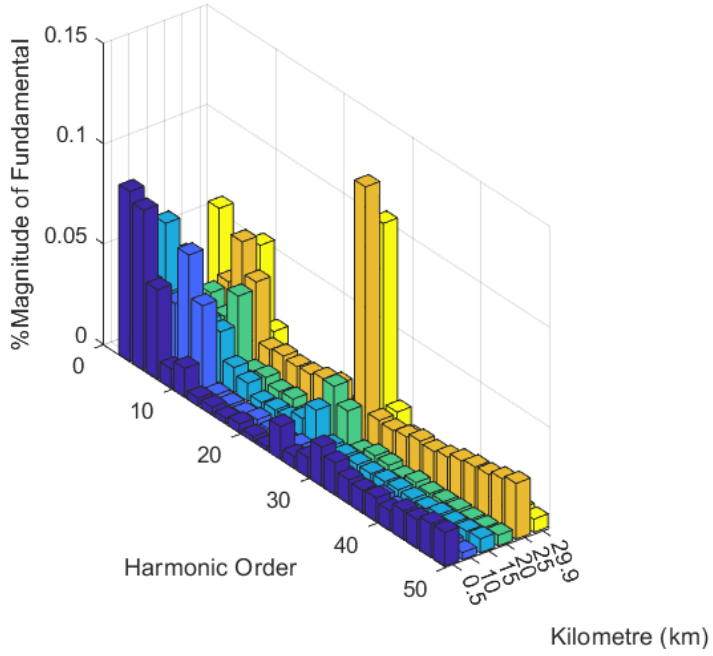

Figure 87: 3D View of Regenerative THD at Varying distances for Tap4

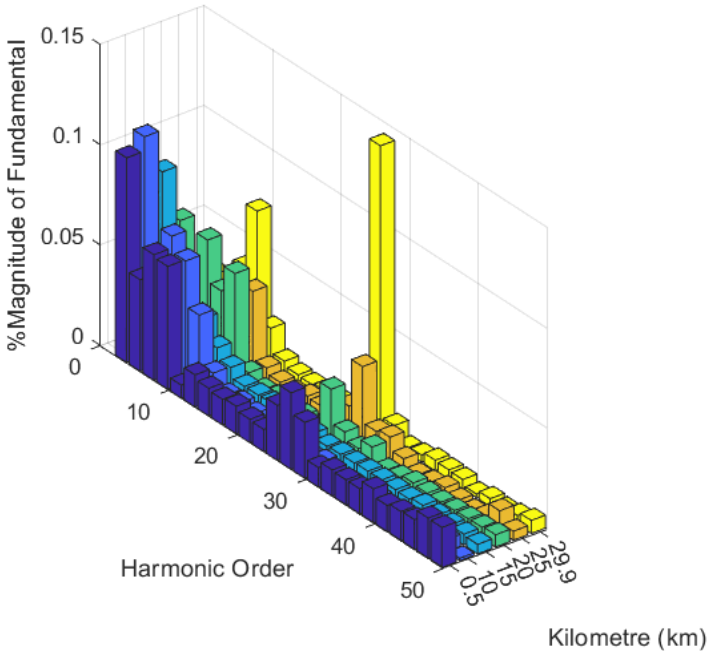

Figure 88: 3D View of Regenerative THD at Varying distances for Tap5

The three-dimensional graphs showing the odd order harmonics per tap changer setting, indicates that the 3rd, 5th, 7th, 9th and 27th order harmonics, are dominant, like for the loaded case. This is verified by the waveforms when the locomotive is at 0.5km away from the traction substation, the plots appear to be similar in nature.

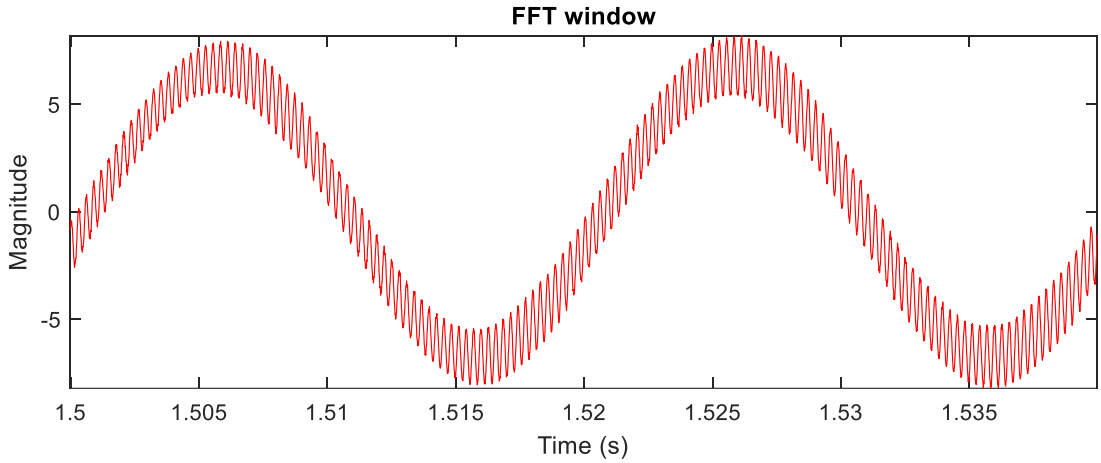

Figure 89: Lineside Current sample under Regenerative conditions for 0.5km at Tap 5

The traction converter outputs at tap changer setting 5 are analysed below. The DC link voltage shows that the converter becomes unstable when the controller attempts to maintain the output of 2.8kV DC. The current also oscillates irregularly.

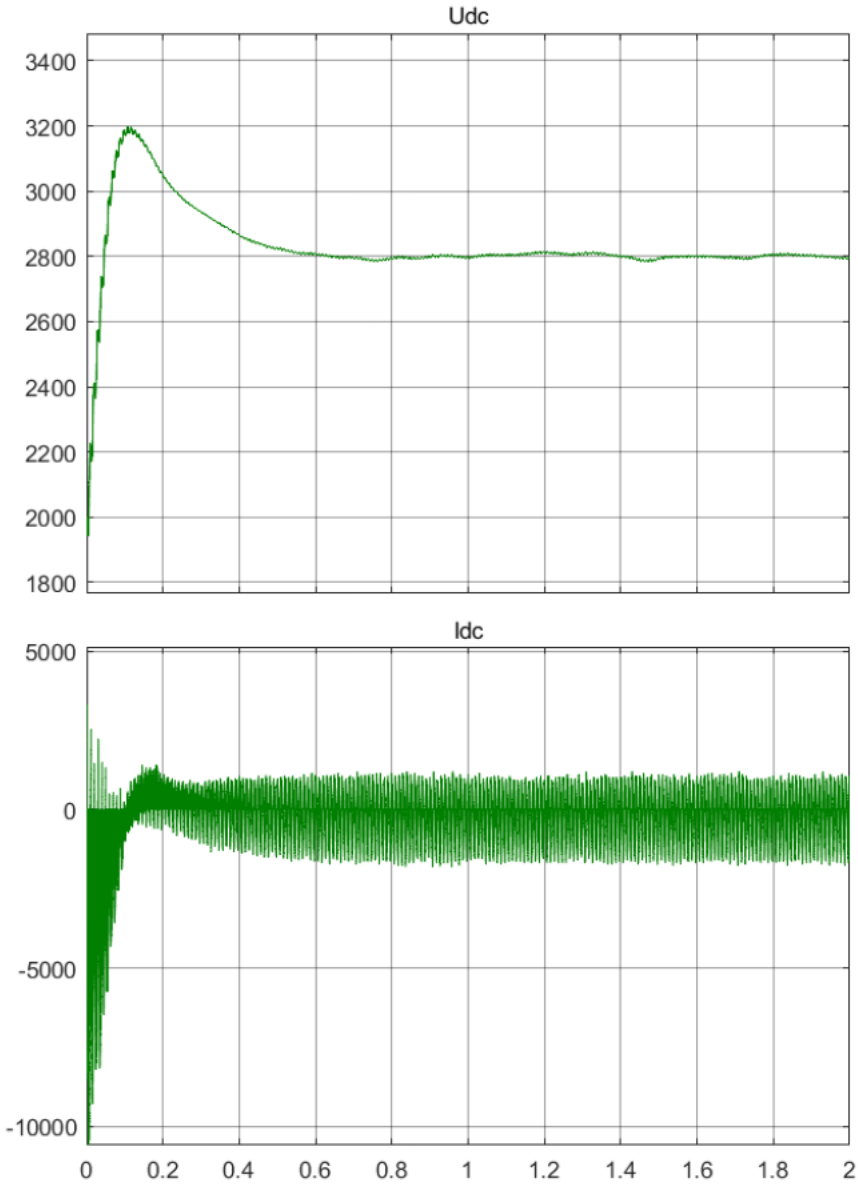

Figure 90: DC Link Voltage and current output of Converter under Regenerative conditions

Under regeneration conditions the line voltage could greatly exceed the maximum of 30kV. In this case if the lineside transformer is set at tap changer 5, which yielded the highest THD value, the transformer

moves towards the saturation region, suggesting that the induced emf is larger at a lower number of winding turns. This essentially increases the induced current exponentially and will hence be transferred to all the lineside equipment connected to the secondary side.

Although comparisons can be drawn between the loaded and regenerative conditions, in that the relationship between the THD calculated and the distance is the same. It needs to be stated that the MATLAB model has simulated ideal regeneration conditions. There are number of external factors to be considered, besides the purely electrical characteristics of the power supply generated from the train and fed back into the system. Aside from the terrain of the railway track, the internal electronic components onboard each locomotive will also contribute to the condition of the regenerated signal. These are known to be extremely sensitive to signal fluctuations and if they aren't protected against them, will have transferred them to the regeneration signal, which will in turn negatively affect the lineside transformer.

6.4 Varying Model Parameters

The total harmonic distortion can be investigated further, through other scenarios, by varying the traction system model parameters. This is done by simulating the train at 0.5km form the traction substation.

6.4.1 Switching Frequency

The switching frequency refers to the rate at which the IGBT's in the converter will operate. By increasing the switching frequency, the converter should perform better, however there will still be issues with the efficiency. All previous simulations were conducted with a switching frequency of 1750Hz. The following cases will show the distortion at switching frequencies of 3750Hz and 4950Hz.

Figure 91, shows the FFT plot when the switching frequency is changed to 3750Hz, whilst the lineside transformer is set to 25kV on the primary side. Since this frequency is greater than the maximum frequency range used throughout this investigation for THD, the limit has been increased to 5kHz. Frequencies between 2kHz and 150kHz is referred to as the supraharmonic region. [33] And according to the figure below, there are harmonics present in this region which will supplement the decrease in life span of the lineside transformer.

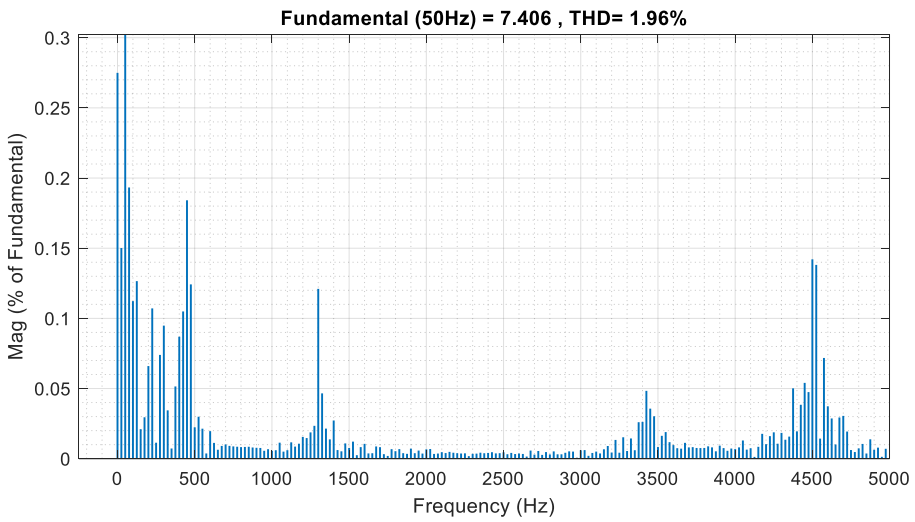

Figure 91: Harmonics Plot when switching frequency is 3750Hz.

Although the THD decreased significantly to 1.96%, after increasing the switching frequency, when the switching frequency is further increased to 4950Hz, it goes up to 2.78%. This is largely due to the increase in the harmonic magnitude. Which is because of the inefficiencies that a higher switching frequency brings and is seen in Figure 92.

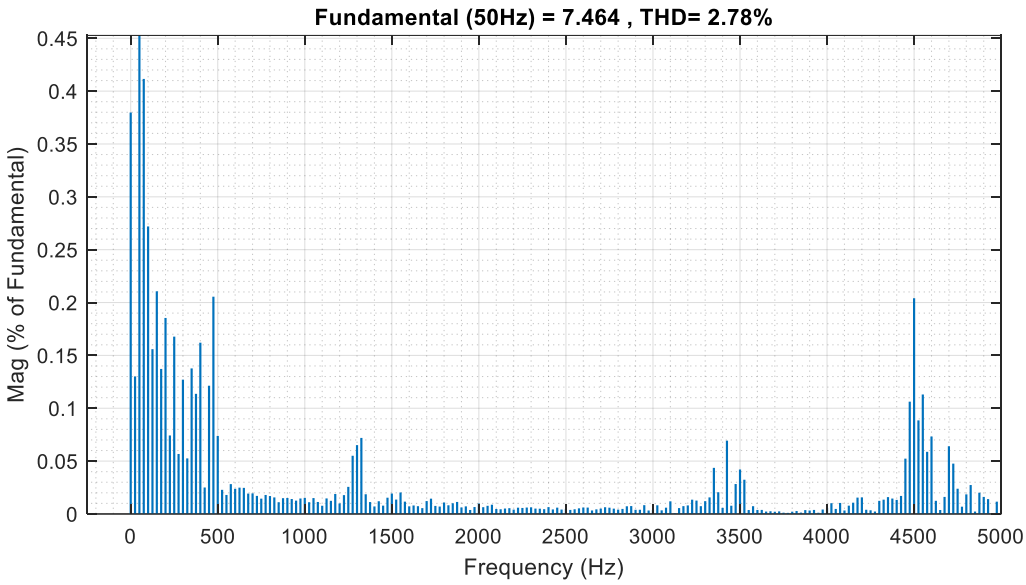

Figure 92: Harmonics Plot when switching frequency is 4950Hz.

The supraharmonics identified in the high frequency region will add to the already identified instabilities in the 25 kV line voltage, during regeneration. This specifically becomes a cause for concern, as the voltage supplied to the line by dynamic braking will affect not only the lineside transformer, but all the equipment it supplies. Essentially, the longevity of all the electrical components, especially the trackside monitoring equipment will be in jeopardy and need to be maintained or replaced more frequently.

6.4.2 Fault level

Next, the source fault level is increased to 100 MVA, whilst reverting the switching frequency to 1750Hz. This returned a THD of 9.56%. Which indicates that although increasing the fault level is known to reduce the harmonics in the system, by allowing the load to draw more current, this does not necessarily diminish the train on the line. Again, the early order harmonics are noted to be significant and the 3^{rd}, 5^{th}, 7^{th}, 9^{th} and 27^{th} order harmonics, have the highest magnitude.

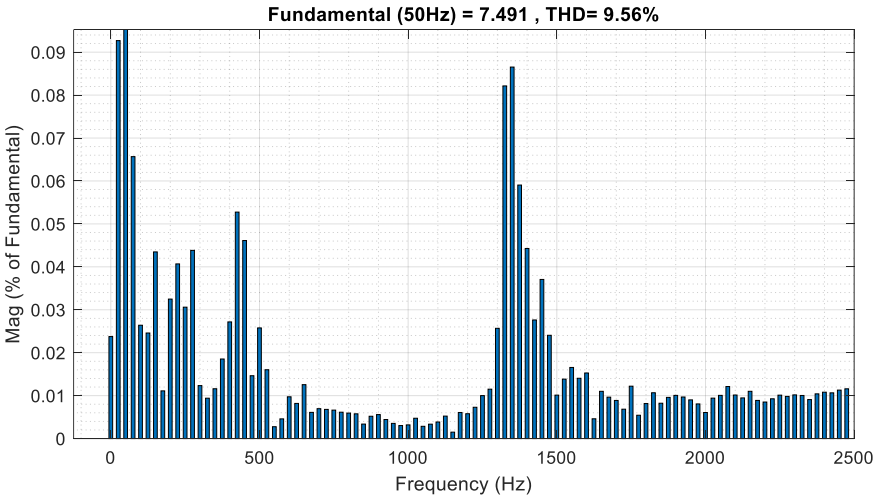

Figure 93: Harmonics Plot when fault level is at 100 MVA.

6.4.3 Overvoltage

To simulate the over voltage worst case conditions, the traction transformer output was changed from 25kV to 27.5kV. the THD has risen to 20.59% and the early order harmonics are again the contributing factors to this. The magnitude in the distortion has increased due to the lineside transformer not being equipped to manage the sudden surge in supply voltage at an operating voltage of 25kV.

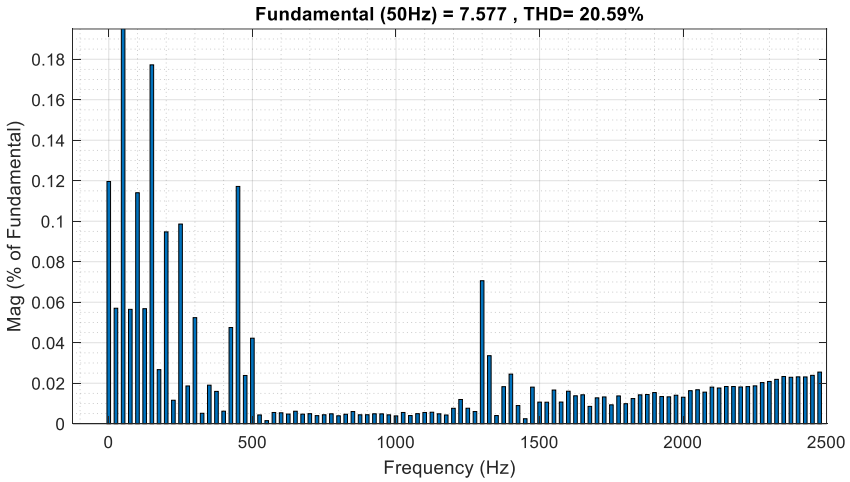

Figure 94: Harmonics Plot at Overvoltage conditions

The purpose of this section was to determine the harmonics experienced by the lineside transformer, which are the most prevalent in different situations. And in all cases, these were found to be the 3rd, 5th, 7th, 9th and in some cases the 27th orders, also keeping in mind that supraharmonics are apparent after 3kHz with higher switching frequencies.

To further illustrate the impact of the harmonics, tap changer is set to 1, which is the lowest operating voltage, and the system is pushed into regeneration, in order to analyse the effects on the transformer's magnetising current. The distance from the traction substation is again set to 0.5km, since this is the point at which the transformer experiences the largest amount of distortion, and the load is disconnected.

Figure 95 shows the magnetising current of the lineside transformer at the lowest tap setting, whilst the system is experiencing an overvoltage. It is noted that there are additional harmonics in the magnetising current waveform. The magnitude of the current is extremely high, compared to no load conditions, when there are no harmonics present. The difference between the two plots indicates an increase of approximately 70%, due to harmonics.

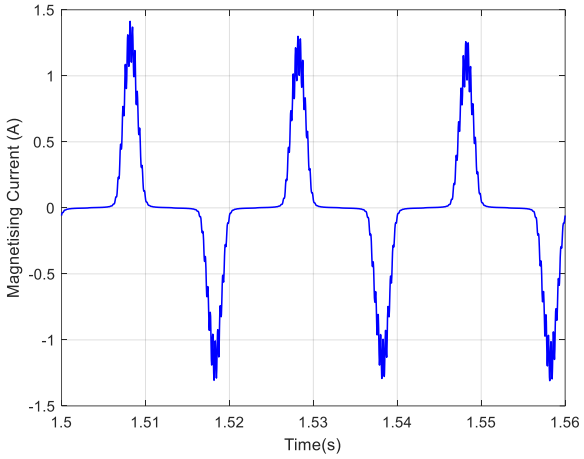

Figure 95: Magnetising current of Lineside transformer at Tap 1 at 0.5km

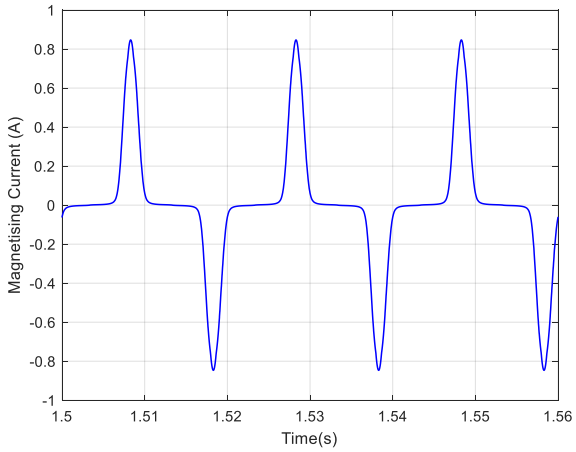

Figure 96: Magnetising current of Lineside transformer at Tap 1 at 0.5km at no load

Figure 97 indicates that although the magnitude of these spikes are lower, they are still present in the transformer. These harmonics will eventually increase the power losses in the transformer, as is seen as an additional source.

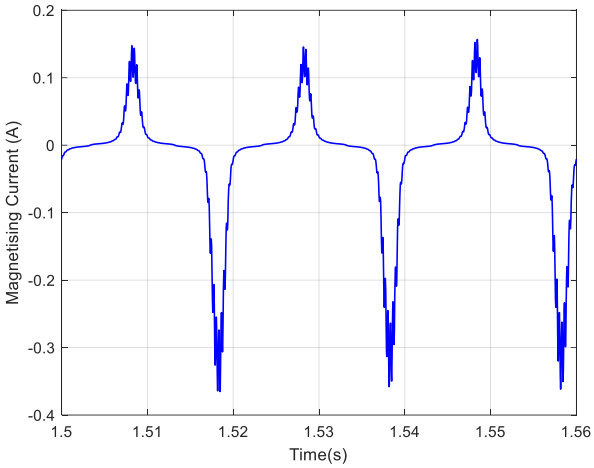

Figure 97: Magnetising current of Lineside transformer at Tap 5 at 0.5km

7 Conclusion

The conclusion to this investigation into the voltage disturbances experienced by the lineside transformer yielded that a specification of the transformer needs to be developed, which is applicable to rail engineering.

During the study of the transformer in chapter 4, it was found that the design flux density level is one of the primary parameters that needs to be accurately stated. This affects the overall function of the transformer and whether it can operate at overvoltage conditions, should they arise. The lineside transformer should, therefore, be rated at 27.5kV/230V instead of 25kV/230V or at a nominal voltage of 44kV. The insulation level also needs to be stipulated, and the corresponding lightning impulse withstand voltage should be 250kV for overvoltage's.

The model is tested at varying distances and tap changer settings from the traction substation, simulating the movement of the train throughout the section. It is found that the highest distortion experienced by the lineside transformer is at 0.5km. This is largely due to the train being in close proximity to the traction transformer in the substation, at the start of the 30km section. The distortion calculated tends to increase in both loaded and regenerative instances, the position of the tap changer increases. As explored, these relationships are not uniform and are dependent on a number of factors.

The harmonics experienced also need to be included in the specification. The most prevalent orders are at the 3^{rd}, 5^{th}, 7^{th}, 9^{th} and the 27^{th}. Although increasing the switching frequency improves the THD, supraharmonics beyond 2500Hz should be noted as possibly affecting the transformer, as well as the presence of transformer resonance after 6kHz.

To reiterate, the following conditions need to be met when developing the lineside transformer specification.

- The flux density design level should ideally be 1.5 T and lower.
- The rated operating voltage should be 27.5kV or the nominal voltage should be 44kV.
- The LIWL rating should be 250kV.

- All harmonics experienced, including those at higher frequencies need to have a THD lower than 5%, according to IEEE 519.

The following aspects should be considered for future work.

- Regeneration characteristics need to be drawn out and analysed in further detail and the possibility of storing the voltage pushed back into the system needs to be investigated. This would aid the trackside equipment and other clients in reducing their consumption from the substation.

- The effects of the terrain gradients and varying train lengths should be simulated. Here, the determination of a tractive effort curve necessary. This will indicate the loading constraints on the traction substation, as well as additional disturbances in supply to the lineside transformer.

References

[1] F. Ajum, C. Godinho, J. Burton, B. McCall and A. Marquad, “A Low-Carbon Transport Future for South Africa: Technical,” Energy Systems Research Group, University of cape Town, 2020.

[2] Transnet, “Rail Development Plan,” Transnet SOC, 2016.

[3] S. Frey, Railway Electrification Systems and Engineering, Delhi: White Word Publications, 2012.

[4] J. J. LaMarca, C. M. King and A. Kusko, “A Survey of Railroad AC Electrification Systems Throughout the World,” U. S Department of Transportation: Federal Railroad Adminstration, Washington, DC, 1979.

[5] W. Sprong, Applying the predictable maintenance approach to DC Traction Substations in South Africa, D.Ing Thesis from University of Johannesburg, 2008.

[6] G. Hailay, Reactive Power Compensation and Harmonic Mitigation in 25 kV AC Railway System Using Shunt Active Filter, MSc Dissertation from Addis Ababa University, 2016.

[7] A. Baxter, Network Rail: A Guide to Overhead Electrification, London, 2015.

[8] Spoornet Infrastructure Electrical, “CEE.0111.99: Specification for 25kV AC traction Substations,” Spoornet, Johanneburg, 1999.

[9] J. M. W. Whiting and H. J. Thompson, “Power converters,” in *The 9th Institution of Engineering and Technology Professional Development Course on Electric Traction Systems*, Manchester, 2006, pp. pp. 101-124..

[10] F. Bordry, “Power converters: definitions, classification and converter topologies,” CERN, Geneva, 2016.

[11] R. D. White, “AC/DC RAILWAY ELECTRIFICATION AND PROTECTION,” in *IET Railway Electrification Infrastructure Systems*, London, 2014.

[12] A. Yuvaraj, “Elimination of Harmonics in Power System Using FFT analysis,” *International Journal of Advanced Research in Computer and Communication Engineering*, vol. 5, no. 11, pp. 468 - 470, 2016.

[13] D. Chapman, “Harmonics Causes and Effects,” Copper Development Association, United Kingdom, 2001.

[14] N. Shah, “Harmonics in Power Systems: Causes, effects and control,” Siemens, Alpharetta, 2013.

[15] M. Khodaparastan and A. Mohamed, “Modeling and Simulation of Regenerative Braking Energy in DC Electric Rail Systems,” in *2018 IEEE Transportation Electrification Conference and Expo*, Long Beach, 2018.

[16] F. Kiessling, R. Puschmann, A. Schmieder and E. Schneider, Contact Lines for Electric Railways: Planning, Design, Implementation, Maintenance, Siemems: Publicis Corporate Publishing, 2009.

[17] A. E. Fitzgerald, C. Kingsley and S. D. Umans, Electric Machinery, Singapore: McGraw-Hill, 2003.

[18] I. P. a. E. Society, “IEEE Recommended Practice for Establishing Liquid Immersed and Dry-Type Power and Distribution Transformer Capability when Supplying Nonsinusoidal Load Currents,” IEEE-SA Standards Board, New York, 2018.

[19] K. B, “Impact of Transformer Inrush Currents on Sensitive Protection Functions,” in *32nd Annual Western Protective Relay Conference*, Washington, 2005.

[20] T. T. Vo, J. Palecek and V. Kolar, “Influence of AC Electric Traction on Harmonic Distortion in 110kV Supply Voltage Network: Measurement and Simulation,” *Electrotechnical Review*, vol. 89, no. 7, pp. 13 - 16, 2013.

[21] H. Hu, Y. Shao, L. Tang, J. Ma, Z. He and S. Gao, “Overview of Harmonic and Resonance in Railway Electrification Systems,” *IEEE TRANSACTIONS ON INDUSTRY APPLICATIONS*, vol. 54, no. 5, pp. 5227 - 5244, 2018.

[22] M. Siranec, A. Bolf, A. Otcenasova, M. Regula and M. Novak, “The Influences of Electrical Traction on Distribution System,” in *13th International Scientific Conference on Sustainable, Modern and Safe Transport*, Slovak Republic, 2019.

[23] C. Sankaran, Power Quality and Reliability - Effects of Harmonics on Power Systems, New York: CRC Press, 1999.

[24] NRS 048-2:2003, “Electricity Supply - Quality of Supply Part 2: Voltage characteristics, compatibility,” 2003.

[25] IEEE, “IEEE 519 - IEEE Standard for Harmonic Control in Electric Power Systems,” IEEE Power and Energy Society, USA, 2022.

[26] SANS 780, “SANS 780: Distribution Transformers,” South African Bereau of Standards, Pretoria, 2009.

[27] IEC, “IEC 60076-3: Power Transformers - Insulation Levels, Dielectric Tests and External Clearances in Air,” IEC, Geneva, 2013.

[28] A. Steel, “Grain Oriented Electrical Steel - Product Data Bulletin,” AK Steel Corporation, West Chester, Revision 04.17.13.

[29] S. Kulkarni and S. Kharpanrde, Transformer Engineering, Marcel Dekker, 2004.

[30] T. Wescott, “PID Without a PhD,” Wescott Design Services, 2000.

[31] M. Shafighy, S. Khoo and A. Kouzani, “Modelling and simulation of regeneration in AC traction propulsion system of electrified railway,” *IET Electrical Systems in Transportation,* vol. 5, no. 4, pp. 145 - 155, 2015.

[32] L. Buhrkall, “TRACTION SYSTEM CASE STUDY,” *Traction Systems and EMC,,* vol. 7, 2004.

[33] C. Waniek, T. Wohlfahrt, J. Myrzik, J. Meyer, M. Klatt and P. Schegner, “Supraharmonics: Root Causes and Interactions between multiple devices and the low voltage grid,” in *2017 IEEE PES Innovative Smart Grid Technologies Conference Europe (ISGT-Europe)*, Turin, 2017.

[34] “JICA,” Japan International Corporation Agency, [Online]. Available: https://openjicareport.jica.go.jp/pdf/12112959_02.pdf. [Accessed 17 April 2020].

[35] South African Department of Transport, “National Rail Policy - First Draft,” Gauteng, 2017.

[36] Quorum Corporation, “Railway Capacity Background & Overview,” October 2005. [Online]. Available: http://www.quorumcorp.net/Downloads/Papers/RailwayCapacityOverview.pdf. [Accessed 28 June 2020].

[37] B. W. Ring, “www.bwring.net,” 06 March 2004. [Online]. Available: http://www.bwring.net/rail/sar/pyramid_south/pyramid_south.html. [Accessed 24 June 2020].

[38] L. Makhatini, “BBB 8204: Medium Voltage Distribution and Supply Transformers in Accordance with SANS 780,” Transnet Freight Rail, Johannesburg, 2018 (Confidential).

[39] Connor, P, “The Railway Technical Website,” PRC Rail Consulting Ltd., 21 January 1998. [Online]. Available: http://www.railway-technical.com. [Accessed 15 February 2019].

[40] Transnet, “Transnet Freight Rail - Heritage,” 2010. [Online]. Available: http://www.transnetfreightrail-tfr.net/Heritage/150years/150YearsRail.pdf. [Accessed 09 September 2020].

[41] H. Naude, Dynamic modelling of traction loads and renewable energy systems on shared power lines for power quality assessment, MSc Dissertation, Stellenbosch University, 2019.

[42] M. Mandic, I. Uglesic and V. Milardic, “Design and testing of 25kVAC Electric Railway Power Supply Systems,” *Technical Gazette,* vol. 3, no. 20, pp. 505-509, 2013.

[43] D. Manton and J. Middleton, “THE ASSESSMENT AND IDENTIFICATION OF WAGONS, COACHES, LOCOMOTIVES AND TENDERS WHICH MERIT HERITAGE STATUS ACCORDING TO SAHRA CRITERIA AND MUST BE PRESERVED FOR FUTURE GENERATIONS,” Heritage Railway Association of South Africa, Johannesburg, 2011.

[44] Z. Fei, T. Konefal and R. and Armstrong, “AC Railway Electrification Systems – an EMC Perspective,” *IEEE Electromagnetic Compatibility Magazine,* vol. 8, no. 4, pp. 62-69, 2019.

[45] C. Fourie and N. T. Zhuwaki, “A MODELLING FRAMEWORK FOR RAILWAY INFRASTRUCTURE RELIABILITY ANALYSIS,” *South African Journal of Industrial Engineering,* vol. 28, no. 4, pp. 150-160, 2017.

[46] J. Seymour, “The Seven Types of Power Problems,” 16 April 2010. [Online]. Available: https://www.se.com/za/en/download/document/SPD_VAVR-5WKLPK_EN/. [Accessed 12 October 2019].

[47] E. Andersson, “Energy Efficiency Technologies for Railways,” International Union of Railways, 02 December 2002. [Online]. Available: https://www.railway-energy.org/static/Regenerative_braking_in_50_Hz__25_kV_systems_104.php. [Accessed 03 11 2020].

[48] T. Wildi, Electrical Machines, Drives and Power Systems, New Jersey: Pearson Education, 2006.

[49] S. Gopalan, “Design and Control of Single Phase PWM,” *International Journal of Advanced Research in Electrical,,* vol. 4, no. 6, p. 2278 – 8875, 2015.

[50] A. A. Elmoudi, Dissertation: Evaluation of Power System Harmonic Effects on Transformers, Finland: Helsinki University of Technology, 2006.

[51] ABB, “Application Guide: Harmonics in HVAC applications,” ABB, 2018.

[52] Transnet, “Transnet Freight Rail,” [Online]. Available: https://www.transnetfreightrail-tfr.net/Heritage/150years/150YearsRail.pdf. [Accessed 22 December 2022].

[53] U. Kotaro, “Power Electronic Devices for Railway Vehicles,” *FUJI ELECTRIC JOURNAL,* vol. 85, no. 3, pp. 175 - 181, 2012.

[54] M. Ahmed, “Simulation and Experimental Verification of Single-Phase PWM Boost -Rectifier with Controlled Power factor,” *International Research Journal of Engineering and Technology,* vol. 4, no. 3, pp. 1689 - 1693, 2017.

[55] Energy Networks Association, P 24: AC Traction Supplies to British Rail, London: Engineering Directorate, 1990.

[56] S. A. Deokar and L. M. and Waghmare, “Impact of Power System Harmonics on Insulation Failure of Distribution Transformer and its Remedial Measures,” in *3rd International Conference on Electronics Computer Technology,* Kanyakumari, India, 2011.

[57] C. V. Tharani, M. Nandhini, S. R and K. Nithiyananthan, “MATLAB based Simulations model for three phases Power System Network,” *International Journal for Research in Applied Science & Engineering Technology,* vol. 4, no. 11, pp. 502 - 509, 2016.

[58] M. Salih, A. K. W and M. Nayef, “Practical Analysis of Harmonics Effects on Transformer,” *Elixir Renewable Energy,* vol. 70, pp. 24362 - 24367, 2014.

[59] D. M. Said and K. M. Nor, “Effects of Harmonics on Distribution Transformers,” in *Australasian Universities Power Engineering Conference,* Sydney, NSW, Australia, 2008.

[60] S. Rustemli, I. Demir and M. Akdag, “Modelling and analysis of line-to-line short circuit fault in 154 kV high-voltage substation,” Bitlis Eren Univ J Sci & Technol, Bitlis, Turkey, 2016.

[61] O. Faten and F. A. Ammar, “Compensation of harmonic disturbances in the Tunisian SAHEL railway supply system,” in *International Conference on Electrical Engineering and Software Applications*, Hammamet, Tunisia, 2013.

[62] A. Bellini, S. Bifaretti and S. Costantini, “High Power Factor Converters For Single-phase AC Traction Drives,” in *Computers in Railways VIII*, Genova, Wessex Institute of Technology, 2002, pp. 559 - 568.

[63] R. Aceiton, J. Weber and S. Bernet, “Validation of a State Composer Algorithm for a Cascaded Multicell Converter via Real-Time Simulation,” in *2018 International Symposium on Power Electronics, Electrical Drives, Automation and Motion (SPEEDAM),* Amalfi, 2018.

[64] Japan International Co operation Agency, “Joint Feasibility Study for Mumbai-Ahmedabad High Speed Railway Corridor,” Delhi, 2015.

[65] W. Jefimowski and A. Szeląg, “Assessment of AC Traction Substation Influence on Energy Quality in a Supply Grid,” *Technical Transactions 12/2018 Electrical Engineering,* vol. 12, pp. 127 - 138, 2018.

[66] V. Matta and G. Kumar, “Unbalance and Voltage fluctuation study on AC Traction System,” in *International Conference on Computation of Power, Energy, Information and Communcation*, Chennai, India, 2014.

[67] N. John, J. James and D. E. Koshy, “The Concept Of Power Electronic Traction Transformer For Indian Railway,” in *International Conference on Control, Power, Communication and Computing Technologies*, Kerala, India, 2018.

[68] N. Raval, S. N. Shivani and M. K. Kathiria, “AC Traction Power Line Fault Analysis and Simulation,” *International Journal of Innovative Research in Electrical, Electronic, Instrumentation and Control Engineering,* vol. 4, no. 4, pp. 258 - 261, 2016.

[69] B. Milesevic and I. Uglesic, “Inductive Influence 0f 25 kV, 50 Hz Electrified Single Rail Traction System,” in *13th International Conference Modern Electrified Transport – MET’2017*, Warsaw, Poland, 2017.

[70] E. Cazacu and L. Petrescu, “Inrush Current Investigation for Single Phase Power Transformers by Means of Magnetic Material Core Characteristics,” *UPB Scientific Bulletin, Series C: Electrical Engineering and Computer Science,* vol. 77, no. 2, pp. 193 - 204, 2015.

[71] S. G. Abdulsalam, W. Xu, W. L. A. Neves and X. Liu, “Estimation of Transformer Saturation Characteristics from Inrush Current Waveforms,” *IEEE TRANSACTIONS ON POWER DELIVERY,* vol. 21, no. 1, pp. 170 - 177, 2006.

[72] A. D. Theocharis, J. Milias-Argitis and T. Zacharias, “Single-phase transformer model including magnetic hysteresis and eddy currents,” *Electrical Engineering,* pp. 229 - 241, 2008.

Appendices

Appendix A : MATLAB CODE

A.1. Controller Waveforms

```
figure
plot(signals.time,signals.signals(1).values, 'b','LineWidth',1)
hold on
plot(signals.time,signals.signals(2).values, 'k','LineWidth',1)
hold on
plot(signals.time,signals.signals(3).values,'r','LineWidth',1)
hold on
plot(signals.time,signals.signals(4).values,'g','LineWidth',1)
hold off
grid on
title('Controller Waveforms')
xlabel('Time(s)')
ylabel('Amplitude')
legend('Step Response','Product','Sum','Gain')


%LineSideTX
figure
plot(LineSideTX.time,LineSideTX.signals(2).values, 'b','LineWidth',1)
%xlim([0 1.5])
grid on
title('V LineSide Transformer HV')
xlabel('Time(s)')
ylabel('Voltage (V)')

%UDC
figure
plot(Loco1.time,Loco1.signals(5).values, 'b','LineWidth',1)
xlim([0 2.5])
grid on
title('DC Voltage')
xlabel('Time(s)')
ylabel('Voltage (V)')
```

A.2. FFT Analysis

```
clear


FFTDATA = power_fftscope(LineSideTX);   % call LTX scope signals
FFTDATA.input = 2;                      % V_LineSide Transformer HV
FFTDATA.signal = 1;                     % Only signal 1
FFTDATA.startTime = 1.5;                  % Start

FFTDATA.cycles = 2;                    % number of cycles to run simulation for
(10 fir now)
FFTDATA.fundamental = 50;               % 50 Hz fundamental frequency
FFTDATA.maxFrequency = 5000;
```

```
FFTDATA = power_fftscope(FFTDATA);
power_fftscope(FFTDATA)         %PLOTS FFT
print('-dpng','-r300','FFT V_LineSide Transformer HV 0.5 km.png');        %png
format at 300dpi



%HARMONICS - ODD AND EVEN
y = 1;
H_ODD = zeros(50,2);


for x = 31:20:1000      %row 31 shows 150Hz - 3rd order harmonic; interval of 20
to 5th and so on

    H_ODD(y,1) = FFTDATA.freq(x,1)/50;      %Harmonic order
    H_ODD(y,2) = (FFTDATA.mag(x,1)/FFTDATA.mag(11,1))*100;      %Percentage of
fundamental magnitude

    y = y +1;

end


%Odd Harmonics Plot Code
bar(H_ODD(:,1),H_ODD(:,2));
grid on;
ylim([0 0.4])
xlabel('Harmonic Order')
ylabel('%Magnitude of Fundamental')


str = sprintf('Odd Harmonics - LineSide Transformer HV 0.5 km')
title(str)
print('-dpng','-r300',' ODD HARMONICS V_LineSide Transformer HV 0.5 km.png');


AA = H_ODD(:,1);
AX = [0.5 10 15 20 25 29.9];
Y = AA;
Z = [AB(:,2) AC(:,2) AD(:,2) AE(:,2) AF(:,2) AG(:,2)];
bar3(Y, Z);
set(gca,'xticklabel', AX)
xlabel('Kilometre (km)')
ylabel('Harmonic Order')
zlabel('%Magnitude of Fundamental')
```

A.3. Transformer Model

```
clear;

rating(1) = 32e3;        % VA
rating(2) = 19.41e3;        % Vrms1 VARY
rating(3) = 480;         % Vrms2 VARY
rating(4) = 50;          % Hz

n = rating(2)/rating(3);
```

```
ff = 0.95;               % fill factor;
Bdes = 1.7;
Dia = 40*(rating(1)/1e3)^0.25/1000;
Area = pi*(Dia/2)^2;
Area = 0.8*sqrt(rating(1)/1e3)/4.44/rating(4)/Bdes
Ac = 0.0125;
lc = 0.65;

Vc = Ac*(lc+lc+lc/2);        %m3
Mc = Vc*1000*7.65;           %kg
Qc = 2.7*Mc;                 %VA (2.7VA/kg at 1.7T)
%Qc = 1.21/0.45*Mc;
im2 = Qc/rating(3)           %Ai
Pc = 1.3*Mc                  %W (1.3W/kg at 1.7T)
%Pc = 0.569/0.45*Mc;
ir = Pc/rating(2);           %Ar
ir2 = Pc/rating(3);          %Ar
Rc2 = Pc/ir2^2;
Rc = Pc/ir^2;

Et = 1*sqrt(rating(1)/1e3)
phim = Et/4.44/50
Area2 = phim/Bdes/ff

core(1) = Ac*ff;          % Core/limb cross sectional area [m2]
core(2) = Ac/2*ff;        % Return limb cross sectional area [m2]
core(3) = Ac/2*ff;        % Return limb cross sectional area [m2]
core(4) = lc;                % Core length [m]
core(5) = lc;                % Yoke length [m]
core(6) = lc;             % Limb length [m]
core(7) = sqrt(Ac*ff);          % Core depth [m]
core(8) = 1e-5;                % Length gap [m]

winding(1) = 0.0225;      % Winding 1 thickness [m]
winding(2) = 0.015;       % Winding 2 thickness [m]
winding(3) = 0.015;       % Gap between windings [m]
winding(4) = 0.005;       % Gap between core and winding [m]
winding(5) = 0.182;       % Winding 1 length [m]
winding(6) = 0.325;       % Winding 2 length [m]
winding(7) = 2;          % Current density [A/mm2]
winding(8) = 59;          % Conductivity of Cu [MS/m]
%winding(8) = 35;         % Conductivity of Al [MS/m]
winding(9) = 0.0607;      % Mean area of winding 1
winding(10) = 0.0264;     % Mean area of winding 2

windinga(1) = 0.0225;     % Winding 1 thickness [m]
windinga(2) = 0.020;      % Winding 2 thickness [m]
windinga(3) = 0.010;      % Gap between windings [m]
windinga(4) = 0.005;      % Gap between core and winding [m]
windinga(5) = 0.164;      % Winding 1 length [m]
windinga(6) = 0.183;      % Winding 2 length [m]
windinga(7) = 2;         % Current density [A/mm2]
winding(8) = 59;          % Conductivity of Cu [MS/m]
%windinga(8) = 35;        % Conductivity of Al [MS/m]
windinga(9) = 0.0607;     % Mean area of winding 1
windinga(10) = 0.0264;    % Mean area of winding 2

% b(1) = 1.3;           % Peak mag flux density [T]
```

```
% b(2) = 1.5;           % Saturated mag flux density [T]
% b(3) = b(1)/2;        % Residual mag flux density [T]

ba(1) = 1.7;              % Peak mag flux density [T]
ba(2) = 2;                    % Saturated mag flux density [T]
ba(3) = ba(1)/10;         % Residual mag flux density [T]

bb(1) = 1.7;
bb(2) = 2;              % Saturated mag flux density [T]
bb(3) = bb(1)/10;       % Residual mag flux density [T]

bc = ba;
bc(1) = 1.7;

load bh_steel2;
%load bh_steel2;
rating(2) = 19.41e3;    %VARY
ratinga = rating;
ratingb = rating;
ratingc = rating;


% This pretty much just selects the turns ratio.
[Na,phia,ima] = static1(ratinga,core,winding,ba,bh_steel2);
[Nb,phib,imb] = static1(ratingb,core,winding,bb,bh_steel2);
[Nc,phic,imc] = static1(ratingc,core,winding,bc,bh_steel2);


Na
Nb
Nc

N = [4118 107];


Na = N;
Nb = N;
Nc = N;

Vthva = ratinga(2)/Na(1)
Vtlva = ratinga(3)/Na(2)
Vtlvb = ratinga(3)/Nb(2)
Vtlvc = ratinga(3)/Nc(2)


% r = 1:3:36;
% s = 2:2:38;

% Ibase = rating(1)/rating(2)*sqrt(2)         % PU rated power / rated voltage
% phibase = rating(1)/4.44/50                 % PU flux (Wb)

% I_pu = ima(r)/Ibase;
% phi_pu = phia(r)*2/1.3/max(phia);
%
% MAG(:,1) = I_pu;
% MAG(:,2) = phi_pu;

v_min = rating(2)%*(1-0.05);
v_max = 2*4.44*50*core(1)*Na(1)/1000;
```

```
v_op = ba(1)*ones(length(ima),1)*4.44*50*core(1)*Na(1)/1000;;
v_over = 1*v_op;
v_under = 19.41e3/v_min*v_op;   %VARY

%fig = figure(1),
% ax1 = axes();
% ax2 = axes('position', ax1.Position);
%
% %linkaxes([ax1,ax2],'x')
%
% plot(ax1,ima*1e3,phia/core(1),imb*1e3,phib/core(1))
% plot(ax2,ima*1e3,phi_op*4.44*50*core(1)*Na(1)/1000)
%
%
% set([ax1,ax2],'Color', 'None', 'Box', 'on')
% set([ax1,ax2], 'YAxisLocation', 'left')
%
% ax1.YTick = 0:0.2:2;
% ax2.Color = 'none';
% ax2.YTickLabel = strcat(num2str(round(ax1.YTick'*4.44*50*core(1)*Na(1)/1000)),{'
'});
% ax2.XLim = ax1.XLim;
%
% ax2.XTick = ax1.XTick;

% ax2.YLimMode = 'manual';
% yl = ax2.YLim;
% ax2.YTick = linspace(yl(1), yl(2), length(ax1.YTick));

%ylabel (ax2,'Voltage (kV)');



figure(1)
yyaxis left
plot(ima*1e3,phia/core(1))
xlabel ('Magnetising Current (mA)');
ylabel ('Flux Density (T)');
grid on
hold on
yyaxis right
plot(ima*1e3,v_op,ima*1e3,v_over,ima*1e3,v_under)
ylabel ('Voltage (kVrms)');
ylim([0 v_max]);
legend('BI Curve for Transformer','Normal Voltage','Overvoltage','Undervoltage')
hold off


%  hold on
%
%  x = [1 1e3];
%  y = [1 2];
%  X = [x,fliplr(x)];
%  Y = [y,fliplr(y)];
%  fill(X,Y,'g','FaceAlpha',0.5,'EdgeColor','none')
%  hold off
```

```
% Na(1) % = 4115
% Nb(1) % = round(Nb(1))

%N(1) = round(N(1)) %5716;
%N(2) = round(N(2)) %60;

% [L_1,Z_pu] = leakage1(rating,core,winding,N)
% [L_1,Z_pua,L_2] = leakage1(rating,core,winding,Na)
% [L_2a,Z_pua,L_2b] = leakage1(rating,core,winding,Nb)

% [R] = winding1(rating,core,winding,N,CA)
% [Ra] = winding1(rating,core,windinga,Na,CA)
% [Rb] = winding1(rating,core,winding,Nb,CA)

dt = 10e-5;
t = 0:dt:1/20;                                  % 0 to 1 sec
td = t(1:length(t)-1);

ratingb(2) = 19.41e3*1.05;      %VARY
ratingc(2) = 19.41e3*0.95;      %VARY


[v_1a,i_ma,L_ma,B_ca,i_ma2] = dynamic1(ratinga,core,winding,ba,bh_steel2,Na,t);
[v_1b,i_mb,L_mb,B_cb,i_mb2] = dynamic1(ratingb,core,winding,bb,bh_steel2,Nb,t);
[v_1c,i_mc,L_mc,B_cc,i_mc2] = dynamic1(ratingc,core,winding,bc,bh_steel2,Nc,t);


% i_rms = sqrt(sum(i_s1.^2)/length(i_s1))*1000
i_rmsa = sqrt(sum(i_ma.^2)/length(i_ma))*1000
i_rmsb = sqrt(sum(i_mb.^2)/length(i_mb))*1000
i_rmsc = sqrt(sum(i_mc.^2)/length(i_mc))*1000

i_rmsa2 = rms(i_ma2)

i_core2 = v_1a/Rc*n;
i_t = (i_core2+i_ma2);



figure(5)
% subplot(3,1,3);
yyaxis left
plot(t,v_1a/1000,t,v_1b/1000,t,v_1c/1000);
xlabel ('Time (s)');
ylabel('Applied Voltage (kV)');
yyaxis right
plot(t,i_ma2,t,i_mb2,t,i_mc2,t,i_t);
ylabel('Magnetising Current (A)');
% %axis([0 0.04 -2 2]);
legend ('Normal Voltage','Overvoltage','Undervoltage')
grid on;

figure(3)
% subplot(3,1,3);
yyaxis left
plot(t,v_1a/n,t,v_1a/n,t,v_1a/n);    % Standardise for verification purposes
xlabel ('Time (s)');
ylabel('Applied Voltage (V)');
yyaxis right
```

```
plot(t,i_ma2,t,i_core2,t,i_t);
ylabel('Current (A)');
% %axis([0 0.04 -2 2]);
legend ('Magnetising Current','Core Loss Current','Total Current')
grid on;


%CURRENT VS VOLTAGE

% LV2 = [128, 240, 299, 327, 403, 420, 444, 471, 480];
% I2rms = [0.1311, 0.1901, 0.2405, 0.2757, 0.4924, 0.6079, 0.9269, 2.2959,
3.3396];
% figure(20)
% plot(I2rms,LV2)
% xlabel('Current (A)')
% ylabel('Voltage (V)')
% %title('Current vs. Voltage')
% grid on
```

Appendix B: Simulation Results - Unloaded System (Locomotive Disconnected)

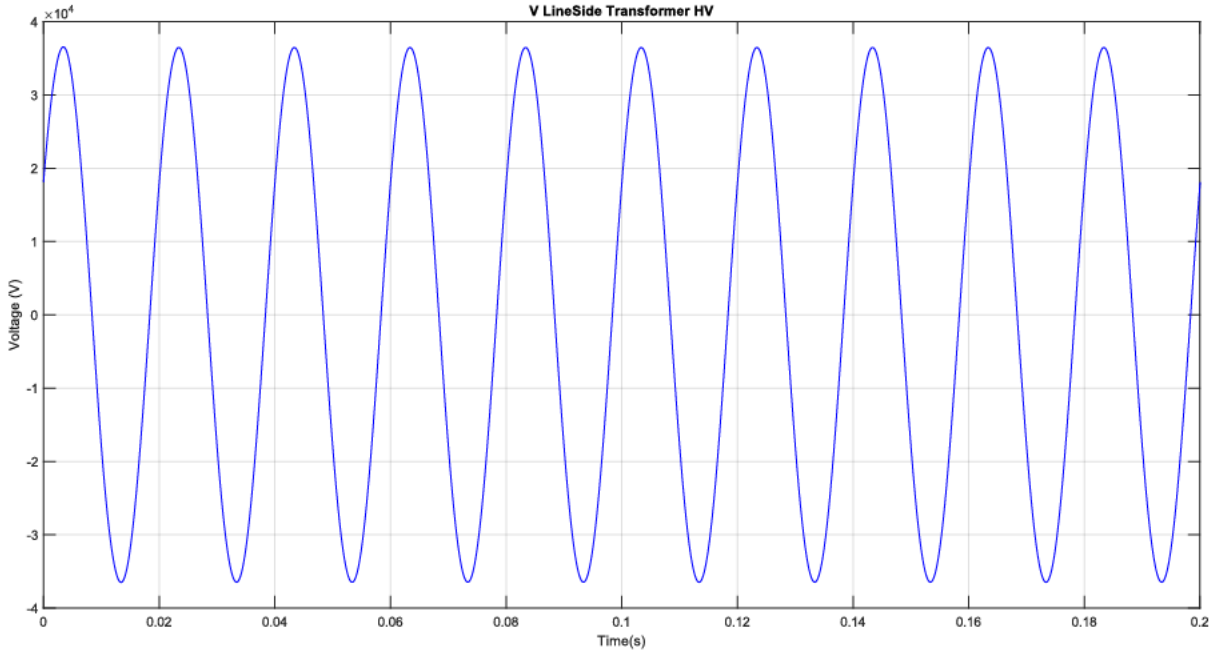

Appendix C: Simulation Results - Loaded System

Distance from Traction Substation = 0.5km

Tap changer setting = 1

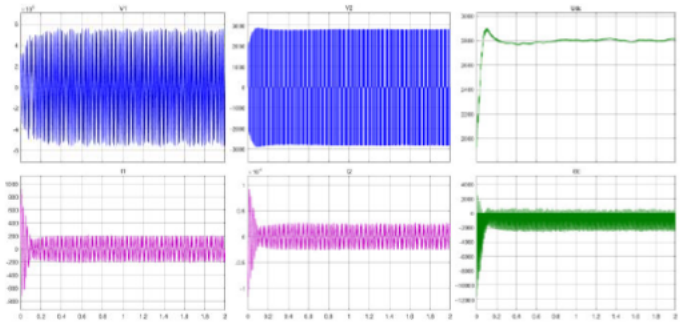

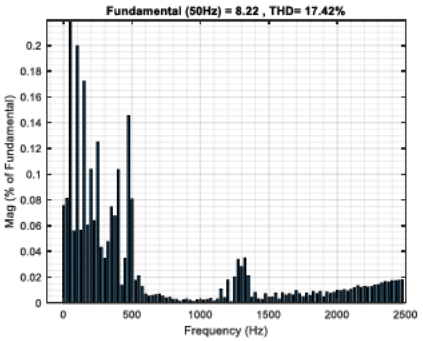

Distance from Traction Substation = 10km

Tap changer setting = 1

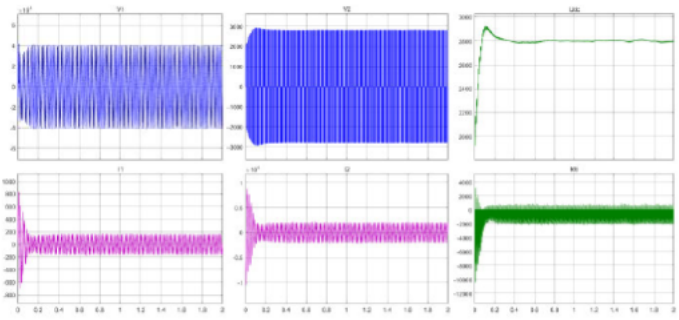

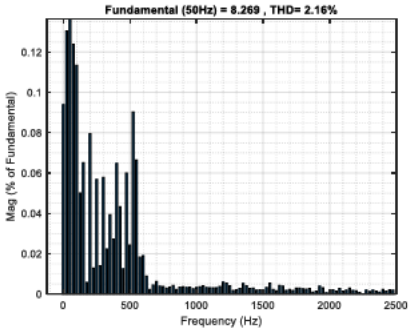

Distance from Traction Substation = 15km

Tap changer setting = 1

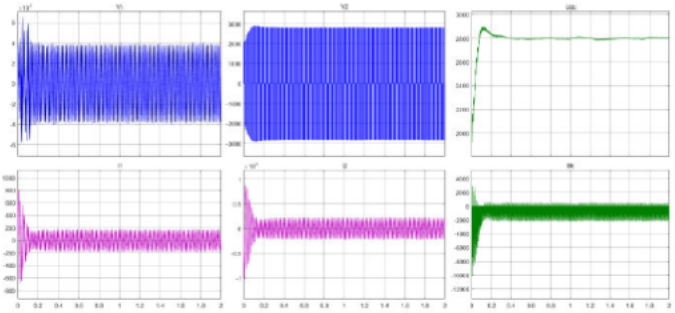

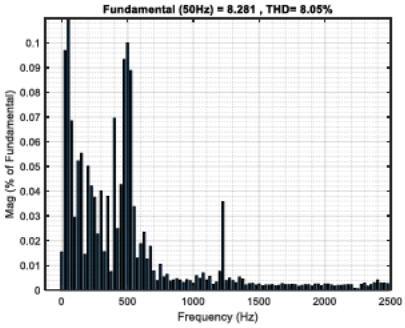

Distance from Traction Substation = 20km

Tap changer setting = 1

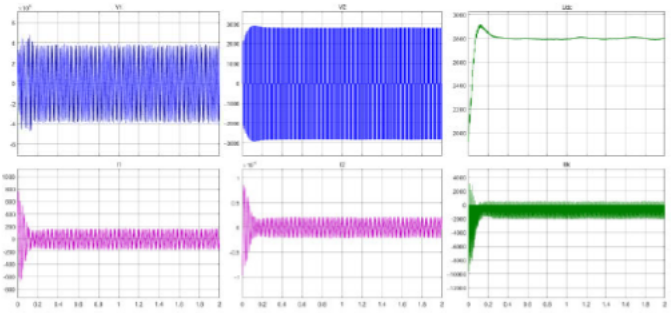

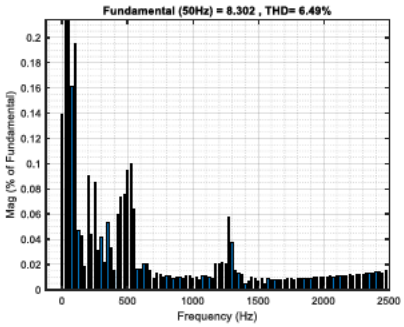

Distance from Traction Substation = 25km

Tap changer setting = 1

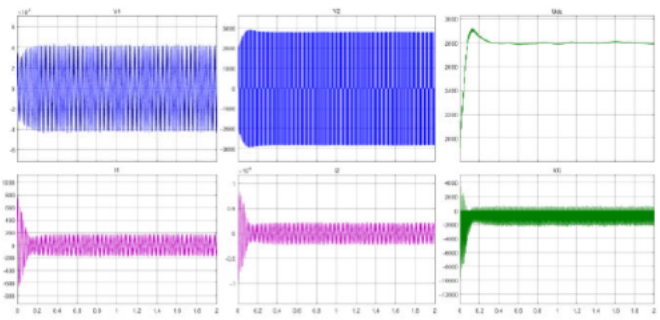

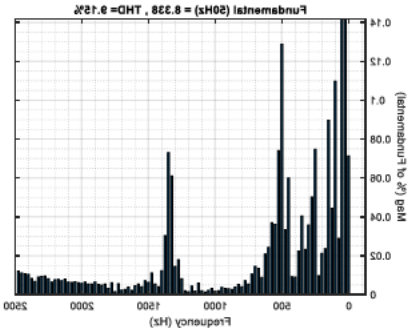

Distance from Traction Substation = 29.9km

Tap changer setting = 1

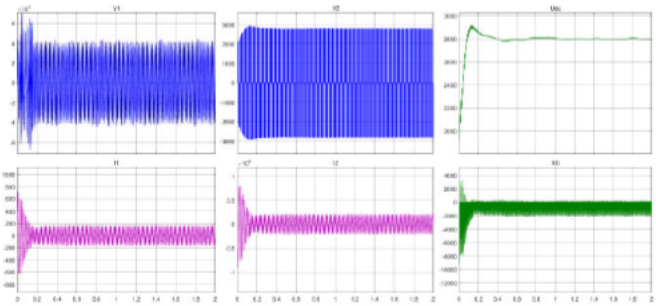

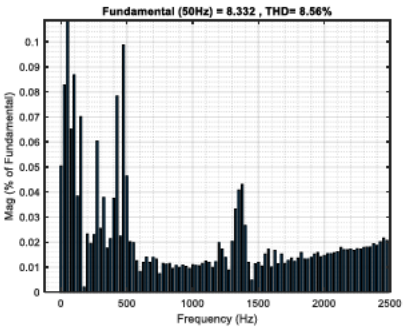

Distance from Traction Substation = 0.5km

Tap changer setting = 2

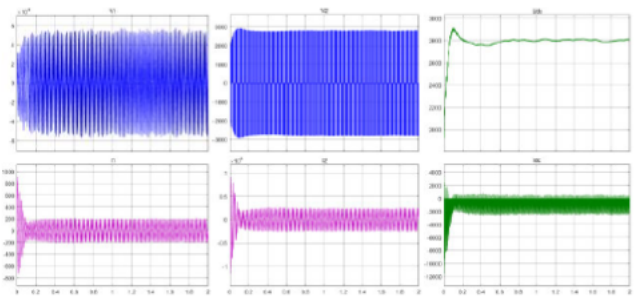

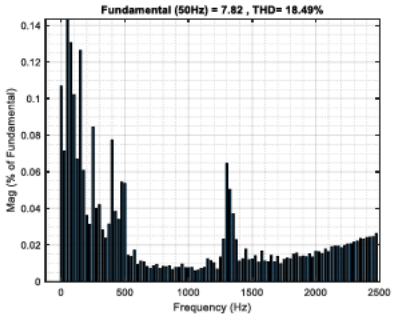

Distance from Traction Substation = 10km

Tap changer setting = 2

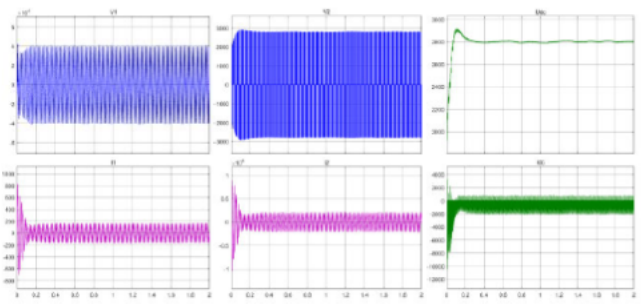

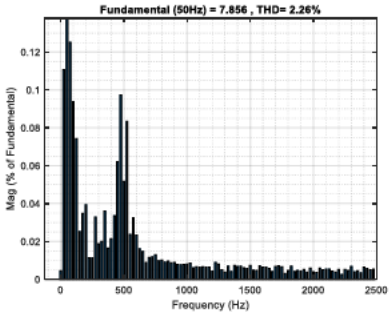

Distance from Traction Substation = 15km

Tap changer setting = 2

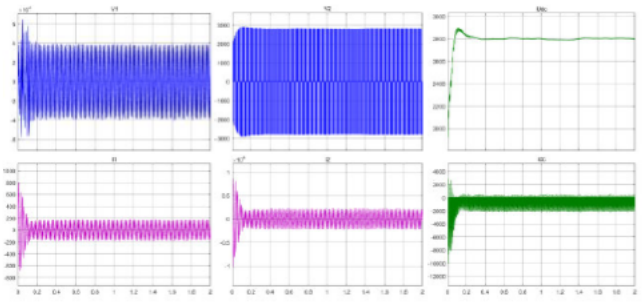

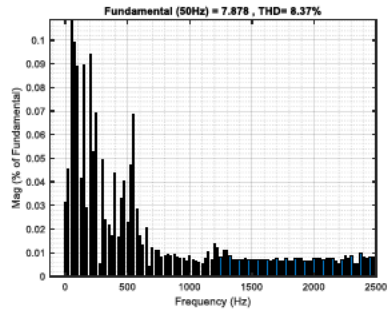

Distance from Traction Substation = 20km

Tap changer setting = 2

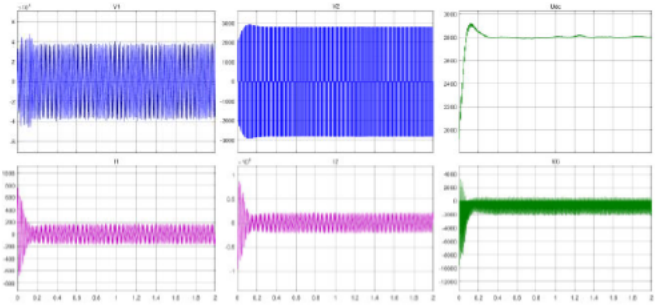

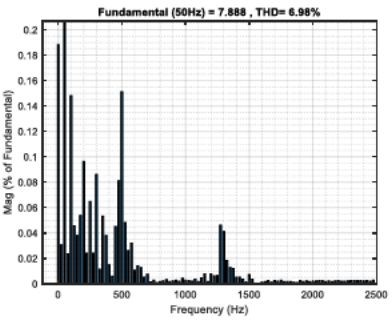

Distance from Traction Substation = 25km

Tap changer setting = 2

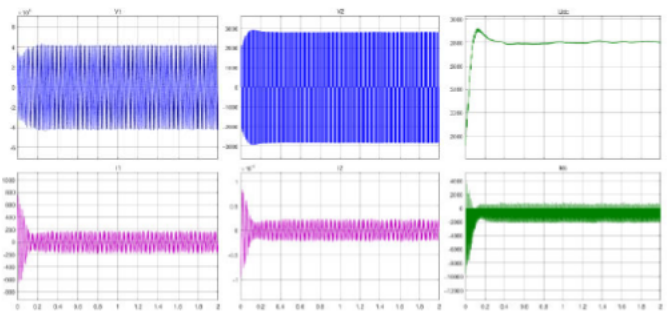

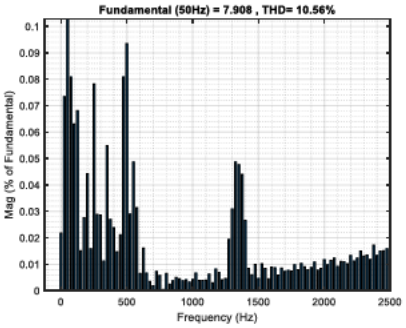

Distance from Traction Substation = 29.9km

Tap changer setting = 2

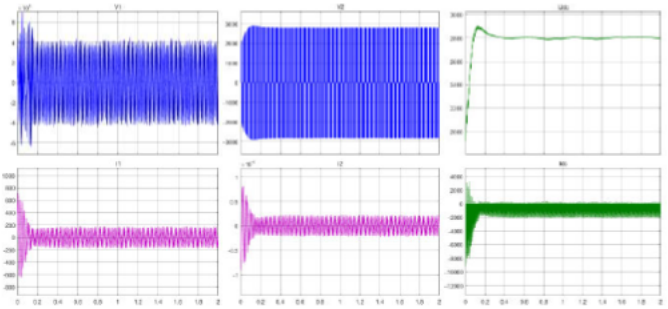

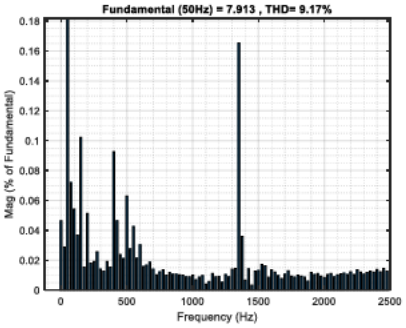

Distance from Traction Substation = 0.5km

Tap changer setting = 3

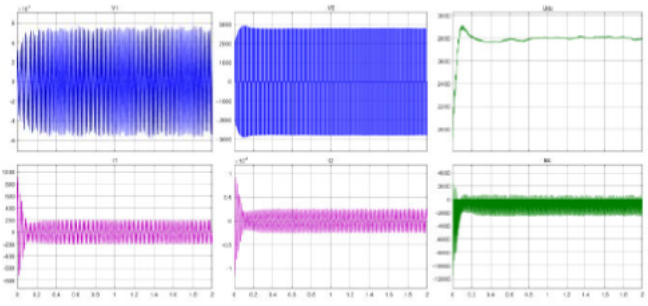

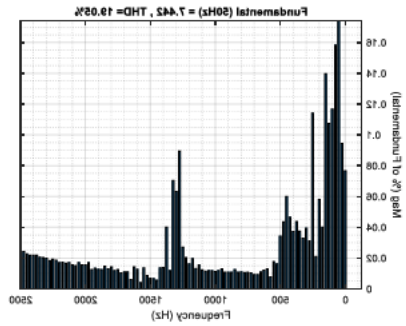

Distance from Traction Substation = 10km

Tap changer setting = 3

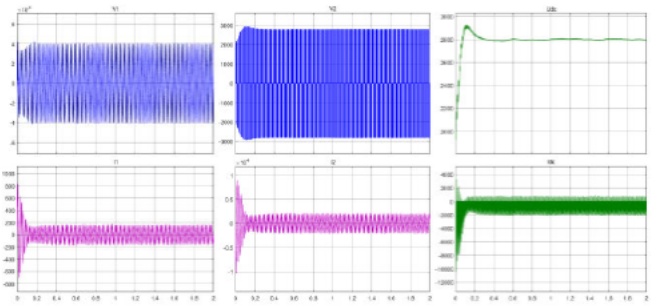

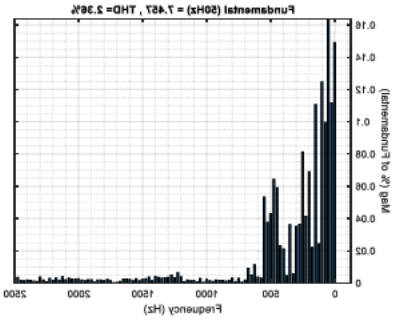

Distance from Traction Substation = 15km

Tap changer setting = 3

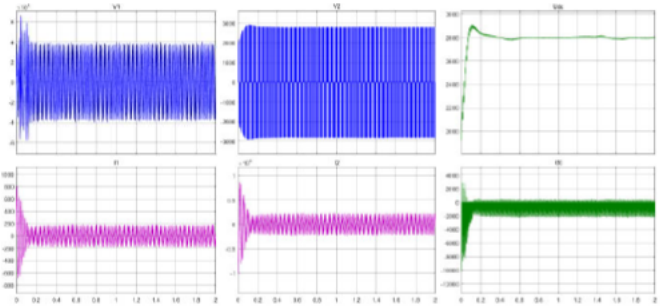

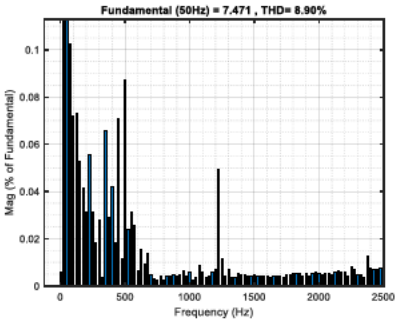

Distance from Traction Substation = 20km

Tap changer setting = 3

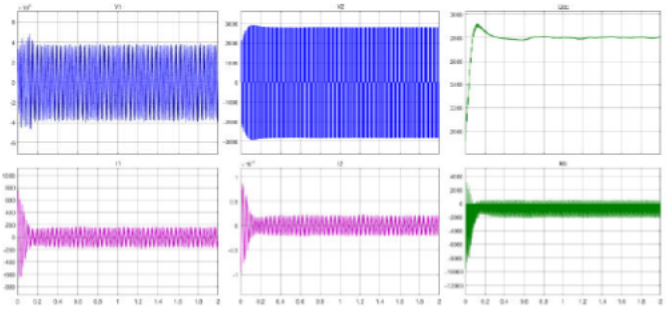

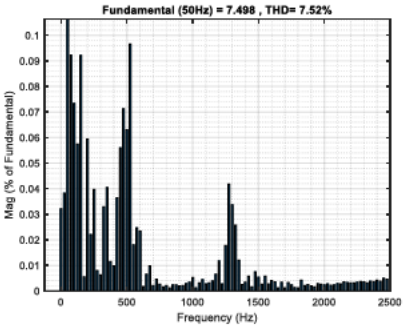

Distance from Traction Substation = 25km

Tap changer setting = 3

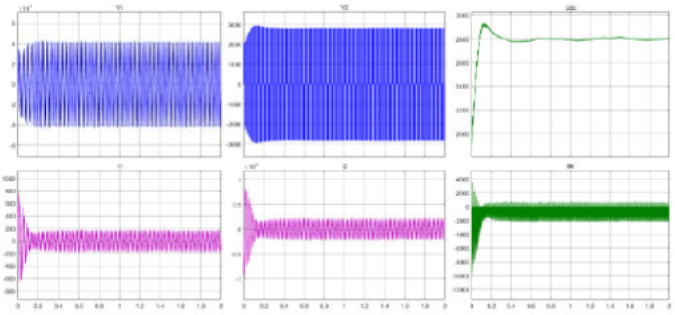

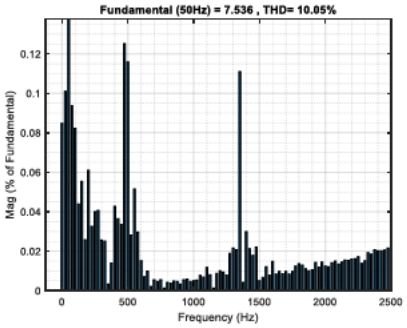

Distance from Traction Substation = 29.9km

Tap changer setting = 3

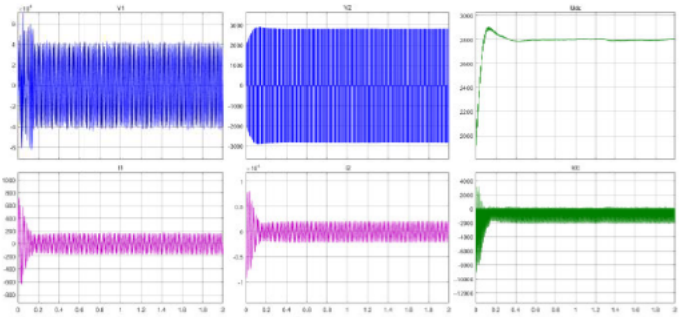

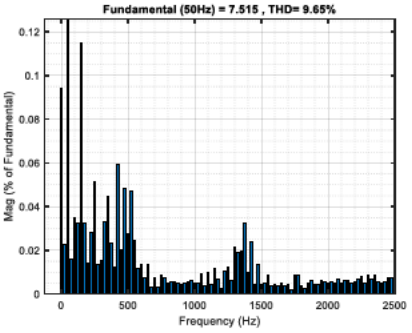

Distance from Traction Substation = 0.5km

Tap changer setting = 4

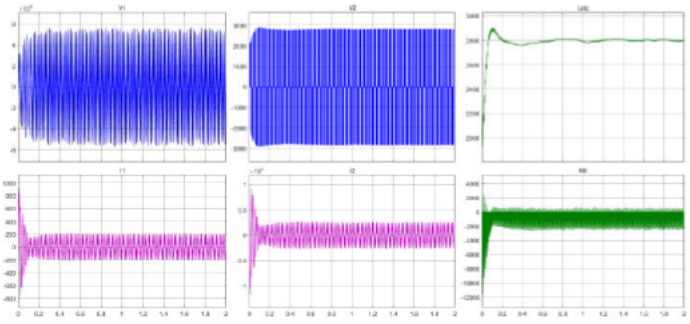

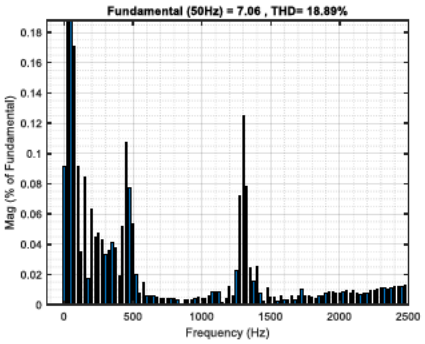

Distance from Traction Substation = 10km

Tap changer setting = 4

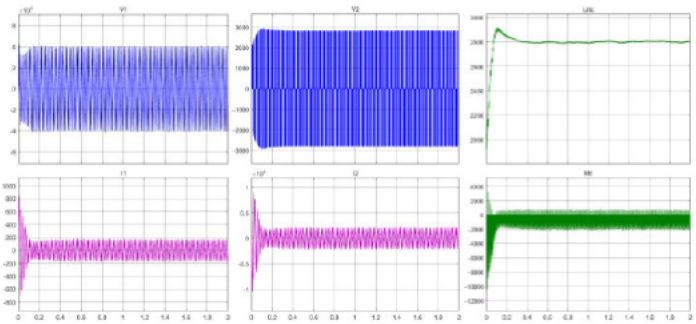

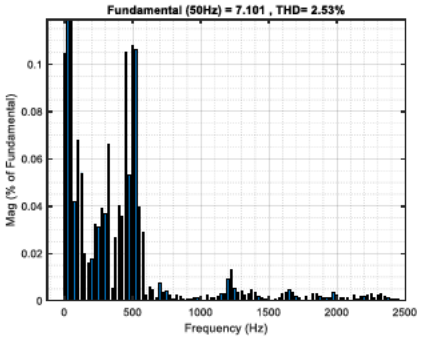

Distance from Traction Substation = 15km

Tap changer setting = 4

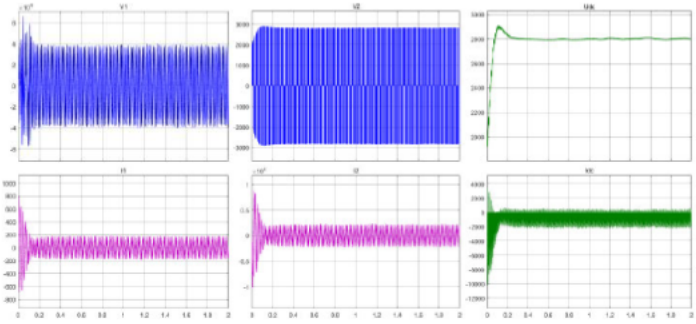

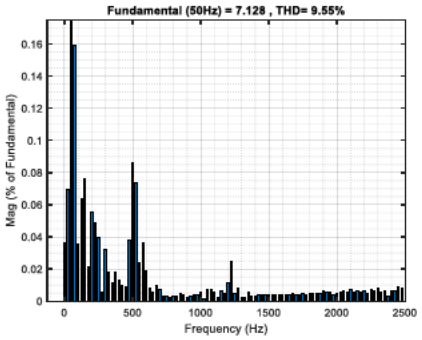

Distance from Traction Substation = 20km

Tap changer setting = 4

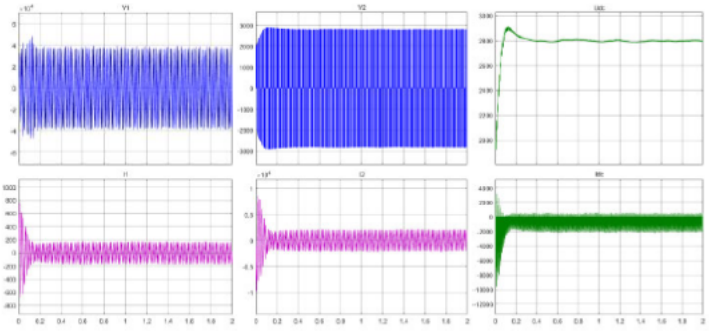

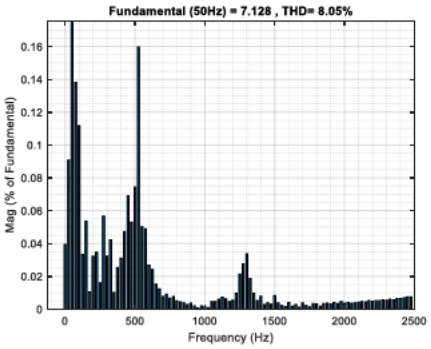

Distance from Traction Substation = 25km

Tap changer setting = 4

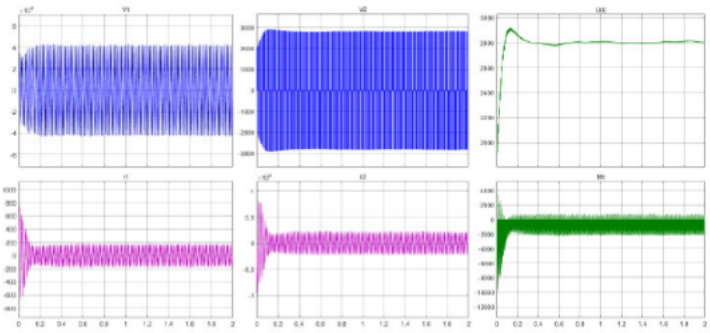

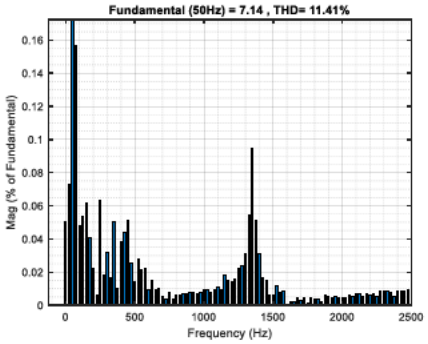

Distance from Traction Substation = 29.9km

Tap changer setting = 4

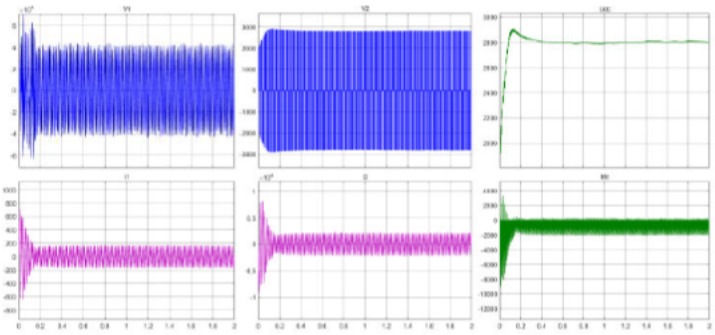

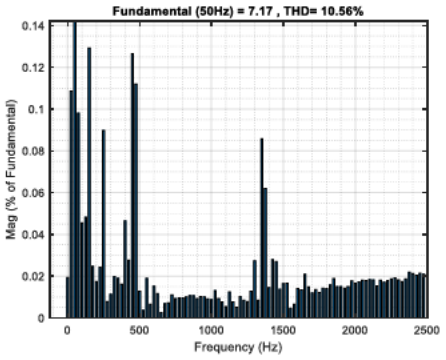

Distance from Traction Substation = 0.5km

Tap changer setting = 5

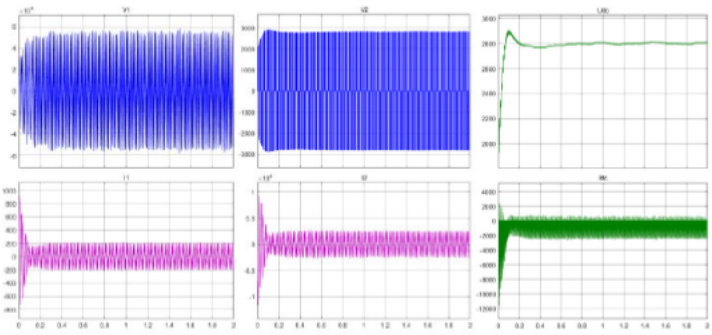

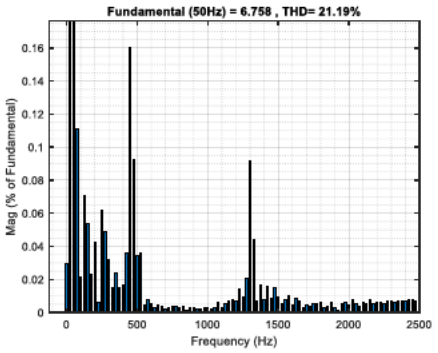

Distance from Traction Substation = 10km

Tap changer setting = 5

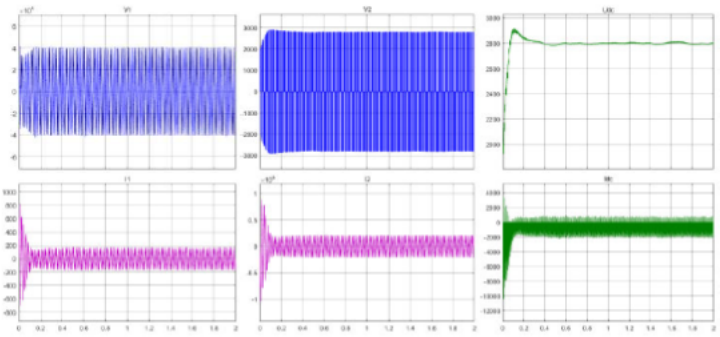

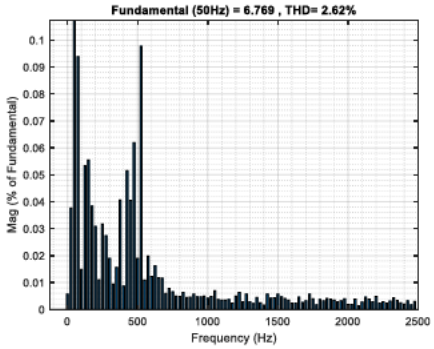

Distance from Traction Substation = 15km

Tap changer setting = 5

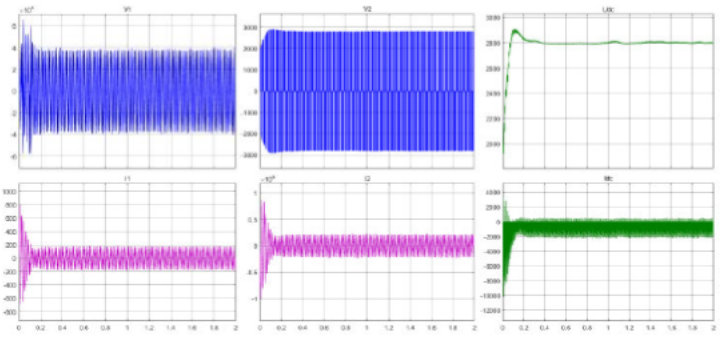

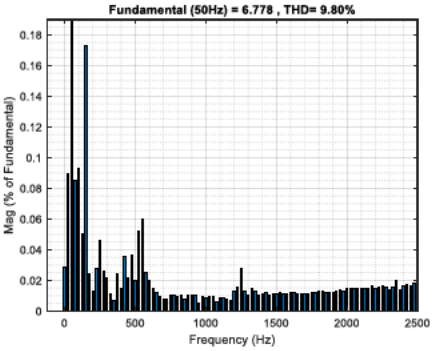

Distance from Traction Substation = 20km

Tap changer setting = 5

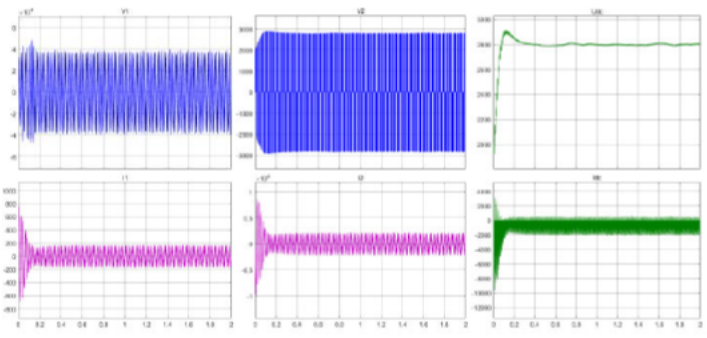

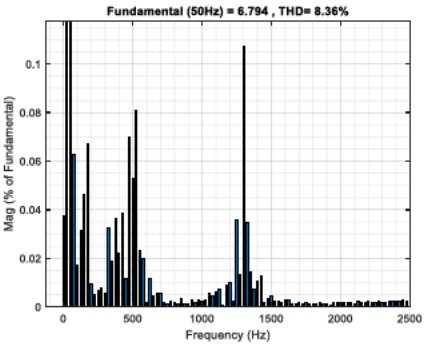

Distance from Traction Substation = 25km

Tap changer setting = 5

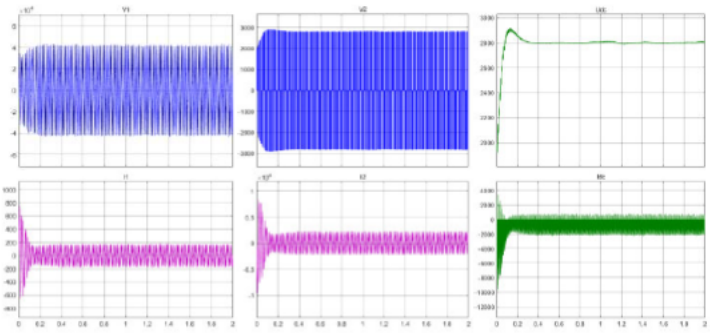

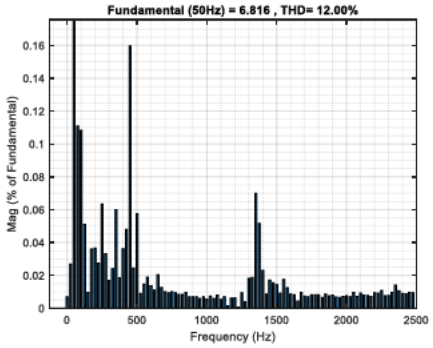

Distance from Traction Substation = 29.9km

Tap changer setting = 5

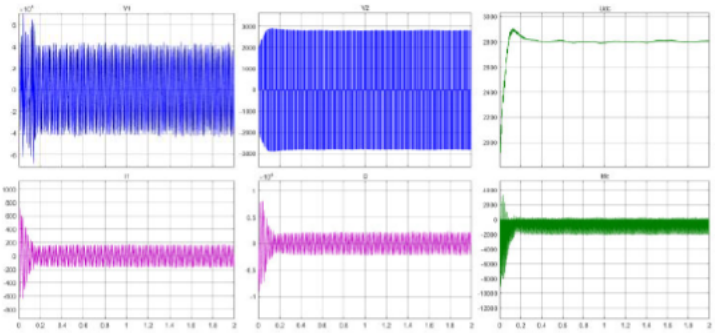

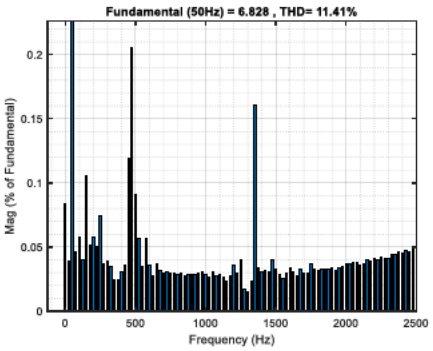

Appendix D: Simulation Results - Regenerating Loaded System

Distance from Traction Substation = 0.5km

Tap changer setting = 1

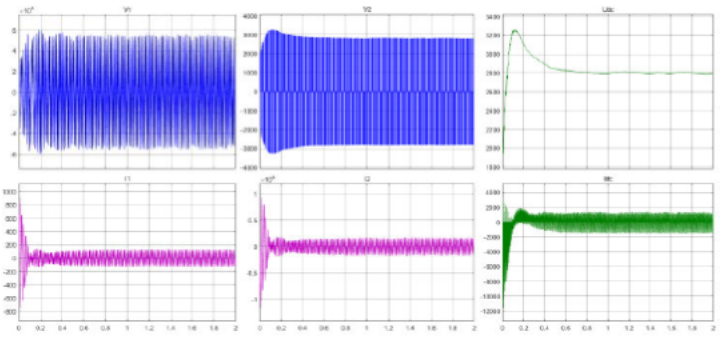

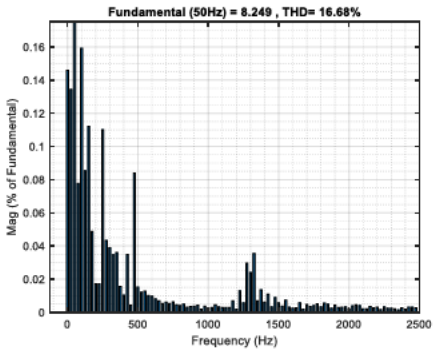

Distance from Traction Substation = 10km

Tap changer setting = 1

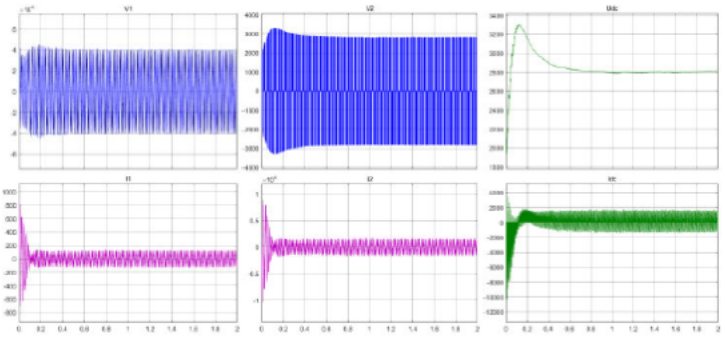

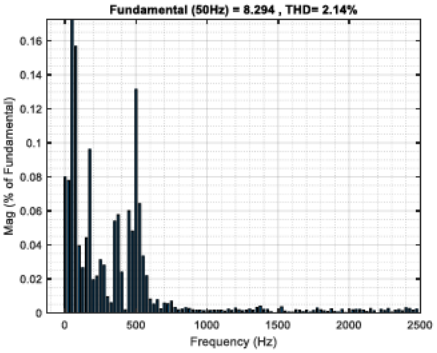

Distance from Traction Substation = 15km

Tap changer setting = 1

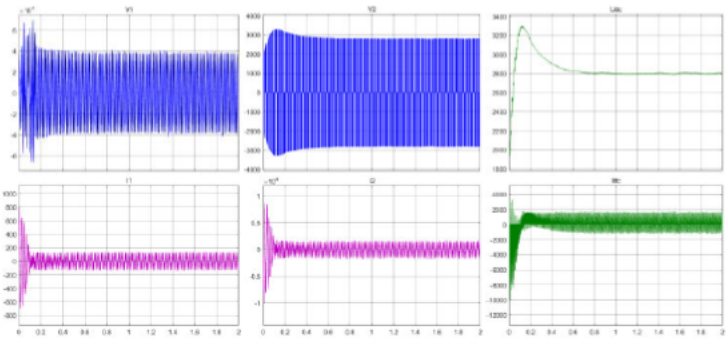

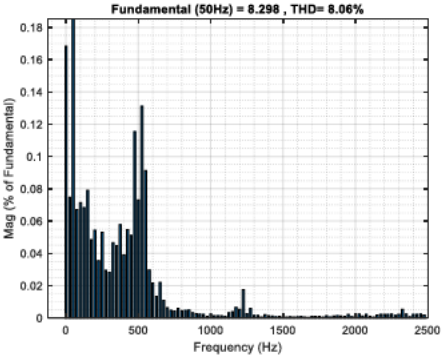

Distance from Traction Substation = 20km

Tap changer setting = 1

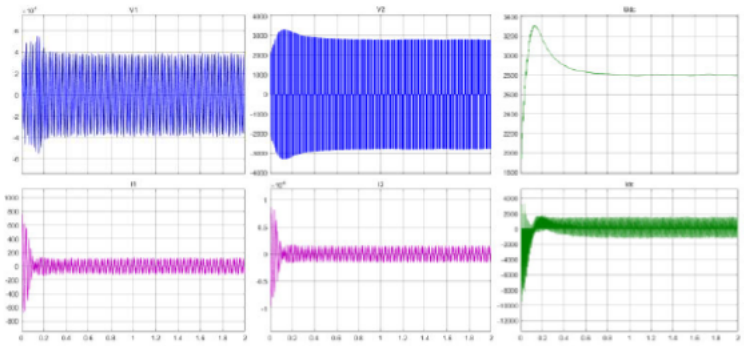

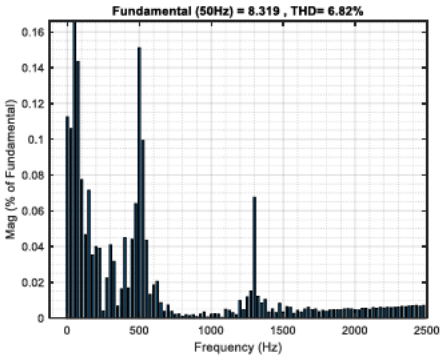

Distance from Traction Substation = 25km

Tap changer setting = 1

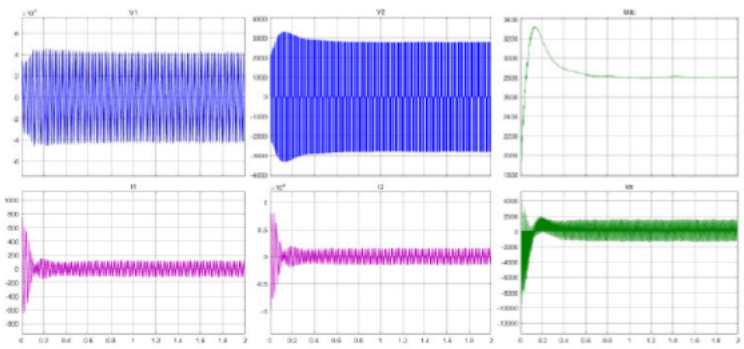

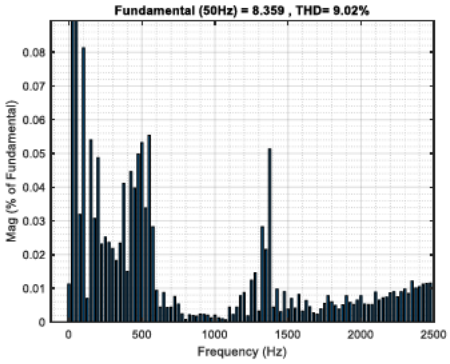

Distance from Traction Substation = 29.9km

Tap changer setting = 1

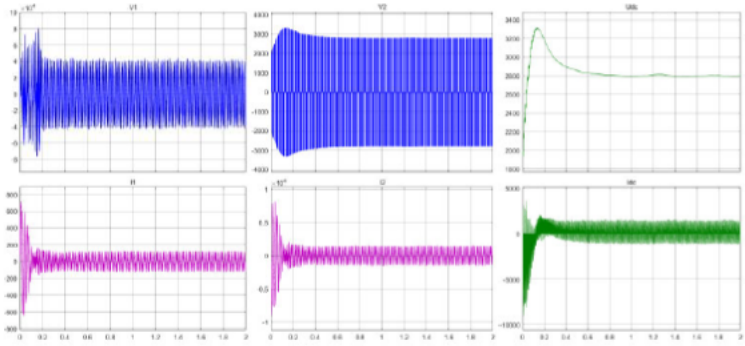

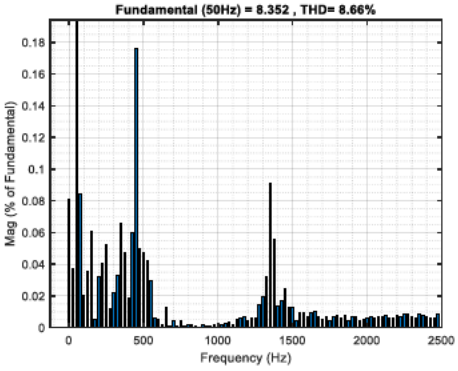

Distance from Traction Substation = 0.5km

Tap changer setting = 2

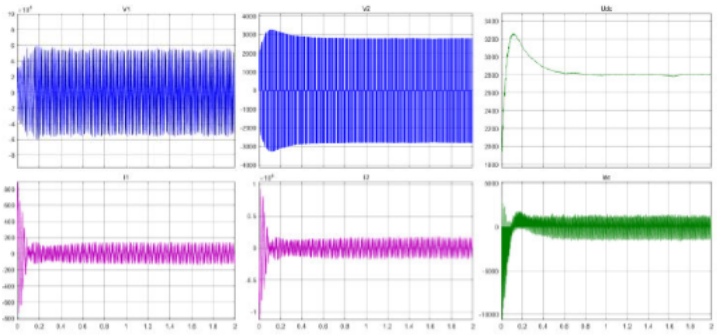

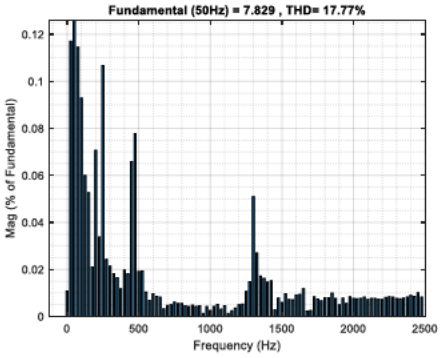

Distance from Traction Substation = 10km

Tap changer setting = 2

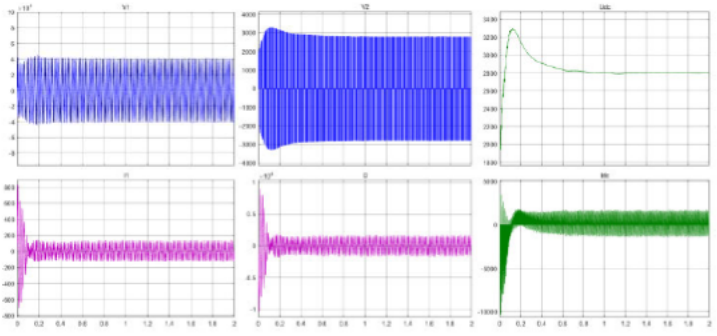

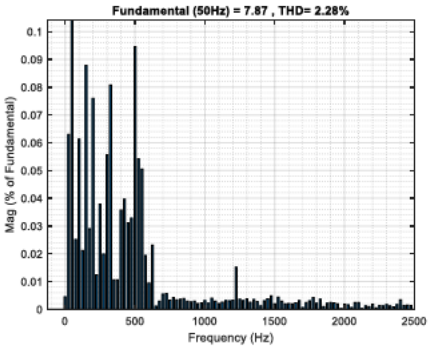

Distance from Traction Substation = 15km

Tap changer setting = 2

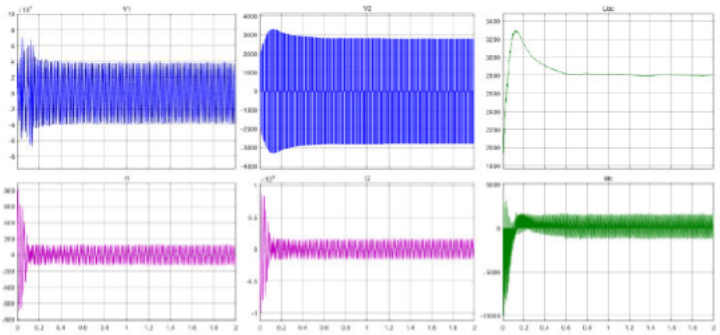

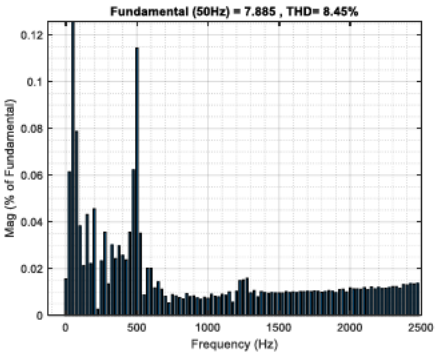

Distance from Traction Substation = 20km

Tap changer setting = 2

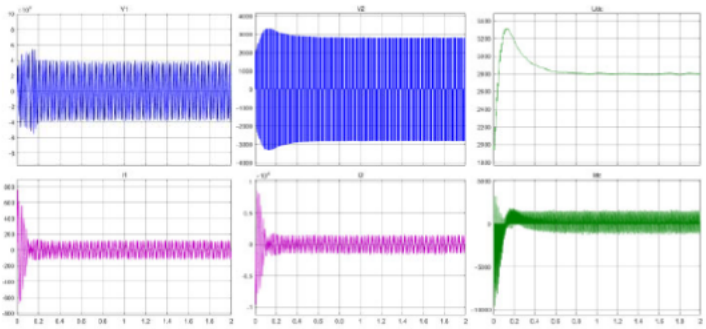

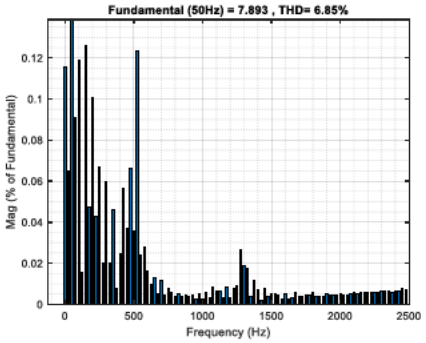

Distance from Traction Substation = 25km

Tap changer setting = 2

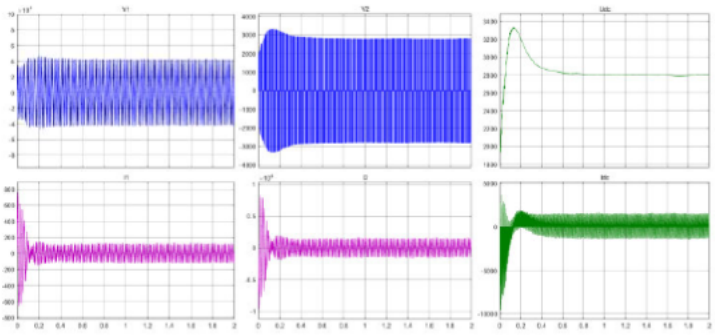

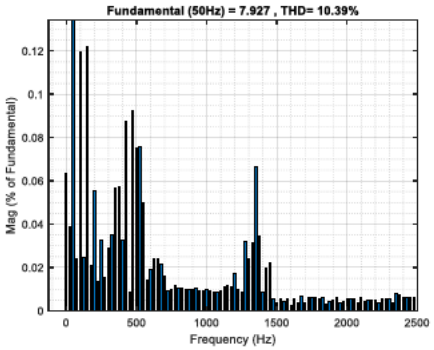

Distance from Traction Substation = 29.9km

Tap changer setting = 2

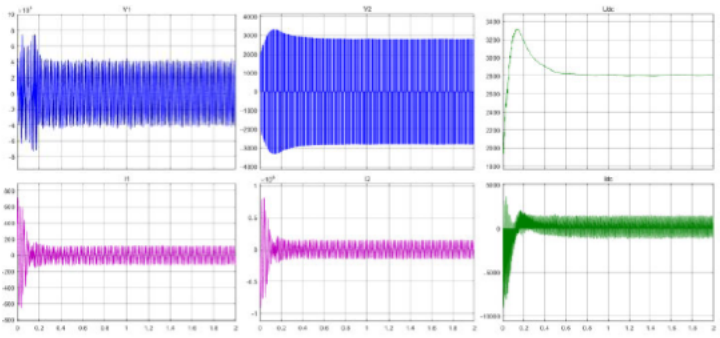

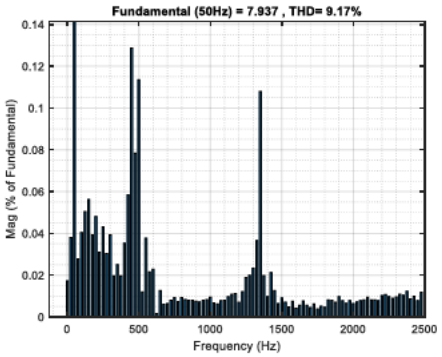

Distance from Traction Substation = 0.5km

Tap changer setting = 3

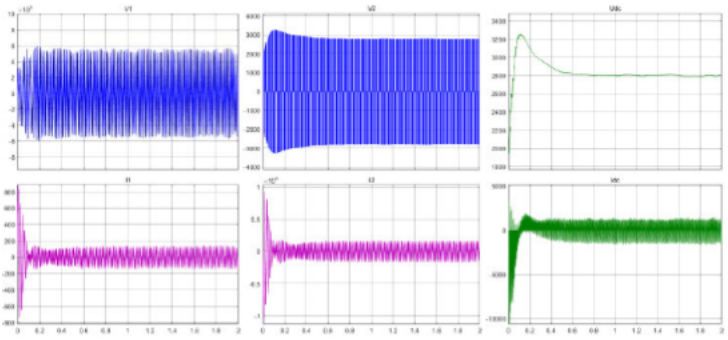

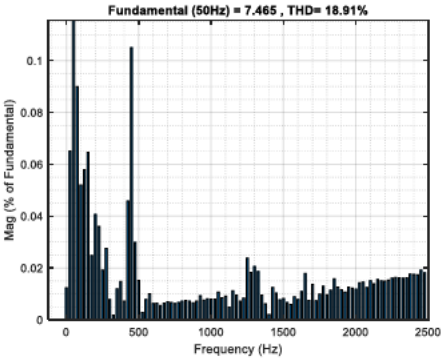

Distance from Traction Substation = 10km

Tap changer setting = 3

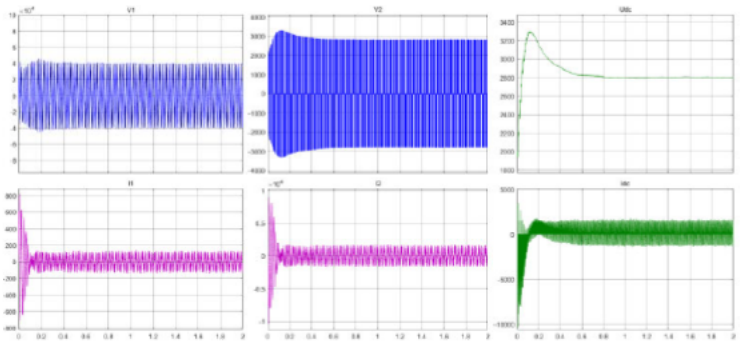

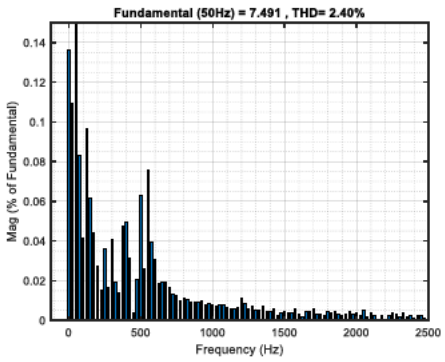

Distance from Traction Substation = 15km

Tap changer setting = 3

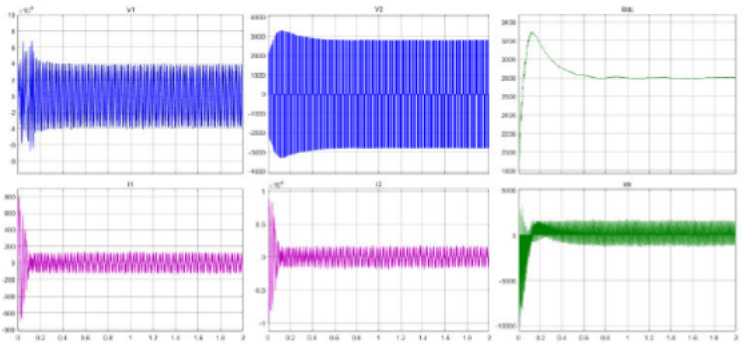

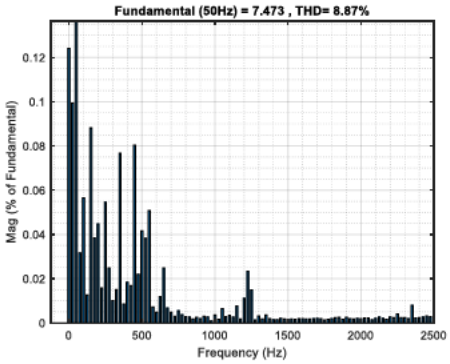

Distance from Traction Substation = 20km

Tap changer setting = 3

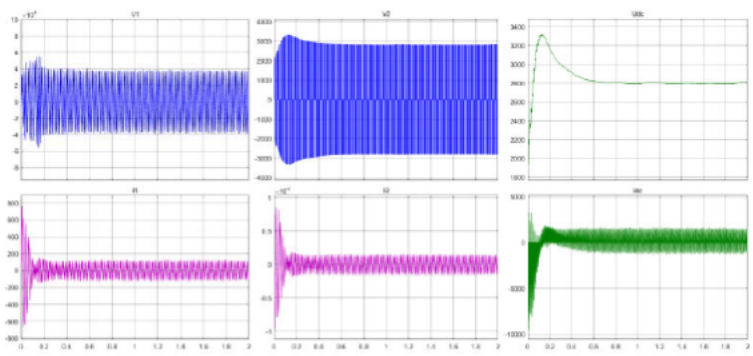

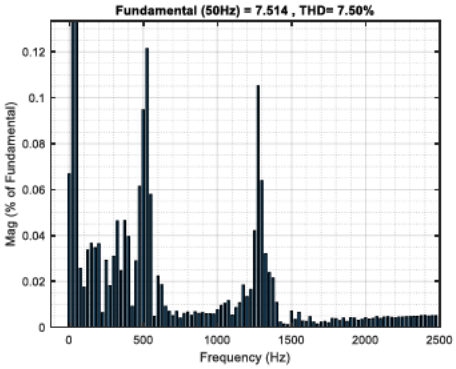

Distance from Traction Substation = 25km

Tap changer setting = 3

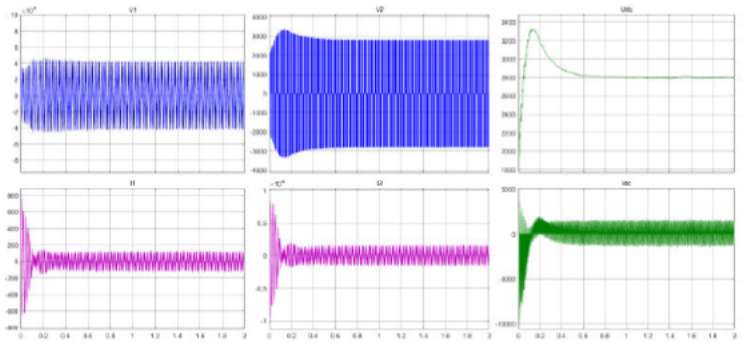

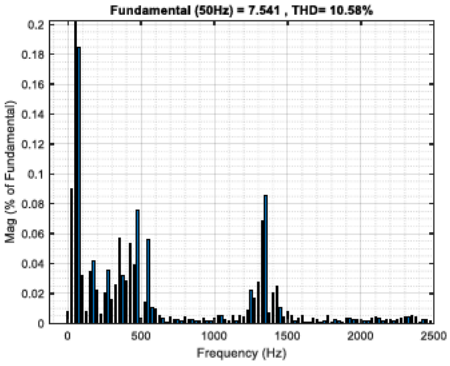

Distance from Traction Substation = 29.9km

Tap changer setting = 3

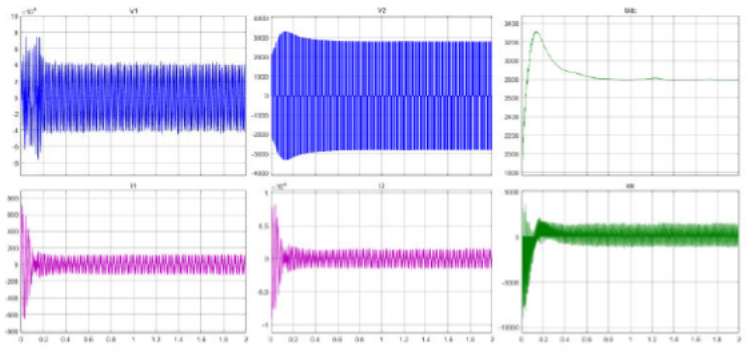

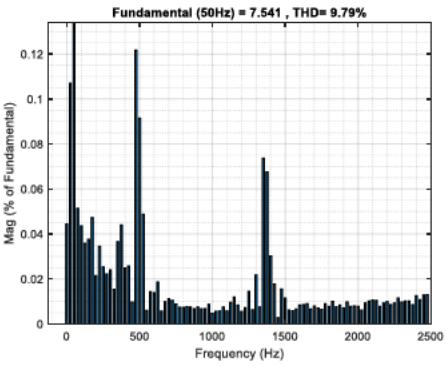

Distance from Traction Substation = 0.5km

Tap changer setting = 4

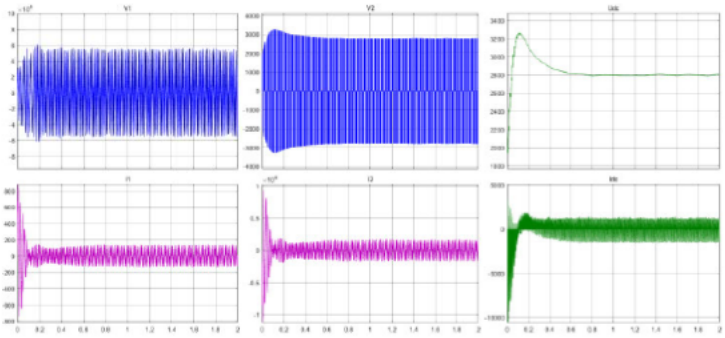

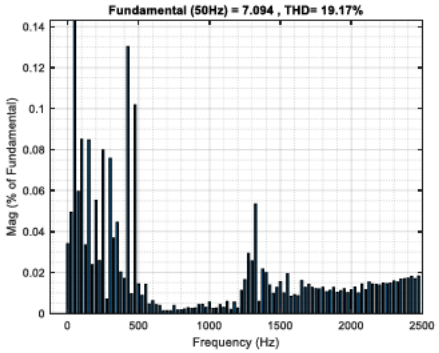

Distance from Traction Substation = 10km

Tap changer setting = 4

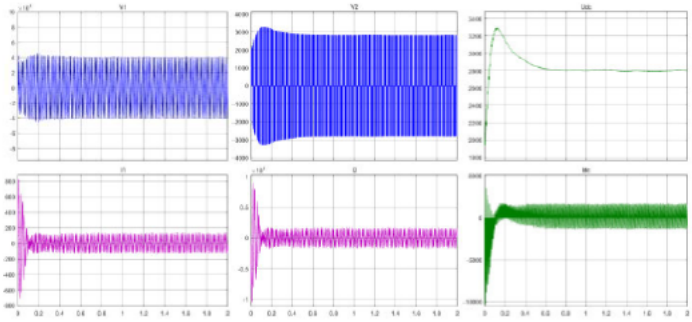

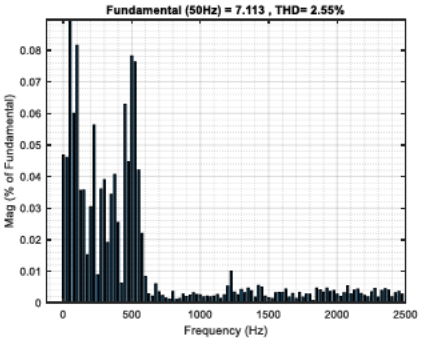

Distance from Traction Substation = 15km

Tap changer setting = 4

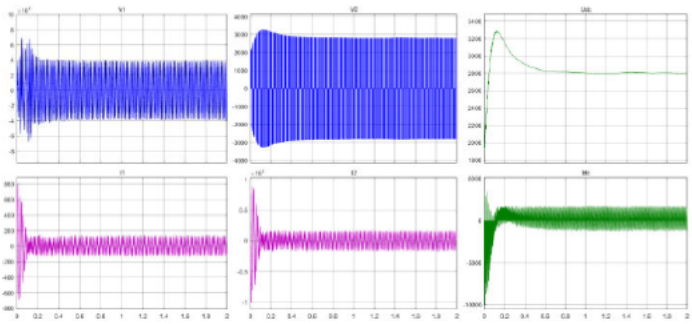

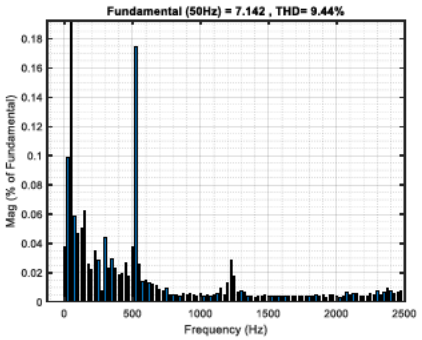

Distance from Traction Substation = 20km

Tap changer setting = 4

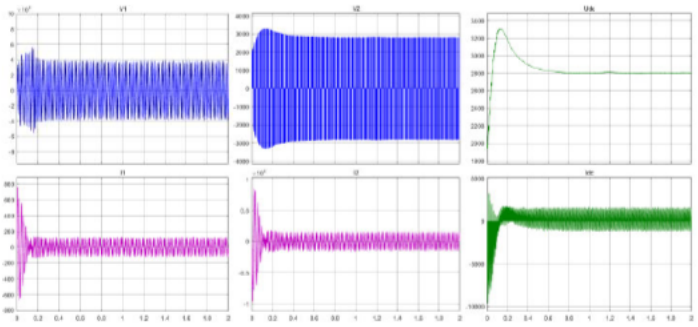

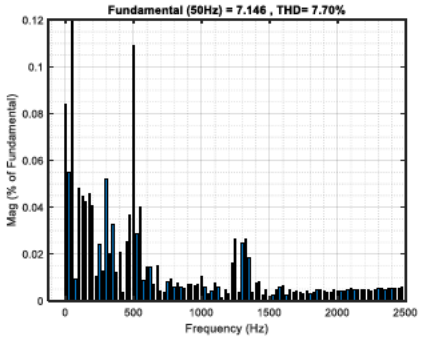

Distance from Traction Substation = 25km

Tap changer setting = 4

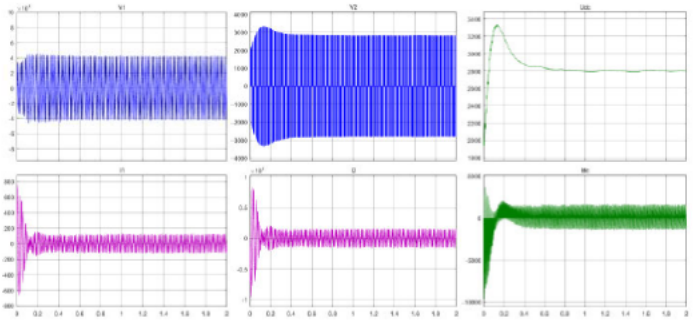

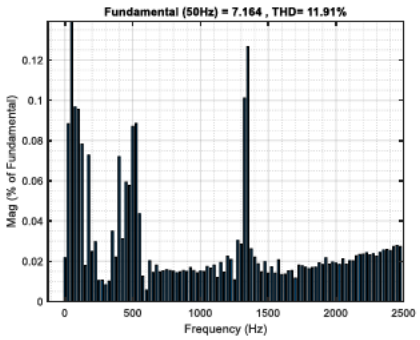

Distance from Traction Substation = 29.9km

Tap changer setting = 4

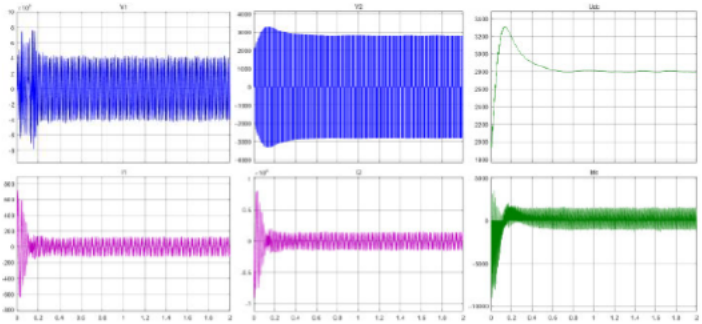

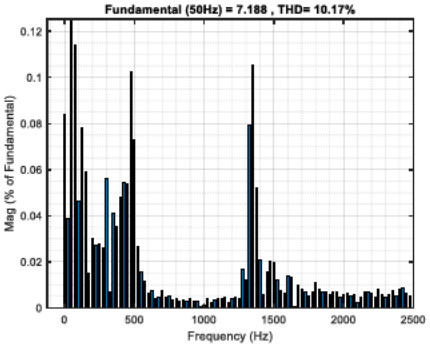

Distance from Traction Substation = 0.5km

Tap changer setting = 5

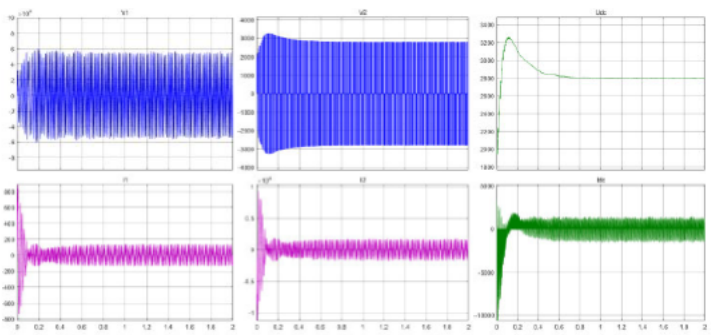

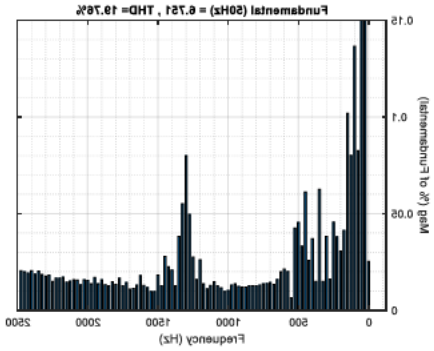

Distance from Traction Substation = 10km

Tap changer setting = 5

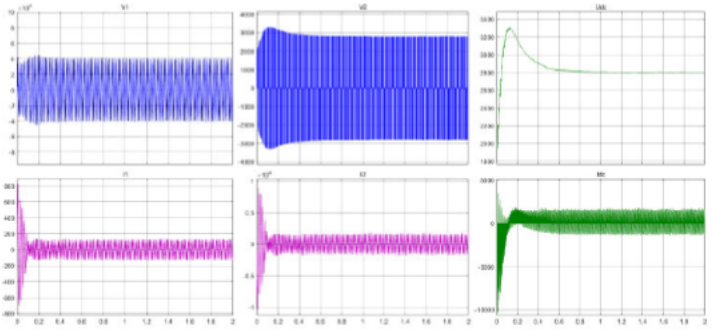

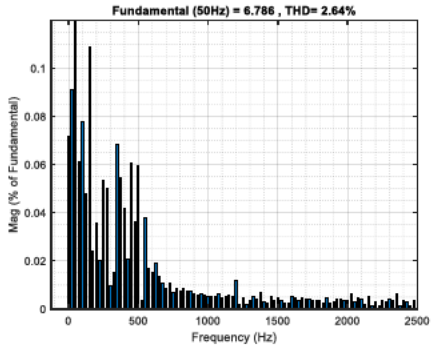

Distance from Traction Substation = 15km

Tap changer setting = 5

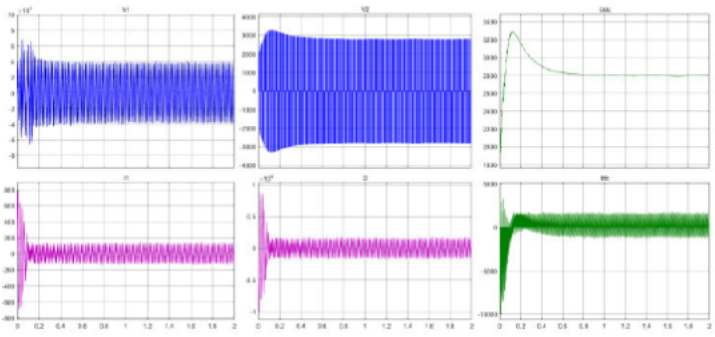

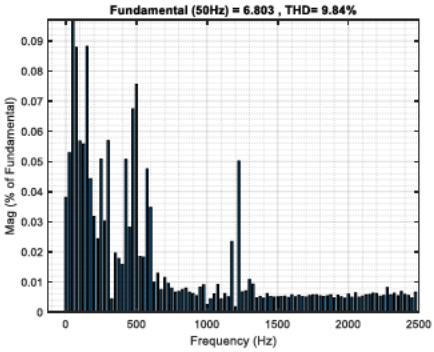

Distance from Traction Substation = 20km

Tap changer setting = 5

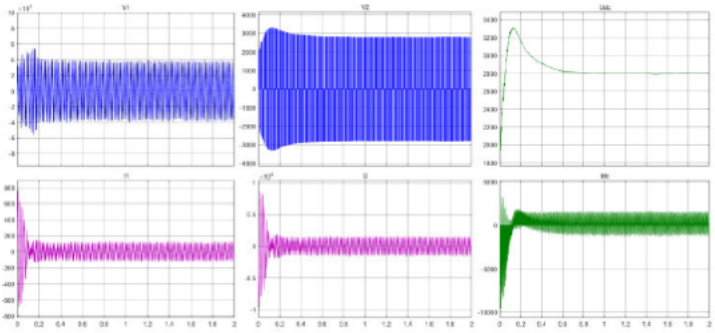

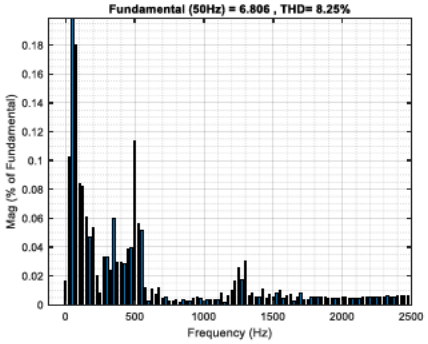

Distance from Traction Substation = 25km

Tap changer setting = 5

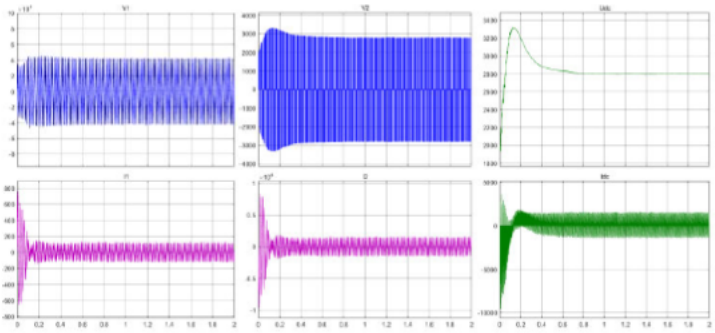

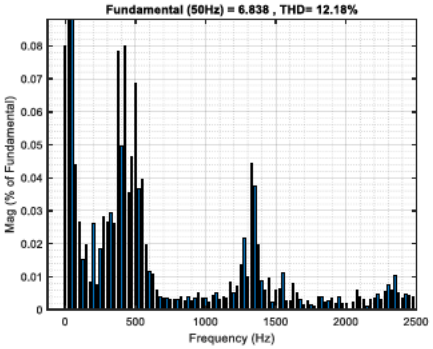

Distance from Traction Substation = 29.9km

Tap changer setting = 5